DEVELOPMENT AND SYSTEM INTEGRATION OF A COMPUTER-ASSISTED TOTAL KNEE REPLACEMENT TECHNIQUE

by:

Stacy J. Bullock

B.Sc.(Eng), University of Guelph 2001

A THESIS SUBMITTED IN PARTIAL FULFILLMENT OF THE REQUIREMENTS FOR THE DEGREE OF

MASTER OF APPLIED SCIENCE

in

THE FACULTY OF GRADUATE STUDIES

(Department of Mechanical Engineering)

We accept this thesis as conforming

to the required standard:

The University of British Columbia

December 2003

Library Authorization

In presenting this thesis in partial fulfillment of the requirements for an advanced degree at the University of British Columbia, I agree that the Library shall make it freely available for reference and study. I further agree that permission for extensive copying of this thesis for scholarly purposes may be granted by the head of my department or by his or her representatives. It is understood that copying or publication of this thesis for financial gain shall not be allowed without my written permission.

STACY BULLOCK — Name of Author *(please print)*

18/12/2003 — Date (dd/mm/yyyy)

Title of Thesis: Development and System Integration of a Computer-Assisted Total Knee Replacement Technique

Degree: Masters of Applied Science Year: 2003

Department of Mechanical Engineering
The University of British Columbia
Vancouver, BC Canada

Abstract

In a total knee replacement (TKR), the deformed articular surfaces of the knee joint are replaced with femoral, tibial, and patella components. Though this procedure is considered successful, component positioning errors, postoperative instability, and component loosening still exist.

Computer-assisted techniques aim to remove the inadequacy of mechanical instrumentation and the visual perception necessary in conventional procedures. Though commercial systems are available, published literature do not entirely support its use. Many systems incorporate algorithms that have not been verified, or that are known to be variable.

Our lab (Neuromotor Control Lab, UBC) has been investigating repeatable algorithms for steps of the total knee replacement procedure. The ultimate goal would be a complete, accurate, and cost-effective system that is an open architecture for research incorporating all the verified algorithms. The overall system must be validated and assessed, before it can be ultimately implemented clinically.

My thesis focused on determining repeatable algorithms for the requirements of the total knee replacement that had not been previously addressed, and integrating the system to take steps towards providing this open architecture for research. With this, the benefits of computer-assistance over conventional surgery may eventually be shown in this area.

In the first study, I investigated the use of a plane probe over a point probe to locate the transepicondylar axis for applications to proper rotational alignment and femoral knee centre. Current computer-assisted systems use a point probe to locate this axis, but this approach has been shown to result in highly variable axis locations. By conducting intra- and inter-operator tests on a cadaveric knee, I found that for this specimen, a sphere-fit based method was more reliable than a convex-hull based method in determining medial and lateral epicondylar estimates, and that this method may be more repeatable than using a point probe.

In the second study, I investigated a way to locate a tibial knee centre based on optimal coverage of the tibial plateau. Current computer-assisted systems digitize the tibial

eminences, and while this may provide a good mediolateral centre, the resulting anteroposterior location is variable. I evaluated the use of an ellipse-fit algorithm on a Sawbones and cadaveric model, and found, upon further verification, that this method could be implemented in computer-assisted systems as it better represents a tibial knee centre than the centre of the tibial eminences currently used in other commercial systems.

I then developed the kinematics for, and integrated a prototype of an adjustable cutting guide into our overall system. This cutting guide is different from those in many commercial systems as it can be roughly positioned on the bone, and then adjusted into place. This reduces error that may result from using visual feedback to manually align cutting blocks to guide lines provided on the screen. I evaluated the use of the cutting guide, and recommended changes for a more improved version.

Finally, I integrated all the algorithms (includes mine and previous graduate students) developed for each stage of the procedure into a full working system complete with a graphic user interface (GUI). The integrated system was designed to be modular, allowing choices in each step of the procedure. I demonstrated the working system on a Sawbones model, and presented it to an expert orthopaedic surgeon for feedback and recommendations.

By combining the contributions of this thesis with those of previous students, and the recommended hardware and software changes, our system provides an open architecture for research in this computer-assisted total knee replacement area. This system should increase the accuracy of TKR thereby increasing implant success and longevity, hence improving the patients quality of life.

Table of Contents

Table of Figures

List of Tables

Acknowledgements

First thanks go to my family for their love, support, and encouragement during the course of this degree, and in all my endeavours. Your trust in my decisions, and support for the choices I have made in my life journey means the world to me.

Thanks also to my supervisor, Dr. Antony Hodgson, who provided me with advice and direction, and to Dr. Bassam Masri for his insightful clinical perspectives.

Special thanks goes to my amazing friends and lab mates – Catherine & Joanne, Iman, Adam, and Mehdi - for being there whenever I needed you; for providing non-stop moral and technical support; and for donating time and agreeing to perform the experimental work detailed. Thanks also to Chris Plaskos for his advice during the course of the project; and my dream come true post-doc, Dr. Carolyn Anglin for her support and advice towards a final goal. This thesis would not be complete without all of you guys.

Finally, thanks to all my wonderful friends in Vancouver - Nicole, Lourette, and everyone from Green College who offered me a smile or a laugh whenever I needed it. This place has truly been like a home, and my experience here would have never been the same without you.

Chapter 1: Development of a computer-assisted total knee replacement system

1.0 Overview

The goal of a total knee replacement (TKR) surgery is to restore limb alignment, improve limb function, and relieve patient pain. This is done by resurfacing the deformed articular surfaces by femoral, tibial and patellar components. In this chapter, I describe the objectives for a successful procedure and the current conventional technique; various approaches that have been taken in computer-assisted surgery; the benefits and limitations of each approach; and the technique chosen by our laboratory. Our technique is further described in detail, both with respect to work that was completed prior to this thesis, and the work performed for this thesis.

The aim of our lab is to have a complete, accurate, cost-effective computer-assisted surgery system that can serve as a research testbed to validate and evaluate our algorithms before they are ultimately implemented clinically.

1.1 Objectives for a proper TKR

Degenerative arthritis of the knee joint is a common pathology seen in orthopaedic patients. Total knee replacement (TKR) otherwise known as total knee arthroplasty (TKA) is indicated for these patients to eliminate pain and improve function. Total knee arthroplasty has been a major advance for the treatment of the arthritic knee, achieving good to excellent results at 10-15 year follow-up in more than 88% of patients (Konig and Kirschner, 2003; Martin et al., 1998; Nicholson et al., 2002; Sharkey et al., 2002). However, failures from component loosening, instability, dislocation, fracture, or infection do occur. In the United States alone, more than 22,000 knee replacements are revised yearly (Sharkey et al., 2002).

In the TKA procedure, the surgeon removes the damaged surfaces of the diseased joint, and replaces them with metal and plastic components. The distal femoral surface is replaced with a metallic femoral component. The proximal tibial surface is replaced with either a tibial tray and polyethylene insert or an all-polyethylene tibial component. The patella is usually resurfaced with an all-polyethylene symmetrical component known as

the patella button (Figure 1.1). The surgeon then balances the soft-tissue structures (ligaments) surrounding the knee joint.

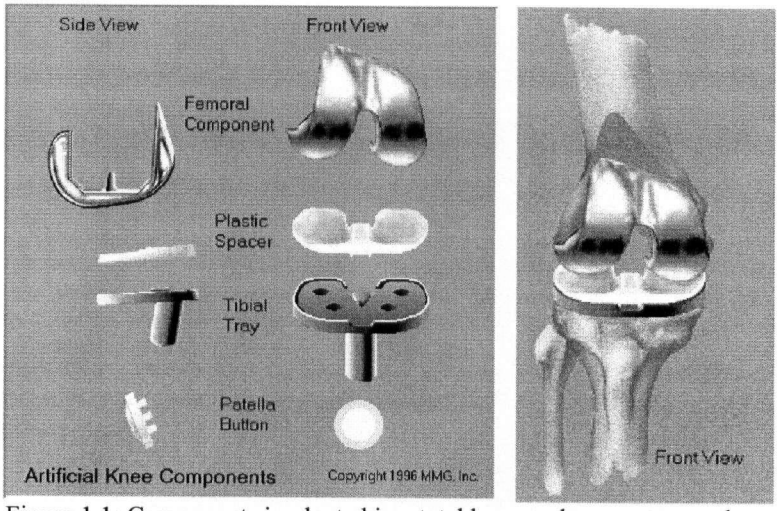

Figure 1.1: Components implanted in a total knee replacement procedure.
(Images courtesy Medical Multimedia Group)

There are many factors that affect the outcome following a TKA procedure. These include patient selection, prosthetic design, alignment, position of the individual components, ligament balance, and fixation. Of these, the surgeon directly controls alignment, component positioning, fixation, and ligament balance during the operation. Overstepping the narrow limits of correct alignment, component position or ligament balance will disturb knee kinematics and lead to adverse short-, and long-term effects (Victor and Sint-Lucas, 1998) such as the need for revision surgery.

Proper knee kinematics is achieved during surgery when implants are centred on the load-bearing or mechanical axis (a line linking the centre of the femoral head through the centre of the knee (femoral and tibial) to the centre of the ankle) and aligned and oriented with the rotational axes of knee motion (indexed by attachments of functionally important ligaments) defined by natural kinematics (Cooke et al., 1998). In addition to alignment through bone cuts, anatomically balanced knee ligaments also properly distribute weight-bearing forces on the surface of the implants (Nicholson et al., 2002).

Proper alignment and positioning of the implant are important in the three anatomical planes (Figure 1.2).

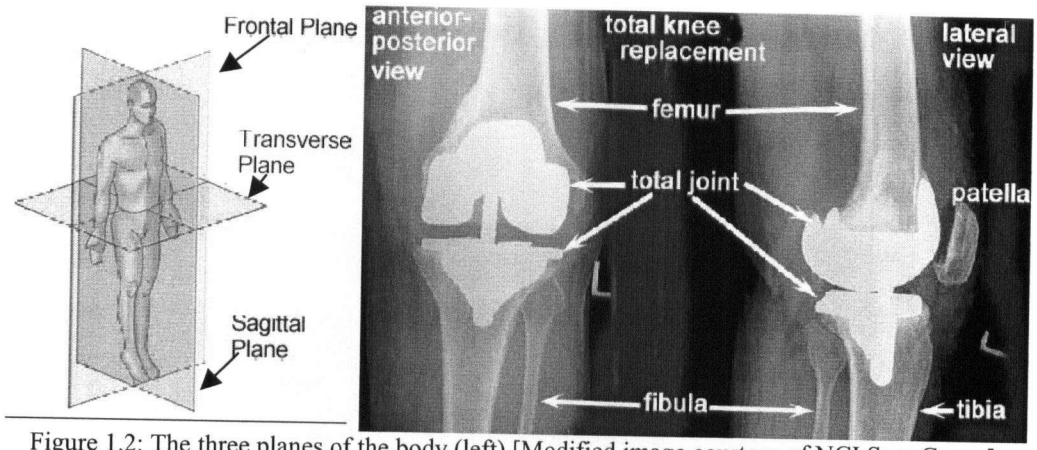

Figure 1.2: The three planes of the body (left) [Modified image courtesy of NCI Seer Group]. The TKR components viewed in the coronal (anterior-posterior view) and sagittal (lateral view) planes (right).[Image courtesy of Access Excellence The Living Skeleton]

- Frontal plane: Alignment of both the femoral and tibial implants should be perpendicular to the mechanical axis. Varus or valgus alignment of more than 3° around the anterposterior axis is a major cause of premature implant loosening (Jeffery et al., 1991).

- Sagittal plane: Alignment about the mediolateral axis defines flexion of the femoral component and posterior slope of the tibial component. Posterior slope and flexion are dependent on the implant type. Posterior slope usually ranges from 3° to as much as 10° to assist femoral 'roll back' on the tibia as the knee is flexed, and flexion of the femoral component can have values of up to 10°. Abnormal posterior tilt of the tibial component negatively affects knee range of motion (ROM), and tibiofemoral kinematics (Delp et al., 1998; Piazza et al., 1998)

- Transverse or horizontal plane: Rotation of the femoral component should be collinear with the transepicondylar axis, a line joining the medial and lateral epicondyles of the femur (Berger et al., 1993). The tibial component should be rotated to be congruent with the femoral component (Dalury, 2001). If these components are not congruent, this will likely lead to patellofemoral complications.

Anatomically balanced knee ligaments are necessary for acceptable passive knee kinematics and knee stability when the new components are implanted. The most

common technique involves balancing the soft tissues in flexion and extension by creating equal flexion and extension gaps of resected bones (Figure 1.3) to be filled by implants (Cooke et al., 1998).

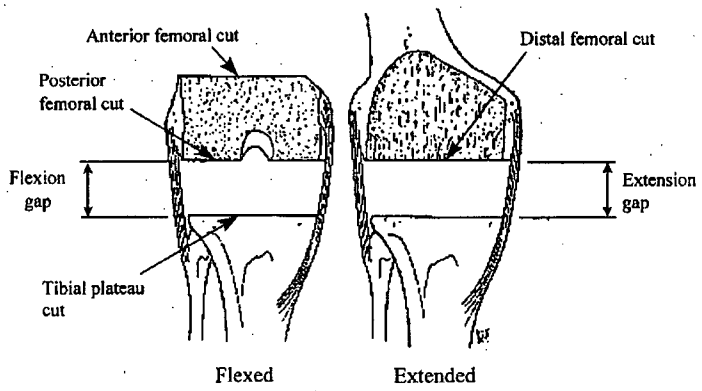

Figure 1.3: Rectangular flexion and extension gap at even ligament tension. Cuts for a TKR are also shown. (Inkpen, 1999 – Image adapted from Krackow, 1991)

Of equal importance to limb-realignment and proper soft tissue balance is component placement and size matching of components. The joint line of the knee must be preserved. An oversized femoral component or a cut that is too distal will cause overstuffing of the joint leading to anterior knee pain. The tibial component must also offer full coverage of the tibial plateau. If the cortical bone of the tibia does not fully support the component, component subsidence or migration can occur leading to implant loosening and failure (Lemaire et al.,1997).

Conventional mechanical alignment systems and guides have been developed to aid the surgeon in proper component sizing and positioning. Within the last 20 years, major efforts have been made in the development of new mechanical instruments that have allowed surgeons to meet their goals (Krackow et al, 2003). However, though the success rate has increased, there are fundamental limitations to these systems that will never allow for predictable alignment 100% of the time (Delp et al., 1998; Krackow et al., 2003; Stulberg et al., 2000).

In general, conventional systems are based on standard bone geometry and their instrumentation is based on a representative femur and tibia (Figure 1.4).

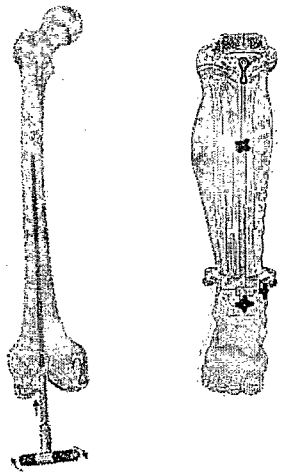

Figure 1.4: Common conventional instruments currently used in total knee arthroplasty. The intramedullary rod (left) is inserted up the femur, and the extramedullary rod (right) is placed on the tibia. (J&J Orthopaedics)

Optimal placement of the components may never be achieved when the patient's bones differ from the bone geometry assumed by the designer. Preoperative planning is also limited to the errors inherent to standard radiographs. With standard instrumentation, the accurate location of crucial landmarks such as the femoral head and ankle centre is limited. This conventional method assumes that the intramedullary rod (Figure 1.4) follows a predictable path in the femur, with a fixed relationship between the rod and the mechanical axis of the leg (Lam and Shakespeare, 2003). This relationship may differ if the intramedullary rod bends as it is inserted up the femur. For the ankle centre, the extramedullary guide is typically offset 5° to overlie the centre of the talus, an angle that can vary across patients (Jeffcote and Shakespeare, 2003). The extramedullary guide is also usually placed over an ankle that is already draped. This increases the uncertainty of its true position.

Some degrees of freedom such as rotation of femoral and tibial components in the horizontal plane, and positioning of the patellar component, are aligned by visual inspection (Delp et al., 1998), and there is no means to assess final implant positions at surgery (Krackow et al., 2003). Even the most elaborate mechanical instrumentation systems rely on this visual inspection to confirm the overall accuracy of the limb and implant alignment. Visual inspection is inherently subjective, and it varies among surgeons (Nizard, 2002).

Computer-based alignment systems have been developed to address and overcome these problems with the mechanical alignment systems. Computer-assisted systems are specific to the patients bone geometry, and try to reduce the number of assumptions that are inherent in conventional systems. These systems are also designed to reduce the amount of visual inspection compared to that that is present in conventional surgeries. This is done by overcoming limitations of 2-dimensional x-ray planning using 3-dimensions, and increasing the precision of implant positioning by real time navigated cutting templates. It is hoped that the use of computer-assisted surgery will reduce surgical failures and the number of extreme malalignment outcomes (outliers) seen in some conventional surgeries. This technology will then provide optimal alignment, component position, and ligament and gap balancing, and should produce stability throughout a maximal range of motion (Krackow et al., 2003).

1.2 Current computer-assisted techniques and their limitations

Most current computer-assisted techniques involve the use of an optoelectronic camera detecting the spatial orientation of infrared emitters that are attached either to digitizing probes or to the patient's anatomy. These systems assist the surgeon in detecting the important components for performing a proper TKA (mechanical axis, rotational alignment and component size) using either image or image-free techniques with robotic or passive guided cutting navigation.

Stindel et al. (2002), distinguishes these systems at two levels: 'Perception of Data' and 'Action Guidance'. Since that article, a few new systems have entered the market making his current taxonomy of computer-assisted systems for perception of data incomplete. At the time of writing, the new taxonomy of computer-assisted systems is shown in Figure 1.5. At the level of perception there are two main categories. These are Image-based and Image-free Systems. Within Image-free Systems, there are Landmark based systems and Bone morphing systems. Within the systems that use Images, there are CT-based and systems with Virtual fluoroscopy.

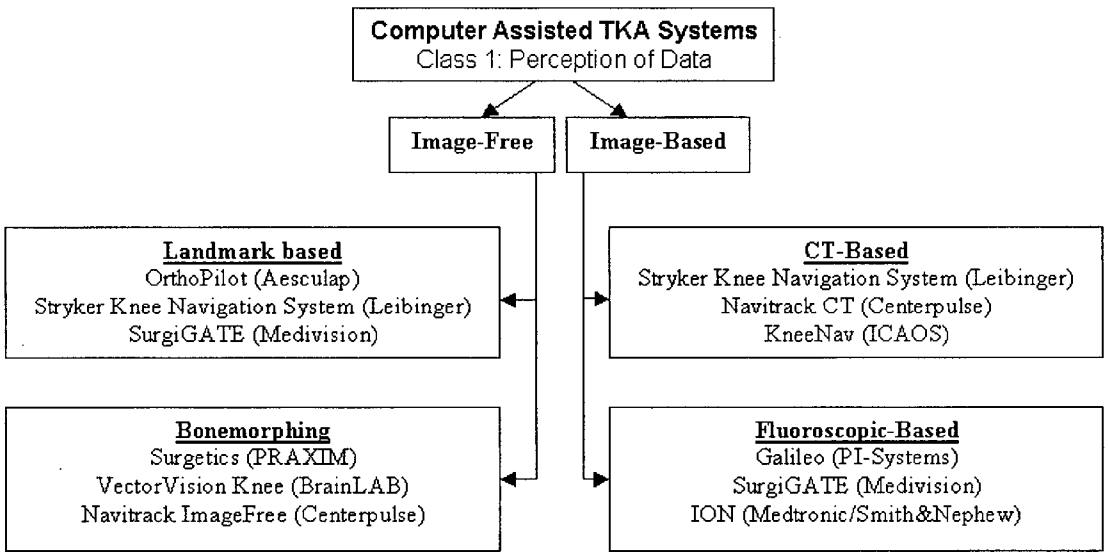

Figure 1.5: The new taxonomy for Class 1:Perception of Data.
(Modified from Figure 1: Taxonomy of computer assisted TKA procedures Stindel et al., 2002)

The Action Guidance level is unchanged as reported in the Stindel et al. (2002) article. Within this level there are five categories. These are passive systems using navigation of cutting blocks, individual templates machined to fit the bone and position a guide intraoperatively, semi-active systems using robotic assistance to position cutting guides, semi-active systems using manual control of robotic milling, and active systems for milling the bone automously.

The trend for current knee navigation systems is passive systems (Nizard, 2002), and hence in this thesis I will only focus on these.

In this category, there are over 10 commercially available systems, either image-based or image-free (Figure 1.5). At the start of this line of research in 1997, three systems were in their development stages with very little clinical testing and no long-term results. Within the last five years every major surgical navigation system has created and commercialized a knee system. Some companies namely Stryker, Navitrack, and VectorVision even offer Image-based and Image-free versions. There have also been randomized prospective studies on some systems, data that had been previously unavailable when these systems were in their initial stages.

1.2.1 Image-based systems

Systems featuring the use of images are either computed tomography (CT)-based or Fluoroscopic-based. Though spine and neuro-surgical applications are well established in this area, total knee replacements are new to this market, entering in 2001. These systems are generally more expensive, and expose the patient to radiation.

1.2.1.1 CT (e.g.: Stryker Knee Navigation System, Navitrack CT, KneeNav)

CT-based knee systems were introduced into the US in December, 2001. These systems require pre-operative imaging in order to reconstruct a 3D model of the knee. During surgery, a registration process is required to match reality to the model seen on the screen. This occurs by identifying special points during the operation that had been chosen preoperatively by the surgeon. This patient specific model is advantageous to the surgeon as he/she is able to align the implant during the operation based on his or her preoperative decisions.

Published results on this class of systems are now being seen for the Stryker system. One study showed an increase in surgical time of 37 minutes (Lionberger et al., 2003) with no statistically significant improvement in the range of joint motion determined between the conventional and computer-assisted groups. Another study (53 patients in each category) showed significantly better alignment for the image-guided patients in the coronal plane for both components, and in the sagittal plane for the femoral component only (Swank, 2003).

1.2.1.1.1 Limitations of CT-based systems

There are minor inaccuracies in CT data at the boundaries and inherent in segmenting (Krackow et al., 2003). However, while these systems may prove to be beneficial for the patient in the case of extreme deformities, for the average total knee replacement patient, the market has been moving away from this area due to the large increase in cost for the hospital, an unreasonable source of radiation for the patient, and unproven benefits for such an expense. In addition, many small hospitals cannot afford a CT-based platform. For these reasons, navigation companies are exploring Fluoroscopic and Image-free options in order to stay in the navigation market.

1.2.1.2 Fluoroscopy (e.g.:Galileo, iON, SurgiGATE)

Fluoroscopic-based systems allow the surgeon to have an image of the knee without the expense of the CT-scans and pre-operative surgical time needed to reconstruct the images. Similar to all computer-assisted systems, reference arrays are attached to the femur and tibia. Fluoroscopic images of the knee are then obtained from a C-arm and matched to the patient's anatomy. Proper alignment is then determined based on intra-operative kinematic manipulations of the limb, incorporating information from the patient-specific fluoroscopic images. Component sizing is obtained by superimposing component images on the patient's fluoroscopic image. Though there are limited published results on clinical trials using these systems, a study performed on 14 cadavers showed minimal increase in time and acceptable frontal and sagittal alignment (Murphy et al., 2002). Lange et al. (2003) also reports good results with a frontal plane alignment of 0.7±1.1° off the mechanical axis for computer-assisted patients compared to 2.2±3.4° for the conventional patients. He reported no computer-assisted patients with more than 5° mal-alignment compared to 11 in the conventional group. Both of these studies were performed using the iON system. The SurgiGATE Image-based system is a CT-based system that registers bones with 3D fluoroscopy instead of the more commonly used digitization present in other CT-based systems.

1.2.1.2.1 Limitations of Fluoroscopic-based systems

Though this group of systems seem to be the current trend in computer-assisted navigation, there is currently insufficient literature to allow objective evaluation of its efficacy. Though there is less radiation exposure than CT scans, radiation exposure does exist, hence the surgeons operating must wear lead in the operating room, which can get uncomfortable. Fluoroscopy is still relatively crude and the lateral plane is still somewhat difficult to see. Fluoro-Navigation systems also need a fluoro-technician in order to operate them. This may be an additional expense that cannot yet be justified.

1.2.2 Image-free systems

Image-free systems require no radiation exposure as well as no additional preoperative time. The two main categories are systems featuring bone morphing, and those that use landmarks. These systems are generally less expensive than image-based options.

1.2.2.1 Bone morphing (e.g.: Surgetics, VectorVision, Navitrack ImageFree)

Bone morphing systems allow the user to use a digitizing probe to gather clouds of points along areas defined by the system. A generic 3D model of the leg is then morphed or fit to the patient's anatomy from which important landmarks can be distinguished. Alignment and component size are proposed, which can be accepted or modified by the surgeon. Alignment of the cutting guide is generally done in real time by following guide lines seen on the screen.

Surgetics introduced their technique to clinical trials in 2002. At the time of writing, there has only been one published paper on the Surgetics technique. The first randomized clinical trial using the Computer Assisted Surgical Protocol (CASP) in association with the De Puy LCS prosthesis reported initial results of 11 patients (Stindel et al., 2002). The computer-assisted procedure took an average of 90 minutes to complete with all post-operative frontal alignment within ±3° of the mechanical axis. A two year clinical study is currently in progress.

The CT-free VectorVision for total knee arthroplasty was also released in 2002. This technique is similar to Surgetics with differences seen only in rotational alignment of the femoral component. The VectorVision knee system provides the surgeon with four different choices for rotational orientation. The femoral component can be oriented with respect to the posterior condyles, the transepicondylar axis, Whitesides line or ligament tension (gap technique) in order to achieve a balanced flexion and extension gap. The ligament balanced orientation procedure allows the surgeon to use a laminar spreader tool to check the flexion and extension gaps. The system measures gap size and deviation of the leg axis, and suggests optimal femoral component orientation with respect to a balanced flexion gap (Bathis et al., 2003). A study comparing 80 conventional patients to 80 computer-assisted patients reported an increase of 15 minutes operating time for the computer-assisted surgeries. Post-operative x-rays revealed 86% of the computer-assisted patients within 3° in the frontal plane compared to 78% of the conventional patients.

1.2.2.1.1 Limitations of Bone morphing systems

This system relies on the accuracy of the digitized points to morph the bone model to the patient's anatomy. For the femur, the probe is passed over the bone surface. A problem may arise if crucial landmarks for alignment of the implants are not explicitly digitized. If the crucial landmarks are missed in the surface digitization, overall implant alignment may be compromised if the patient's anatomy varies greatly from the generic model.

1.2.2.2 Landmark-based (e.g.: OrthoPilot, Stryker Knee Image-free, SurgiGATE)

Landmark-based systems were first introduced in 1997 and paved the way for navigation in total knee replacement procedures. These systems are the simplest, with no image or model requirements. Kinematic manipulation and direct digitization are used to determine the hip, knee, and ankle centres. In the case of kinematic manipulations, specific modelling algorithms are then used to define the actual centres. Rotational alignment is typically determined by direct digitization.

The first system to be introduced on the market was the OrthoPilot. The first published report on this system was in 1997 (Leitner et al., 1997). In 1999-2001 clinical results reported on this system were not much better than that of conventional systems. Most studies reported no statistical difference between the numbers of cases that fell within 2-3° of the desired mechanical axis angle for conventional vs computer-assisted systems (Table 1.1), and a general increase in surgical time.

Since the OrthoPilot's inception, there have been updates in software and procedures. The 3rd software version eliminated the screw placed in the iliac crest, and adopted a 'worm' algorithm to find the hip centre (Confalioneri et al., 2002). The latest version (OrthoPilot 4.0) includes an adjustable cutting guide. However, the most recent conference publications (2003) on the OrthoPilot system still show variable success rates that overlap considerably with those of the conventional technique (Table 1.1).

Stryker Image Free Navigation system (Leibinger) joined the Image-free Systems very recently. It is uncertain whether this system is purely based on landmarks or has integrated bone morphing as there is no published literature on the working of the system. Assuming that the system is landmark based, published data on clinical trials show

statistically better alignment and fewer outliers in the computer assisted procedure over conventional procedures (Donnelly et al., 2003; Chauhan et al., 2003a; Chauhan et al., 2003b). There was an increase in surgical time of about 13 minutes.

Table 1.1: Reported results using the OrthoPilot system vs conventional procedures.

Study - patients (OrthoPilot/Conventional)	Completion time(minutes)		Reported Success	
	OrthoPilot	Conventional	OrthoPilot	Conventional
Confalonieri, 2000: (25/25)	102 (80-130)	70 (50-100)	75% < 3° mean = 181.2°	84%< 3° 179.0
Stulberg, 2000: (5/15)	101	74	100% < 3°	66.6% < 3°
Confalioneri, 2002: (worm)(60/40)	105	80	mean = 181.2°	mean = 178.5°
Kiefer, 2001: (100/50)	Conv+15	Conv	73% < 2°	40% < 2°
Jenny, 2001a: (30/30)	N/a	N/a	83% < 3°	70% < 3°
Jenny, 2001b: (50/50)	N/a	N/a	94% < 3°	78% < 3°
Saragaglia, 2001:(25/25)	102	70	179±2.53	181.2±2.72
Kiefer, 2003a: (50/50)	N/a	N/a	< 3° 94%[1] 82%[2]	< 3° 58%[3] 74%[4]
Kiefer, 2003b: (80/80)	No increase	N/a	79% < 3° [179.1°] (173-185)	63% < 3° [178.4°] (169-188)
Hart, 2003: (60/30)	N/a	N/a	mean = 174.3° (170-179)	mean = 174.9° (172-179)

(1) E-motion implanted with OrthoPilot 4.0 (2) navigated Search™ prostheses implanted with OrthoPilot 3.0 (3) conventional Search™ prostheses. (4) conventional DePuy LCS prostheses

Wendl et al. (2002) presented the only other published result on Image-free systems at the Computer Assisted Orthopaedic Surgery (CAOS) 2002 conference. His results on 50 surgeries performed using the SurgiGATE system reported an operating time increase of 20 minutes over the conventional procedure, with all patients within 2° deviation from the mechanical axis in the frontal plane.

1.2.2.2.1 Limitations of landmark-based systems

A major concern for the OrthoPilot system is in its location of the knee centre. The OrthoPilot uses a kinematic analysis of the diseased knee joint to find its knee centre. This can be seen as controversial (Stindel et al., 2002), as changes in shape and the surrounding soft tissues are known to influence the kinematics between a diseased knee

and a normal knee. The OrthoPilot also allows the surgeon to digitize the transepicondylar (TE) axis with a point probe, and allows the surgeon to choose whether he/she accepts the kinematic centre or digitized centre as the knee centre. Digitizing the lateral and medial epicondyles with a point probe results in a highly variable identification of axes (Jerosch et al., 2002).

These systems do not report their proprietary algorithms, and the repeatability and robustness of these algorithms are unknown. It is our belief that each system should have all of its individual algorithms tested for repeatability before being implemented into a final system. In this way, final standard deviations reported from clinical trials can be attributed to certain parts of the system, and one can identify which part of the procedure contributes the most to this variability. Computer assisted systems would then be more accepted by the patient and surgeon.

1.3 Status of the computer-assisted technique previously developed in the lab

The Neuromotor Control Lab (NCL) has been developing a Computer Assisted Total Knee Replacement (CATKR) system since 1997. This open architecture platform enables the development and testing of specific algorithms to be used in an overall total knee replacement system. We chose the to develop a system in this category as this is an inexpensive system that is most likely to be widely deployed clinically.

At that time, there were no commercial systems (Figure 1.5) available in the North America, and an opportunity to create such a system was also seen as beneficial to this North American market. Inkpen (1999) outlined the initial procedure adopted by the NCL lab (Figure 1.6). Though his work adopted similar algorithms to other Image-free Landmark based systems (such as the OrthoPilot), it provided the first publication on the repeatability of identifying these important landmarks. He showed that using digitization to calculate the ankle centre showed high inter-operator variability. In addition, there were large differences measured between the desired plane and the actual resulting plane that had been cut with a bone saw.

Another important contribution was the design and validation of a pelvic tracker that eliminated the use of the invasive anterior iliac spine pin and array that was present in other systems during that time. In these image-free systems, the hip centre is determined

by manipulating the femur and fitting a cloud of points from the femoral array in the hip array reference frame. The hip array accounts for the movement of the pelvis during the manipulation. Using the hip modeled as a ball and socket joint, a sphere fit centre is employed with the centre of the sphere designated as the hip centre. The sphere-fit algorithm with the greatest repeatability used in our system solves a non-linear least square fit with homogeneous transforms.

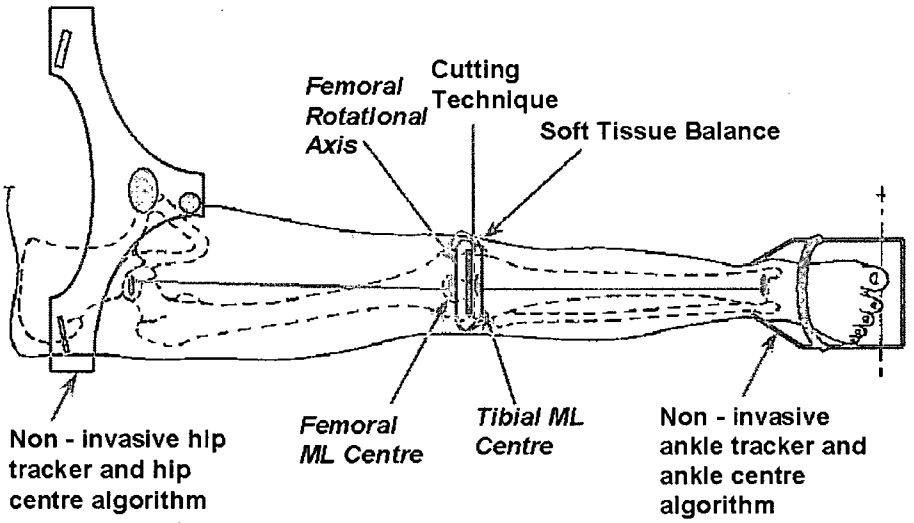

Figure 1.6: The components that have been developed for the NCL system in our lab. The non-italicized components were addressed previously. The italicized components will be addressed by the author.

Though the other systems have since eliminated the use of the pelvic pin hinting at 'worm' algorithms that account for pelvic movement during the manipulation, the algorithm for this is proprietary and no publications have been presented about it, or its repeatability.

Since Inkpen (1999), research has been performed in our lab on determining a more repeatable way of locating the ankle centre, with weight-bearing considerations. All other systems perform non-weight bearing kinematic manipulations or digitize the medial and lateral malleoli in order to determine the ankle centre for the tibial mechanical axis. Though this is the most feasible in the operating room, it was our belief there was need to investigate the location of a weight-bearing centre as this represents the load path from the leg to the foot. Shute (2002) performed research on the relationship between the non-weight bearing centre and the weight-bearing centre in different individuals, as well as on

finding a repeatable algorithm to determine a non-weight bearing centre. He found that a centre determined from using kinematic manipulations of the ankle, corrected with a lateral and posterior shift was on average a repeatable way of identifying a weight bearing centre.

Research has also been performed in our lab on the cutting aspect of the total knee replacement system as earlier research had shown inaccuracies of cutting with a bone saw. Plaskos (2002) documented these inaccuracies, and compared them to a novel milling technique. He recommended that for a high accuracy TKA, a milling tool is required for a more accurate cut. Research is still in progress on the actual tool tip and angle requirements needed for the best cut.

Another important aspect of the total knee replacement system developed in our lab is the issue of soft tissue balancing. Most current computer-assisted TKA systems do not incorporate quantitative intra-operative soft tissue guidance. Instead, they perform motion measurements to check the degree of slackness of the collateral ligaments after cuts have been performed (Kunz et al., 2001; Stulberg and Sarin, 2001). The surgeon's component selection and placement may change after soft tissue releases are made and balance assessed (Illsley, 2002). Additional bone cuts may have to be made, increasing surgical time, and resecting more bone. This problem would be eliminated if soft tissue balancing were performed prior to performing bone cuts. Illsley's (2002) research in this area provided an option of component placement based on balanced soft tissues using intra-operative kinematic manipulations of the knee ligaments.

All of the previous work in our lab has focused on specific areas of the total knee replacement system, trying to improve the specific algorithms for each component of the procedure. Future work is still necessary in other components of the procedure before a complete system can be implemented (Figure 1.7).

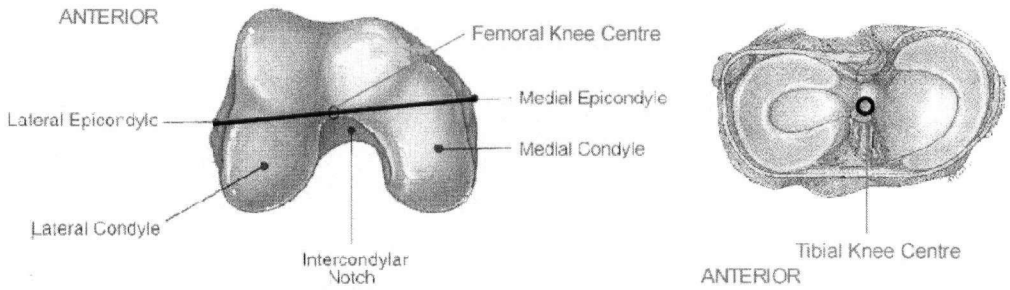

Figure 1.7: Research not yet performed in our lab is the identification of the femoral knee centre and a reference for rotational alignment (left), and the tibial knee centre on the tibial plateau (right).

1.4 Further requirements for a complete system

The aim of our lab is to have a complete computer-assisted total knee replacement research testbed that could be used to validate algorithms on cadavers so that the algorithms can be implemented clinically. In order for that to occur, research is necessary on the remaining requirements of our total knee replacement system that have no published repeatability results. These requirements are outlined below.

1.4.1 Method to repeatably determine the femoral and tibial centres for the mechanical axis

Femoral and tibial knee centre identification is important to complete the determination of the mechanical axis of the leg. While research had been performed in our lab on repeatably identifying hip and ankle centres (Inkpen, 1999; Shute, 2002), it was still necessary to determine and validate repeatable ways for finding the femoral and tibial knee centres (Figure 1.7).

Other CATKR systems identify the mediolateral and anteroposterior femoral centre by digitizing the transepicondylar (TE) axis, and using the mid-point as the centre. There is high inter-operator variability for identifying the TE axis with a pointed instrument (Fuiko et al, 2003; Jerosch et al., 2002; Kessler et al., 2003). It is therefore beneficial to explore other ways to determine the TE axis, and hence determine the femoral knee centre.

The tibial knee centre is typically found as the centre of the implant that has the most coverage of the tibial plateau. Conventionally, the cut is made perpendicular to the extra-medullary rod that is visually positioned by the surgeon over the tibia, and hence perpendicular to the anatomical/mechanical axis of the tibia. In computer-assisted

techniques, the tibial cut is made perpendicular to the mechanical axis of the tibia, defined by a vector joining the two points. It is therefore important for these centres to be in the right place so an anterior/posterior or varus/valgus cut is not made.

In the category of Computer-assisted techniques using Landmarks, the OrthoPilot system never distinguishes a femoral or tibial knee centre. Instead, it uses an overall knee centre in its definition of the mechanical axis. This overall knee centre is based on kinematic manipulations of the leg, even though the knee is diseased. Though we are unsure of the algorithms behind the other Image-free Landmark based systems, our system was in need of a way to determine a tibial knee centre based on optimal bone coverage (Lemaire et al, 1997), as well as to validate the repeatability of this algorithm.

1.4.2 Method to repeatably determine rotational alignment

Rotational alignment of the femoral implant was also necessary for completion of our system. Conventionally, there have been four ways used to determine rotational alignment. These are the transepicondylar (TE) axis, posterior condylar reference line, Whitesides line, and flexion gap technique (Berger et al., 1993; Martelli and Visani, 2002) [details in Figure 2.1]. It has been established that the transepicondylar axis best approximates the flexion axis of the knee; so most systems have adopted this technique (Churchill et al., 1998). Determining the TE axis with a point probe is highly variable (Fuiko et al., 2003; Jerosch et al., 2002; Kessler et al., 2003). It was therefore necessary to determine the TE axis in a more repeatable manner, and incorporate this into our system.

1.4.3 Design, manufacture and validation of an adjustable cutting guide to make final cuts (distal femoral, proximal tibial, and anterior-posterior femoral cuts [Figure 1.3])

Current computer-assisted cutting guides are hand positioned in real time by the surgeon while watching the screen. This method is greatly influenced by minor movements of the surgeon's hand. As well, there is an associated difficulty with using visual feedback to simultaneously line up the component in two planes (sagittal and frontal), and then fix the guides to the bone. It was desired for our system to have adjustable cutting guides that can be roughly positioned into place, and then sequentially adjusted into its final position while being tracked by the camera. In this way, the planar cuts could be made

perpendicular to the desired mechanical axis, and the anterior-posterior femoral cuts made with the cutting guide aligned with the transepicondylar axis.

1.4.4 Design and integration of the system in one graphical user interface

Finally, in order to test the complete system that is made up of validated algorithms, a graphical user interface (GUI) had to be created that incorporated the whole procedure. It was our goal to produce an interface that is modular, with all options possible to carry out the procedure. There are many valid algorithms for each component, and it is up to the surgeon to decide which order and technique he or she would like to use.

It is our hope that incorporation of validated algorithms in each component of our procedure will produce an overall accurate cost-effective computer-assisted system that can be tested in the future first on cadavers, and then clinically.

1.5 Thesis Overview

In my thesis, I have investigated most of the further requirements of our total knee replacement system so that it can be further tested on cadavers.

Chapter 1: Objectives, background and literature review. Includes a review of the success rates for other computer-assisted systems currently in use.

Chapter 2: Description and testing of two methods to determine the transepicondylar axis defined by the location of the medial and lateral epicondyles. I evaluate a convex-hull and sphere-fit method for variability in the mediolateral and anterioposterior locations of the femoral knee centre (contributing to mechanical axis alignment) and for proper rotational alignment of the femoral component.

Chapter 3: Description and testing of an ellipse-fit method to determine the tibial knee centre based on proper bone coverage. I evaluate this method for mediolateral and anteroposterior variability and bias from other techniques.

Chapter 4: Evaluation and kinematics of a cutting guide that has been developed and designed by another group for use in this system. This cutting guide is for distal femoral and proximal tibial cuts only. I use an optoelectronic system to quantify its accuracy and repeatability.

Chapter 5: Description of the integrated system designed in a Matlab GUI. The modular system can be demonstrated on a sawbones model, with future use for validation or testing of algorithms on cadavers. Includes changes and recommendations from the evaluation of an expert orthopaedic surgeon.

Chapter 6: Summary of thesis, conclusions, and direction of future work.

Appendix A: Details of the convex hull algorithm used in determining medial and lateral epicondylar estimates.

Appendix B: Conference publication on a pilot study on wooden model involving the convex-hull algorithm: A plane probe repeatably identifies anatomical features in computer assisted total knee replacement surgery. Third Annual Meeting of Computer Assisted Orthopaedic Surgery (CAOS) – International - June 2003 – Marbella, Spain. (Abstract/Poster)

Appendix C: In-house technical details of the overall computer-assisted total knee replacement program created.

Not specifically addressed in this thesis are the manufacture, validation and associated algorithms of an adjustable cutting guide for the anterior-posterior femoral cut. As well, the alternative method of alignment by soft-tissue balance (Illsley, 2002) has not yet been integrated into the overall system. Using computer guidance to implant the patella component is also not addressed in this thesis.

1.6 References:

Bathis, H., Perlick, L. Luring, C., Kalteis, T., and J. Grifka (2003) Results of the BrainLAB CT-free navigation system in total knee arthroplasty. In Langlotz, F, Davies, B.L., and A. Bauer (Eds): *3rd Annual Meeting of CAOS-International Proceedings*: 20-21.

Berger, R.A., Rubash, H.E., Seel, M.J., Thompson, W.H., and L.S. Crossett (1993) Determining the rotational alignment in total knee arthroplasty using the epicondylar axis. *Clin Orthop* (286): 40-7.

Chauhan, S.K., Clark, G.W., Lloyd, S.J., and J.M. Sikorski (2003a) A comparative study of computer navigated knee arthroplasty versus a conventional technique. In Langlotz, F, Davies, B.L., and A. Bauer (Eds): *3rd Annual Meeting of CAOS-International Proceedings*: 50-51.

Chauhan, S.K., Scott, R.G., Lloyd, S.J., Sikorski, J.M., Briedahl, W., and R.A. Beaver (2003b) A prospective randomized controlled trial of computer assisted vs conventional

knee replacement. In Langlotz, F, Davies, B.L., and A. Bauer (Eds): *3rd Annual Meeting of CAOS-International Proceedings*: 52-53.

Churchill, D. L., Incavo, S. J., Johnson, C. C., and B.D. Beynnon (1998) The transepicondylar axis approximates the optimal flexion axis of the knee. *Clin Orthop* (356): 111-118.

Confalonieri, N., Saragaglia, D., Picard, F., Cerea, P., and K. Motavalli (2000) Computerised OrthoPilot system in arthroprosthesis surgery of the knee. *J Orthopaed Traumatol* **2**: 91-98.

Confalonieri, N., Cerea, P.,Motavalli, K., and A. Manzotti (2002) The computer navigation system in TKA – Three years experience with OrthoPilot. *2nd Annual Meeting of the International System for Computer Assisted Orthopaedic Surgery and CAOS Surgical Academy,* 19-23 June, Santa Fe, New Mexico, USA: 175-178.

Cooke, T.D.V., Kelly, B., and J. Li (1998) Prosthetic reconstruction of the arthritic knee: considerations for limb alignment, geometry and soft tissue reconstruction. *Knee* **5:**165-174.

Dalury, D. (2001) Observations of the proximal tibia in total knee arthroplasty. *Clin Orthop* (389): 150-155.

Delp, S.L., Stulberg, D.S., Davies, B., Picard, F., and F. Leitner. (1998) Computer assisted knee replacement. *Clin Orthop* (354): 49-56.

Donnelly, W., Rimmington, T.D., Crawford, R., Whitting, K.A., and I. Schleicher (2003) Radiographic alignment with and without the aid of a knee navigation device. In Langlotz, F, Davies, B.L., and A. Bauer (Eds): *3rd Annual Meeting of CAOS-International Proceedings*: 94-95.

Hart R., Janecek, M., and P. Bucek (2003) Kinematic navigation of the total knee replacement – The prospective randomised radiological study. In Langlotz, F, Davies, B.L., and A. Bauer (Eds): *3rd Annual Meeting of CAOS-International Proceedings*: 134-135.

Illsley, S.G. (2002) Intraoperatively measuring ligamentous constraint and determining optimal component placement during computer-assisted total knee replacement. MASc Thesis. University of British Columbia, Vancouver, B.C.

Inkpen, K.B. (1999) *Precision and accuracy in computer-assisted total knee replacement.* MASc Thesis. University of British Columbia, Vancouver, B.C.

Jeffcote, B. and D. Shakespeare (2003) Varus/valgus alignment of the tibial component in total knee arthroplasty. *Knee* **10** (3): 243-247.

Jeffery, R., Morris, R., and R. Denham. (1991) Coronal alignment after total knee replacement. *J Bone Joint Surg Br* **73-B** (5): 709-714.Jenny, J., and C. Boeri (2001) Computer-assisted implantation of total knee prostheses: A case-control comparative study with classical instrumentation. *Comp Aid Surg* **6** (4): 217-220.

Jerosch, J., Peuker, E., Phillips, B., and T. Filler (2002) Interindividual reproducibility in perioperative rotational alignment of femoral components in knee prosthetic surgery using the transepicondylar axis. *Knee Surg Sports Traumatol Arthrosc* **10** (3): 194-7.

Kiefer, H., Langemeyer, D., Schmerwitz, U., and F. Krause (2001) Computer-aided knee arthroplasty versus conventional technique – first results. *Comp Aid Surg* **6** (2): 111-130.

Kiefer, H., Nagel, J., Gebhard, F., Schmerwitz, U., Fuckert, O., Keppler, P. (2003a) Mechanical axis deviation after conventional versus navigation of TKA. In Langlotz, F, Davies, B.L., and A. Bauer (Eds): *3rd Annual Meeting of CAOS-International Proceedings*: 188-189.

Kiefer, H., Schmerwitz, U., and O. Fuckert (2003b) Improvement of knee arthroplasty by CT-free navigation technique including soft tissue balancing – a comparative study. In Langlotz, F, Davies, B.L., and A. Bauer (Eds): *3rd Annual Meeting of CAOS-International Proceedings*: 186-187.

Konig, A., and S. Kirschner (2003) [Long term results in total knee arthroplasty] (*In German) Orthopade* **32** (6): 516-526.

Krakow, K.A. and D.S. Hungerford (1991) Sequence of reconstruction and alignment in total knee arthroplasty. In Goldberg VM (ed): *Controversies of total knee arthroplasty.* Raven Press N.Y. Chapter 20.

Krackow,K.A., Phillips, M.J., Bayers-Thering, M., Serpe, L., and W.M. Mihalko (2003) Computer-assisted total knee arthroplasty: navigation in TKA. *Orthopedics* **26** (10): 1017-1023.

Kunz, M., Strauss, M., langlotz, F., Deuretzbacher, G., and W. Ruther (2001) A non-CT based total knee arthroplasty system featuring complete soft-tissue balancing. In Niessen, W., and M, Viergever (Eds): *MICCAI 2001, Lecture Notes in Computer Science* **2208**: 409-415.

Lam, L.O., and D. Shakespeare (2003) Varus/valgus malalignment of the femoral component in total knee arthroplasty. *Knee* **10** (3): 237-241.

Lange, J., Schwartz, P., Mallamo, D., and J. Pearson (2003) Total knee arthroplasty alignment results in patients who underwent knee replacement operations, which were performed using a computer aided surgery alignment system. In Langlotz, F, Davies, B.L., and A. Bauer (Eds): *3rd Annual Meeting of CAOS-International Proceedings*: 200-201.

Leitner, F., Picard, F. Minfelde, R., Schulz, H.J., Cinquin, P., and D. Saragaglia (1997) Computer assisted surgical total knee replacement. In J. Trocacaz, E. Grimson, and R. Mosges (Eds.), *CVRMed-MCRAS Proceedings'97*: 629-637.

Lemaire, P., Piolette, D., Meyer, F., Meuli, R., Dorfl, J., and P. Leyvraz. (1997) Tibial component positioning in total knee arthroplasty: bone coverage and extensor apparatus alignment. *Knee Surg Sports Traumatol Arthrosc* **5**: 251-257.

Lionberger, D., Noble, P., Conditt, M. Thompson, M. and B. Ding (2003) Nuances of navigation – The learning curve in total knee replacement. In Langlotz, F, Davies, B.L., and A. Bauer (Eds): *3rd Annual Meeting of CAOS-International Proceedings*: 214-215.

Martelli, S., and A. Visani (2002) Computer investigation into the anatomic location of the axes of location of the knee. In Dohi, T., and R. Kikinis (Eds) MICCAI 2002. *LNCS* **2489**: 276-283.

Martin, S.D., Scott, R.D., and T.S. Thornhill (1998) Current concepts of total knee arthroplasty *J Orthop Sports Phys Ther* **28** (4): 252:261.

Murphy, S. Goberlie, R., Lyons, C., Herber, C., and G. Goodchild (2002) Applications of surgical navigation to primary TKA. *Poster presented at the 2nd Annual Meeting of CAOS International,* Santa Fe, USA.

Nicholson, P., Sharif, I., and J. McElwain (2002) Total knee joint arthroplasty: A 5 to 10 year follow-up. *J Ir Coll Physicians Surg* **31** (3): 141-144.

Nizard, R. (2002) Computer assisted surgery for total knee artroplasty. *Acta Orthop Belg* **68** (3): 215-230.

Piazza, S.J., Delp, S.L., Stulberg, S.D., and S.H. Stern (1998) Posterior tilting of the tibial component decreases femoral rollback in posterior-substituting knee replacement – a computer simulation study. *J Ortho Res* **16** (2): 264-270.

Plaskos, C. (2002) *Bone sawing and milling in computer-assisted total knee arthroplasty.* MASc Thesis. University of British Columbia, Vancouver, B.C.

Saragaglia, D., Picard, F., Chaussard, C., Montbarbon, E., Leitner, F., and P. Cinquin. (2001) Computer-assisted knee arthroplasty: Comparison with a conventional procedure. Results of 50 cases in a prospective randomised study. *Revue de chirurgie orthopedique* **87**: 18-28.

Sharkey, P.F., Hozack, W.J., Rothman, R.H., Shastri, S., and S. Jacoby (2002) Why are total knee arthroplasties failing today. *Clin Orthop* **404**: 7-13.

Shute C. (2002) *Ankle joint biomechanics applied to computer assisted total knee replacement.* MASc Thesis. University of British Columbia, Vancouver, B.C.

Stindel, E., Briard, J.L., Merloz, P., Plaweski, S., Dubrana, F., Lefevre, C., and J. Troccaz (2002) Bone morphing: 3D morphological data for total knee arthroplasty. *Comp Aid Surg* **7:** 156-168.

Stulberg, S.D., Picard, F., and D. Saragaglia (2000) Computer-assisted total knee arthroplasty. *Opere Techn in Orthop* **10** (1): 25-39.

Stulberg, S.D. and V.K. Sarin (2001) The use of a navigation system to assist ligament balancing in TKR. *CAOS international 2001 First Annual meeting of the International Society for Computer Assisted Orthopaedic Surgery,* Davos, Switzerland.

Stulberg, S.D., Loan, P., and V Sarin (2002) Computer-assisted navigation in total knee replacement: results of an initial experience in 35 patients *J Bone Joint Surg* **84A** (S2): 90-98.

Swank, M.L. (2003) CT based image guided surgery vs conventional intramedullary instrumentation in total knee arthroplasty. In Langlotz, F, Davies, B.L., and A. Bauer (Eds): *3rd Annual Meeting of CAOS-International Proceedings*: 358-359.

Chapter 2: Repeatability in identifying the transepicondylar axis with a plane probe for identification of the rotation axis and femoral knee centre in computer-assisted total knee arthroplasty

2.0 Abstract

Variability in locating the transepicondylar axis (TEA) of the femur leads to malpositioning of the femoral component, which in turn adversely affects the kinematics and stability of the reconstructed knee joint. In order to improve the repeatability of finding the TEA, we developed and tested the use of a plane probe rather than the point probe that has traditionally been used in other landmark-based computer-assisted surgery techniques. Four subjects performed 5 trials and one subject performed 20 trials on a cadaveric knee. Two alternative algorithms, a convex-hull based algorithm and a sphere-fit based algorithm were developed, and used to determine medial and lateral epicondylar estimates. The algorithms were compared based on intra-operator variability, inter-operator variability, and total variability (SD) in the mediolateral and anteroposterior directions, and ultimately the effect on the rotational variation and knee centre variation that would result for placement of the femoral component. We show that the sphere-fit based method is more repeatable than the convex-hull method, and may be more repeatable than use of the point probe.

2.1 Introduction

2.1.1 Clinical application for repeatably locating the proper rotation axis and knee centre of the femur

Locating the proper flexion/extension axis of the femur in the transverse plane is important for accurate rotational alignment of the femoral component. Current literature suggests that for a total knee replacement procedure, the best approximation of this rotational alignment is lining up the component in the horizontal plane with the transepicondylar axis of the knee, a line that joins the origins of the medial and lateral collateral ligaments (Martelli and Visani, 2002). Hence, most implant manufacturers require the implant to follow this rotational alignment. Errors in placing the component askew to this axis can lead to many consequences affecting the kinematics and stability of the knee joint as will be described.

Locating the femoral knee centre accurately is important in determining the mechanical axis of the femur. This mechanical axis joins the hip centre to the femoral knee centre in the frontal and sagittal planes. Errors in locating the femoral knee centre can lead to varus/valgus errors in the frontal plane, and flexion/extension errors in the sagittal plane.

2.1.1.1 Rotational alignment in the horizontal plane

Accurate rotation of the femoral component in total knee arthroplasty (TKA) is important for (Anouchi et al., 1993; Barrack et al., 2001; Echkoff et al., 1995; Fehring, 2000; Hofmann et al., 2003; Whiteside and Arima, 1995):

- normal patellar tracking.
- symmetrical patellofemoral joint contact.
- neutral varus-valgus positioning in flexion.
- correct rotational alignment of the tibia in extension.
- the avoidance of anterior femoral notching.

Many references have been used to rotationally align the femoral component. These are the surgical and anatomical transepicondylar axis (TEA), posterior condylar axis (PCA), anterior-posterior axis (Whiteside's line), and the balanced flexion gap technique (Olcott and Scott, 2000) (Figure 2.1).

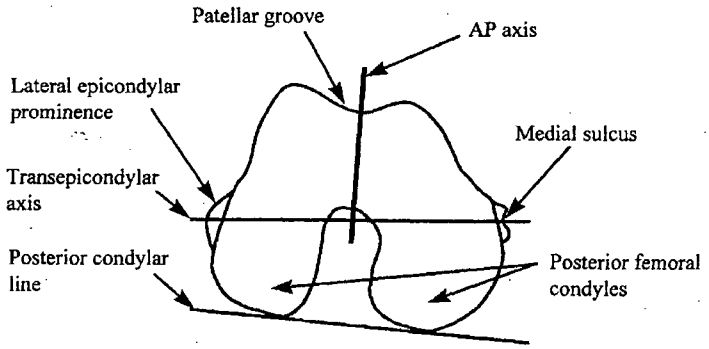

Figure 2.1: Rotational landmarks of the femur – distal-proximal view.
(Inkpen, 1999 – Image adapted from Berger et al., 1993)

These references were mainly developed for use in conventional surgery. The PCA is easy to find with conventional instruments; the anteroposterior (AP) axis is easy to locate (Arima et al., 1995; Katz et al., 2001); and the surgical TEA easy to detect on radiographs

(Berger et al., 1993). However, recent studies have shown that alignment should be parallel to the transepicondylar axis to avoid patellofemoral and tibiofemoral complications (Miller et al., 2001; Scuderi and Insall, 2000). This is because the TEA approximates the optimal flexion axis of the knee (Churchill et al., 1998; Martelli and Visani, 2002), being parallel to the primary centre of rotation of the knee joint (Nordin and Frankel, 1989). Muller (1983) also noted the importance of the TEA as the origin of the collateral ligaments, important in the theory of four-bar linkage for movement around the knee joint. Elias et al. (1990) found a similar relationship stating that the origin of the collateral ligaments is located in the centre of circles created from lateral and medial condyles.

For these reasons, the trend in computer-assisted surgery has been to align the femoral component with the TEA, as most surgeons do not use the other references due to their variation in angle from the TEA (Olcott and Scott, 2000; Tanavalee et al., 2001). While on average the anterior-posterior axis (Whiteside's Line) and PCA should be 90 degrees and 3 degrees respectively from the TEA, this is not always the case; Whiteside's line deviates as much as 95 degrees from the TEA, and the PCA-TEA angle varies as much as 7 degrees (Tanavalee et al., 2001). These references are usually only used if the TEA is difficult to locate.

The TEA is also important for alignment in revision surgery or severely degenerated knees with bone loss because it is the only landmark not defined by a diseased articular surface or removed in previous surgery (Tanavalee et al., 2001).

2.1.1.2 Frontal plane alignment

Frontal/Coronal plane alignment of the femoral component is crucial in total knee replacement surgery and numerous studies have correlated valgus/varus malalignment (Figure 2.2) to early failure (Jeffery et al., 1991; Lotke and Ecker, 1977; Moreland, 1988). In this plane, the femoral component should be placed perpendicular to the mechanical axis of the knee, with the centre of the component on the femoral knee centre (Dorr and Boiardo, 1986). This ensures an equal balance of loads in the lateral and medial compartment. If the centre of the femoral implant is located medial/lateral to the true tibial knee centre, the mechanical axis passes medial/lateral to the centre of the knee

and creates a moment arm acting to increase the force balance between the medial and lateral compartment (Tetsworth and Paley, 1994). It has been shown that as little as 3 degrees of varus deformity transfers 90% of the knee force through the medial compartment. This malalignment alters the stress distribution on the contact surface of the implant-bone interface and increases the soft tissue tension at the knee joint resulting in an accelerated breakdown at the bone-prosthesis or bone-cement interface (Andriacchi, 1994).

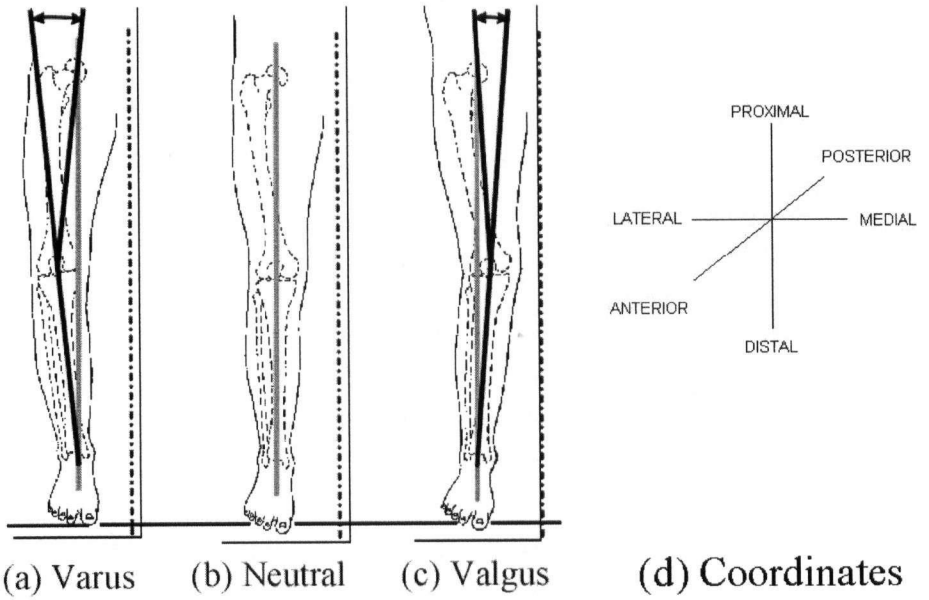

Figure 2.2: Frontal plane alignment errors.
a) Varus malalignment, the mechanical axis shifts medially
b) Neutral alignment, the mechanical axis passes through the knee centre
c) Valgus malalignment, the mechanical axis shifts laterally
d) Anatomic co-ordinate system, anterior direction out of page (Plaskos, 2002)

In general, the accepted window in frontal plane alignment is typically 3 degrees. An angle of more than 3 degrees increases the incidence of loosening from 3% to 24% (Jeffery et al., 1991). This component loosening represents about 24.1% of failed total knee arthroplasty (Sharkey et al., 2002). In particular, radiographic studies have shown varus alignment to be more detrimental, with worse reported outcomes and more cases resulting in premature aseptic loosening (Insall, 1985).

2.1.1.3 Sagittal plane alignment

The femoral knee centre in the sagittal plane influences the flexion/extension alignment of the femoral component. Flexion/extension malalignment can result in abnormal knee kinematics, soft tissue imbalances, and component subsidence (Hofmann et al., 1991). The range of motion of the leg is altered if the femoral and tibial components do not line up due to these errors. A distal femoral error in this plane also results in incorrectly referenced anterior and posterior resections determined by the TE axis as these cuts are usually keyed by the location of the distal cutting plane determined by the mechanical axis. This may then lead to notching of the anterior femoral cortex or fixed flexion contractures.

2.1.2 Current approaches in computer-assisted TKA

Image-free systems using landmarks currently on the market (OrthoPilot, Stryker Knee Navigation, SurgiGATE) use anatomic digitization to determine the TE axis. Surgeons use a point probe to digitize the lateral and medial condyles (Stulberg et al., 2002). They typically palpate the epicondyles, and place the tip of a point probe on the location that they judge to be the most extreme peak (Figure 2.1). An optical localizer detects infrared light emitted by diodes in the point probe, and returns the pointer's tip location.

The midpoint of this TE axis may be considered to be the mediolateral femoral knee centre (Kunz et al., 2001). Published literature on the OrthoPilot also states that identification of the knee centre occurs kinematically by flexing and extending the knee from 0 to 90 degrees, and rotating the tibia on the femur at 90 degrees knee flexion. This manipulation creates a plane that the femoral component should be aligned with. It is unclear what additional algorithms are used in this manipulation and whether this value is compared to the one calculated by the midpoint of the TE axis or uses other geometric references.

2.1.3 Limitations of current approaches

A recent study performed by three surgeons on the identification of the transepicondylar axis with a pointed instrument (in this case a hypodermic needle) used on Thiel-embalmed specimens showed high inter-operator variability in determining this axis, with rotational discrepancy as high as 23° (Jerosch et al., 2002). Another study that used a

Stryker Navigation system to register epicondylar co-ordinates digitized with a point probe showed a rotation range as high as 18°, with the selected points located in an area of 278 mm^2 around the medial epicondyles and an area of 298 mm^2 around the lateral epicondyles (Kessler et al., 2003). Fuiko et al. (2003) also reported a rotation range of 11° with landmarks collected using a photogrammetric system. In addition, the OrthoPilot's use of kinematic manipulation of a pathological knee may not truly represent the desired frontal plane for a proper knee centre.

2.1.4 Digitizing with a plane probe

To reduce the variability in identifying the TEA with a point probe, we propose to use a plane probe (Figure 2.3). With a plane probe one can rock the flat surface tangent to the epicondyles.

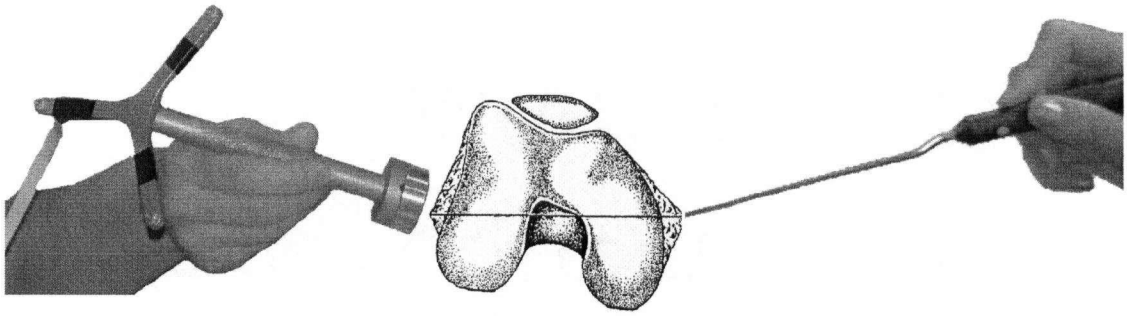

Figure 2.3: Diagram of the plane probe (left), and the point probe (right).

This technique was formulated for four reasons:

- A plane probe is easier and faster to use that a point probe.
- The technique eliminates the need for the surgeon to visually distinguish/palpate an extreme point.
- With a plane probe redesign, the technique can be used in minimally invasive surgery when the epicondyles are not exposed.
- Planar tangents essentially map out the surface of the condyles.

We propose to use this method in conjunction with two different algorithms in order to determine the transepicondylar axis. These algorithms are a convex-hull algorithm and a sphere-fit algorithm (Explained in Section 2.2.3.1 and 2.2.3.2 respectively).

Figure 2.4 shows the three different techniques, the original point probe estimates, the convex-hull algorithm, and the sphere-fit algorithm and how they compare with respect to two criteria: robustness and use of assumptions. For a particular application, an ideal place for a particular method is the top left hand corner. This means that the method is assumption free and robust (based on many data points).

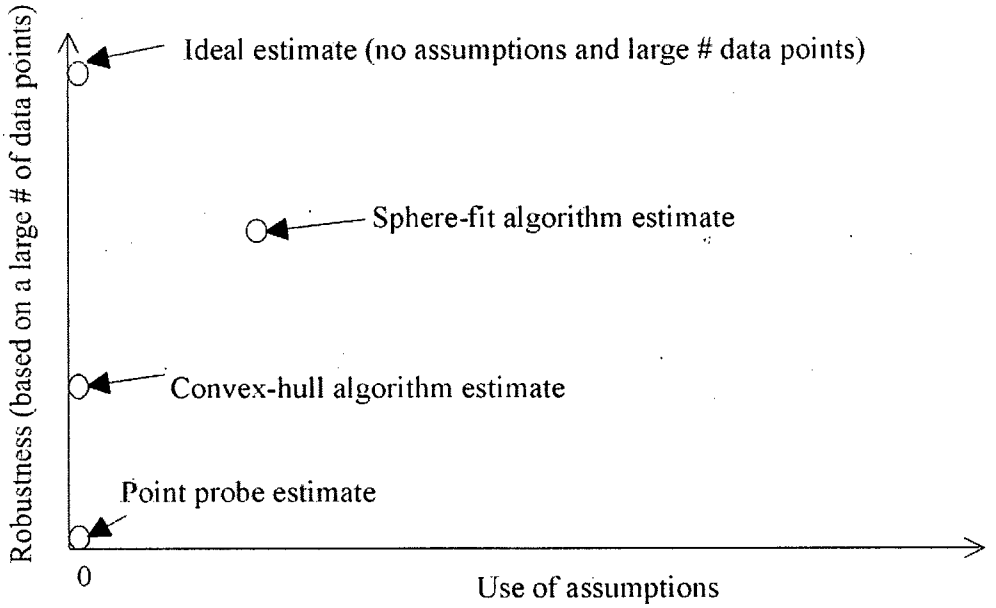

Figure 2.4 shows a comparison of the three different techniques.
The original point probe estimates, the convex-hull algorithm, and the sphere-fit algorithm are compared with respect to two criteria: robustness and use of assumptions. For a particular application, an ideal place for a particular method is the top left hand corner. This means that the method is assumption free and robust (based on many data points).

The point probe estimates currently used by other computer-assisted systems falls on the bottom right hand side based on a small number of readings without any assumptions. The convex-hull algorithm is based on more data points than the point probe but the nature of the algorithm can eliminate a percentage of the input points. The sphere-fit algorithm is based on more data points than the point probe and convex hull algorithm, however it assumes that the condyles can be fitted by a sphere. It was not known which algorithm would provide more repeatable results in determining the epicondyles making up the transepicondylar axis.

We hypothesized that the transepicondylar axis determined by these identification techniques is more repeatable than those obtained by a point probe.

2.1.4 Purpose of study

In order to determine if the plane probe produces more repeatable condylar tip estimates than other computer-assisted techniques, we conducted an in-vitro study to compare original point-probe digitization methods to the planar probe sphere-fit and convex hull methods. Specifically, we addressed the research question: which method most reliably predicts the location of the epicondyles with respect intra-, inter-operator, and total variability, and how does the repeatability of these methods compare to that of the point probe method?

2.2 Design and methods

2.2.1 Probe design

A probe was built previously in our lab by a former graduate student (Kevin Inkpen). It consists of a circular planar surface 3.8 cm in diameter instrumented with a triad of infrared emitting diodes (IREDs) arranged in an equilateral triangle 120 mm on a side (Figure 2.5). This triad defines a local reference frame in which the equation describing the location of the planar contact surface may be defined.

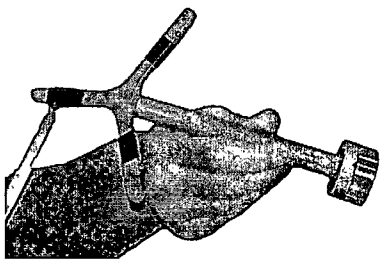

Figure 2.5: Photo of the plane probe used in this study.

This equation of the plane in the plane probe reference frame was calibrated by using a point probe to digitize the planar probe surface in the plane probe reference frame. A plane was fit to these points using a multidimensional non-linear minimization.

The cost function is the sum of squared normal distances between the points (d_i) and a point on the candidate plane ($d_{estimate}$):

$$Q_1 = \sum_{i=1}^{Npoints} (d_i - d_{estimate})^2$$

These planes in the plane probe reference frame are then transformed into the other reference frames (such as the femur or tibia) by first transforming the normal, and then a point on the plane to the other reference frame.

2.2.2 Measurement equipment, subject information and procedure

We performed tests on an intact fresh cadaveric knee from a complete person (76 yr old female) in a simulated computer-assisted TKA setting. An experienced surgeon drilled a hole through the skin into the femur approximately 15cm proximal to the knee joint. He firmly inserted a bone pin in the hole, and securely attached a marker array to the pin (Figure 2.6). This created a fixed reference frame for measurements made on the femur. He then made a midline incision on the knee, approximating that performed in a total knee replacement surgery, and exposed the knee joint.

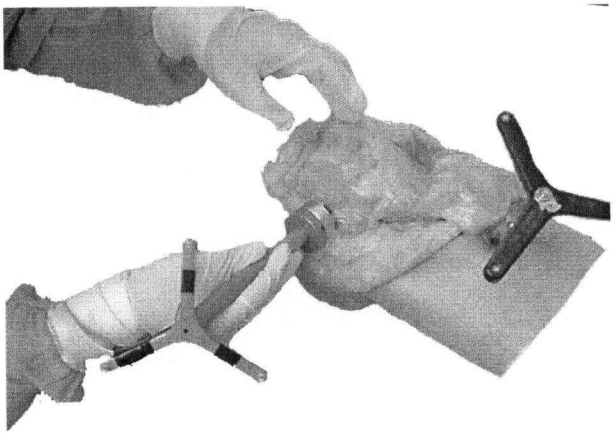

Figure 2.6: Photo using the plane probe to collect tangential planes on the lateral epicondyle of a left cadaveric knee.
(Photo from a pilot study where the quadriceps tendon was snipped)

We used a Flashpoint 5000 localizer (SD of noise 0.35 mm RMS; Boulder Innovator Group, Boulder, CO, USA) to measure the planar face locations while an operator rotated the probe in a spiral fashion on first the medial epicondyle, then the lateral epicondyle (Figure 2.6). The operator was careful to always maintain contact between the planar face and the area of the epicondyles. We performed this manipulation for 5s in order to gather a minimum of 100 sample planes. In order to measure inter-operator variability, five operators performed the procedure 5 times. A single operator (the author) also repeated the procedure an additional 15 times (20 total). The five operators were 27±3 years old, with no prior experience in knee surgery or with the plane probe.

An initial estimate of the medial and lateral epicondylar locations is needed for both algorithms. The accuracy of this initial estimate is not critical. Each operator used a standard 135 mm point probe to digitize the locations of the medial and lateral epicondyles on the cadaveric knee specimen. Each of the five operators palpated the condyles and then digitized what they perceived to be the most extreme point on the medial and lateral side.

2.2.3 Data analysis

The plane probe and point probe data collected in the femoral array frame is used to calculate extrema estimates to define the transepicondylar axis.

2.2.3.1 Convex-hull based algorithm

Planes collected tangent to the epicondyles can map out the surface of the epicondyles without significant error if a large number is collected. In this algorithm, the 3-dimensional planar tangents acquired are processed and entered into a convex hull algorithm.

This algorithm is used because the intersection of half-spaces[1] about an origin is equivalent to the convex hull of the points in dual space[2] (Barber et al., 1996). In dual space, what was once infinity becomes the origin. This reduces the complexity of the problem. Once the tangential planes are dualized, the convex hull of these points around the origin can be easily computed.

[1] half-space - portion of n-dimensional space obtained by removing that part lying on one side of an (n-1) dimensional hyperplane

[2] dual space – an alternate geometric form that uses the unique representation of converting planes to points or points to planes in order to view problems in a different way and hence use alternative algorithms

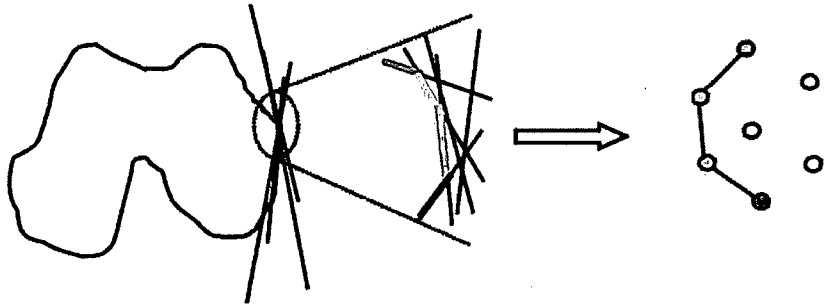

Figure 2.7: Diagram of intersection of half-spaces - and how a convex hull is the dual of this.

Figure 2.7 shows a diagram of the intersection of half-spaces (in 2D). If each epicondyle of the knee is imposed on this diagram, one can see how application of this algorithm maps out the surface of the epicondyle. The diagram (and algorithm) is easily extended into three dimensions. A complete explanation of the convex hull algorithm for this application can be found in Appendix A.

The planar tangents were collected with respect to the femoral reference frame (f). We define another co-ordinate frame (o) with the origin as the midpoint between the estimate medial and lateral epicondyles collected with the point probe, and the +z $axis_{bone}$ as the vector joining the midpoint to the estimate epicondyle of interest. We transform all tangents into this new co-ordinate frame (o). The normal to each plane was then checked to ensure that all were pointed in the same +z $axis_{bone}$ direction.

We apply a duality transform to the transformed planes by the following equation:

$$Ax + By + Cz + D \Leftrightarrow \left(-A/C, -B/C, D/C\right)$$

These resulting points can then be entered into a 3D convex hull algorithm. We use the Matlab function *convhulln* that uses the Quickhull algorithm (Barber et al., 1996) for computing the convex hull.

A convex hull of a set of points is the smallest convex set that contains all the points (Figure 2.8). The algorithm starts with an initial simplex[3], and expands for each visible point seen by each face. A simplified 2D version of the algorithm is illustrated in Appendix A.

[3] simplex – smallest possible polytope for any given space (eg. a triangle in 2D; tetrahedron in 3D)

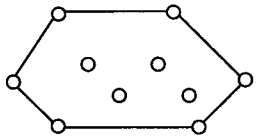

Figure 2.8: Diagram of a convex hull of a set of points.

In 2D, the algorithm returns the indices to vertices of the lines formed for the convex hull. In 3D, the convex hull algorithm returns the vertices of the triangular facets of the points that form the convex hull (Barber et al., 1996). Therefore three indices for vertices are returned for each facet of the convex hull.

These points that make up the triangular facets are then used to create planes in the dual space. The normals of these planes are checked with the +z axis to determine if they lie on the upper or lower hull. Only lower hull planes are kept, as the upper envelope of intersection points and halfspaces define the surface. When this lower hull plane is dualised back to a point, this point actually represents the intersection of three planes in the primal space.

These points were considered to be candidate epicondylar tips (Figure 2.9). In order to calculate the distance between the candidate points, we projected them onto a horizontal plane. This method is an extension to 3D of a 2D scheme used in CT analysis of the TEA (Uehara et al., 2002; Yoshino et al., 2001). In CT scans, once the surface has been mapped out, horizontal slices (transverse plane) are examined in order to determine the most extreme points of the condyles, thus defining the TE axis.

In this case, we defined a body frame by digitizing a point in the centre of the knee (origin), a point medial to that representing the x axis, and another defining the xy plane. The most widely separated pair of points on the medial and lateral convex hulls in this plane was taken to define the transepicondylar axis (in its original location).

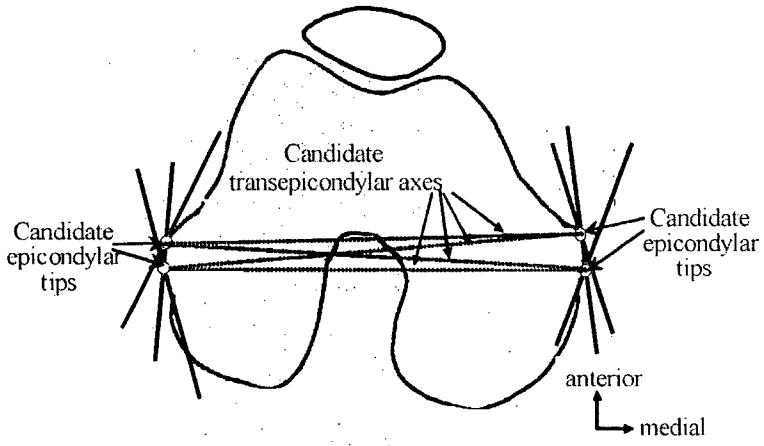

Figure 2.9: Application of convex hull algorithm to determine the transepicondylar axis.

The mean location of the medial and lateral epicondylar estimates was compared for each operator. We then calculated a pooled mediolateral, and a pooled anteroposterior intra-operator variability in identifying the transepicondylar axis. We evaluated inter-operator variability based on the means of each operator, and calculated total variability using the first 5 trials from each operator.

In order to compute a pooled intra-operator variability, we assumed the same variance but different bias for each operator. We computed the standard deviation (SD) for all the medial and lateral epicondylar estimates by:

$$\overline{SD} = \left.\sum_{p=1}^{5}\left(\sum_{i=1}^{n(p)}\left(x_{p,i}-\bar{x}_p\right)^2\right)\right/\sum_{p=1}^{5}n(p)-5$$

where p is each subject and n(p) is the number of estimates per subject (40 trials - 5 trials from 4 operators, and 20 trials from 1 operator). The 95% confidence interval (CI) on this standard deviation was then computed using m-5 degrees of freedom, where m is the total number of estimates from all subjects.

$$LowerLimit = \sqrt{\frac{(m-5)\sigma^2}{\chi^2_{m-5,1-\alpha/2}}}, UpperLimit = \sqrt{\frac{(m-5)\sigma^2}{\chi^2_{m-5,\alpha/2}}}$$

Intra- and inter- and total angular variability and midpoint frontal and sagittal plane variability was also calculated for applications to rotational alignment and the femoral

knee centre. For this angular variability, the intra-operator variability was computed for each individual operator.

2.2.3.2 Sphere-fit based algorithm

The sphere-fit algorithm assumes that planes collected tangential to the epicondyles can be fitted to a sphere, as the epicondyles can be considered spherical in shape (Elias et al., 1990; Kurosawa et al., 1985) with the femoral attachments of the collateral ligaments in the centre.

We entered the tangential planes into a non-linear least squares algorithm (Matlab 6.0 'lsqnonlin') that minimises the difference in distance between each plane and an initial point, and the distance between the average of all the planes and that point. The initial point for the optimization was the midpoint of the estimate medial and lateral epicondyles digitized with the point probe.

The cost function for this optimization is:

$$Q_2 = \sum_{i=1}^{Nplanes} \left(d_i - d_{average}\right)^2$$

d_i = distance between each plane and the initial point.
$d_{average}$ = distance between average of all planes and that point.

This is evaluated for each epicondyle. The absolute tolerance on the function value was $1*10^{-6}$. When the maximum number of evaluations was set to 2000, all procedures converged prior to reaching this number of function evaluations. We did not perturb the solution and re-solve to verify that our solution was a global rather than local minimum, but this problem tends to occur in higher-dimensional optimizations where the data is comparatively noisy. Since the sphere-fitting problem is set in only three dimensions, and since previous pilot studies suggested good repeatability within operators, we do not believe that a multiple local minima problem exists.

A unit vector and distance was then calculated between the two epicondyles. The radius of each fitted sphere was then added in the positive and negative direction of the unit vector to determine the actual medial and lateral epicondylar locations (Figure 2.10).

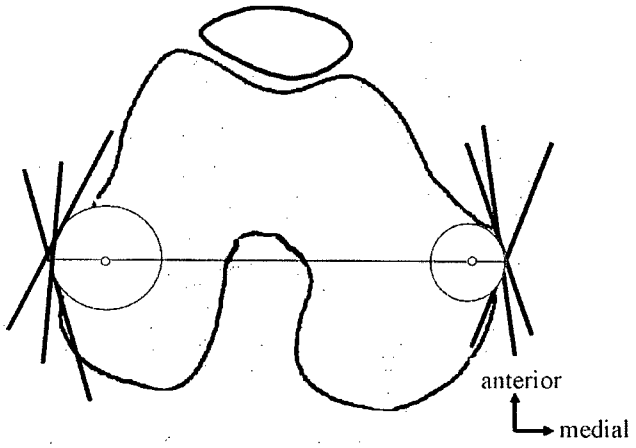

Figure 2.10: Application of sphere-fit algorithm to determine the transepicondylar axis. This is a 2D representation of a 3D algorithm

The mean location of the medial and lateral epicondylar estimates was compared for each operator. We then calculated a pooled intra- mediolateral and anteroposterior variability, used the means to evaluate inter-operator variability, and calculated total variability based on the first 5 trials from each operator. We computed the pooled intra-operator variability based on the same calculations stated for the convex hull algorithm estimates (Section 2.2.3.1). Inter-, intra- and total angular variability and midpoint frontal and sagittal plane variation was also calculated for applications to rotational alignment and femoral knee centre. F-test comparisons were made between the resulting standard deviations of this method compared to the convex-hull method.

2.2.3.2.1 Bootstrapping of the sphere-fit algorithm

In order to further investigate the robustness of the sphere-fitting algorithm, we incorporated a bootstrapping approach into our analysis. Bootstrapping is a process of generating estimates for statistical approaches by direct computation rather than analysis. This technique uses packets of data based on random resampling of original data (Montecarlo technique) with replacement (DiCiccio and Efron, 1996).

We used this bootstrapping technique to assess:

- the bias differences between each operators trials (intra-operator variability).
- the bias differences between the operators (inter-operator variability).

These assessments are dependent on the way we pool the original data for resampling with replacement.

To determine a standard deviation for each operator, we bootstrapped each trial by randomly picking 100 planes from each set of planes 1000 times. The sphere-fit algorithm was then used to find the medial and lateral epicondyles. A standard deviation and associated 95% confidence interval was calculated for these 5000 (1000/operator) medial and lateral epicondylar estimates.

To assess the overall variability of each operator, we put all the planes from the 5 trials of each operator together (~500 planes), and randomly drew 1000 sets of 100 planes to use in the sphere-fit technique. We then computed the standard deviation and 95% confidence interval. This was repeated for all operators. For each operator, we used F-tests to compare this standard deviation (based on 1000 epicondylar estimates) to that computed by the agglomeration of medial and lateral epicondyle estimates from bootstrapping the individual trials (5000 epicondylar estimates). This comparison shows us whether any operator had bias differences in the collecting of planes at each trial.

To assess bias differences between operators, we combined all the planes from all trials of all the subjects (~2500 planes), and random sets of 100 planes were resampled 1000 times. The sphere-fit algorithm was used to find the medial and lateral epicondyle locations, and the standard deviation was calculated for the bootstrapped trials. The increase in standard deviation would tell us the degree of bias differences between the operators. We then compared the variability from bootstrapping all the subjects' planes (1000 medial and lateral epicondyle estimates) to the inter-operator variability from the means of the individual bootstrapped trials computed earlier (means from 1000 bootstrapped trials/trial/operator ~ 5 medial and lateral epicondyle estimates). Though the number of trials varied for the comparison, the 95% confidence interval was also compared, taking into account the differences in degrees of freedom for each comparison.

Standard F-tests were used to compare all variances. For the bootstrapping approach, pairs of epicondylar locations were eliminated if there was no convergence for locating the centre of either sphere.

2.3 Results

2.3.1 Convex Hull Algorithm

The mean locations and range of the medial and lateral epicondylar estimates for each operator using the convex hull method can be seen in Figure 2.11.

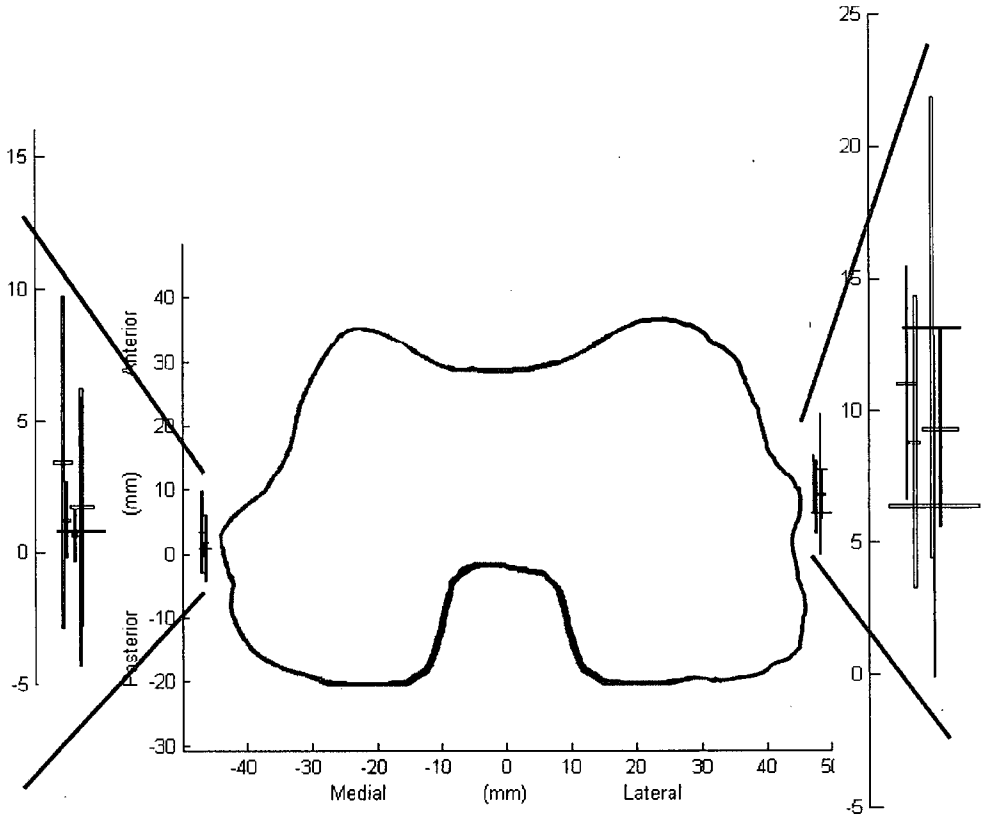

Figure 2.11: Mediolateral and anteroposterior locations of the mean medial and lateral epicondylar estimates for the five operators determined using the convex hull method.
Vertical bars show the range in the anteroposterior direction and horizontal bars show the range in the mediolateral direction. The axes are expanded on both sides to show more detail.

We see that there is a larger range in the anteroposterior direction over the mediolateral direction for the locations of the medial and lateral epicondylar estimates. The range in the anteroposterior direction is also larger for the lateral epicondylar estimates over the medial epicondylar estimates in this study.

The mean location of all estimates, and the pooled intra-operator variation and associated 95% CI on the SD are shown in Figure 2.12.

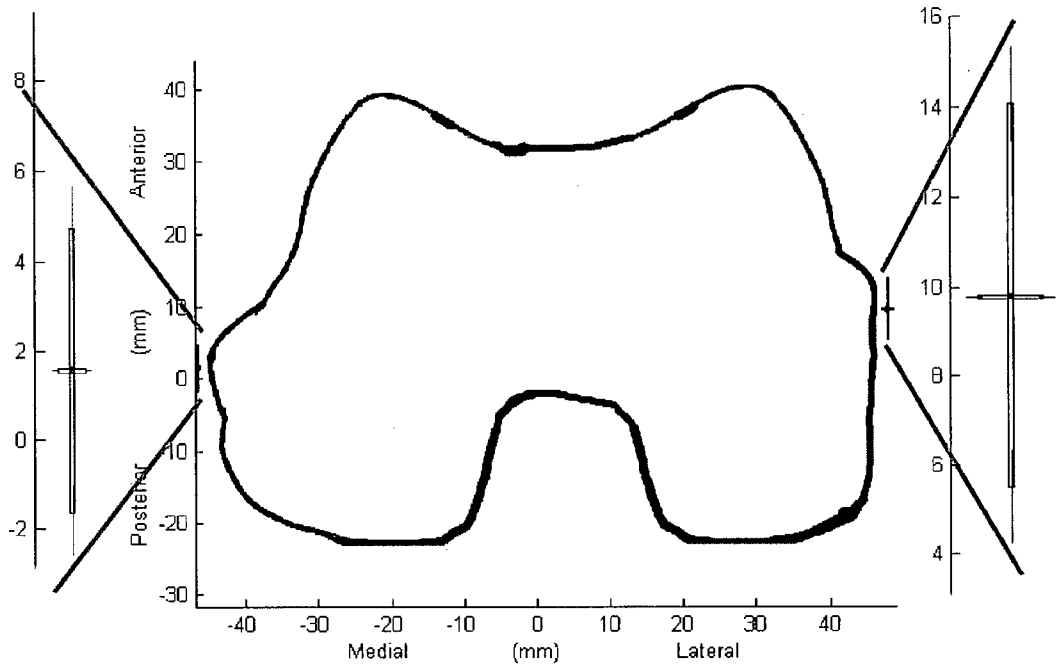

Figure 2.12: Mean epicondylar estimate location for the convex-hull method.
Horizontal bars represent the pooled standard deviation in the mediolateral direction computed for 40 trials, and vertical bars represent the pooled standard deviation in the anteroposterior direction for the 40 trials. Lines represent 95% CI on the SD. [40 trials = (4 operators*5 trials + 1 operator*20 trials)].

The pooled intra-operator, inter-operator, and total variability using the convex-hull method for determining the medial and lateral epicondylar estimates are shown in Table 2.1. In terms of locating the femoral knee centre, this translates to a pooled intra-operator variability of 0.4 mm and 2.7 mm SD in the mediolateral and anteroposterior directions respectively, and an inter-operator variability of 0.2 mm and 0.9 mm SD in the mediolateral and anteroposterior directions respectively. Total variability for the femoral knee centre was calculated using 5 trials from the four operators and the first 5 trials from the fifth operator (25 trials total), and was 0.4 mm and 2.8 mm SD in the mediolateral and anteroposterior directions respectively.

Table 2.1: Mediolateral (ML) and anteroposterior (AP) variability for the medial and lateral epicondyles using the convex-hull method.
All measurements in mm. 95% confidence interval (CI) on each standard deviation is shown in brackets.

Pooled Intra-Operator Variability	ML SD (95% CI)	AP SD (95% CI)
Lateral Epicondyle	0.7 (0.6-0.9)	4.3 (3.5-5.6)
Medial Epicondyle	0.3 (0.25-0.4)	3.2 (2.6-4.2)
Knee Centre	0.4 (0.3-0.5)	2.7 (2.2-3.5)
Inter-Operator Variability	**ML SD (95% CI)**	**AP SD (95%CI)**
Lateral Epicondyle	0.5 (0.3-1.3)	2.3 (1.4-6.5)
Medial Epicondyle	0.3 (0.2-0.8)	1.0 (0.6-2.9)
Knee Centre	0.2 (0.1-0.6)	0.9 (0.5-2.5)
Total Variability	**ML SD (95% CI)**	**AP SD (95% CI)**
Lateral Epicondyle	0.8 (0.6-1.0)	4.9 (3.8-6.8)
Medial Epicondyle	0.5 (0.3-0.6)	2.3 (1.8-3.2)
Knee Centre	0.4 (0.3-0.5)	2.8 (2.2-3.9)

The pooled mediolateral intra-operator variability for the convex hull method for the lateral epicondylar estimates was significantly higher ($p<0.05$) than medial epicondylar estimates. However, there was no significant difference in the anteroposterior variability using this method. There was also no significant difference in inter-operator variability comparing the medial and lateral epicondylar estimates.

The total variability for the lateral epicondylar estimates using the convex-hull method was significantly higher ($p<0.05$) than the medial epicondylar estimates in both mediolateral and anteroposterior directions.

Each medial epicondylar estimate was paired with every other lateral epicondylar estimate to determine rotational alignment variability. Figure 2.13 shows the computed rotation angles for each operator from a standard axis. The intra-operator rotational variability ranged from 1.7° SD (95% CI from 1.4 to 2.4) to 4.4° SD (95% CI from 3 to 8.5), the inter-operator variability was 1.5° SD (95% CI from 0.9 to 4.3) and the total rotational variability was 2.9° SD (95% CI from 2.6 to 3.4). The range of rotational alignment seen for all operators was 15°..

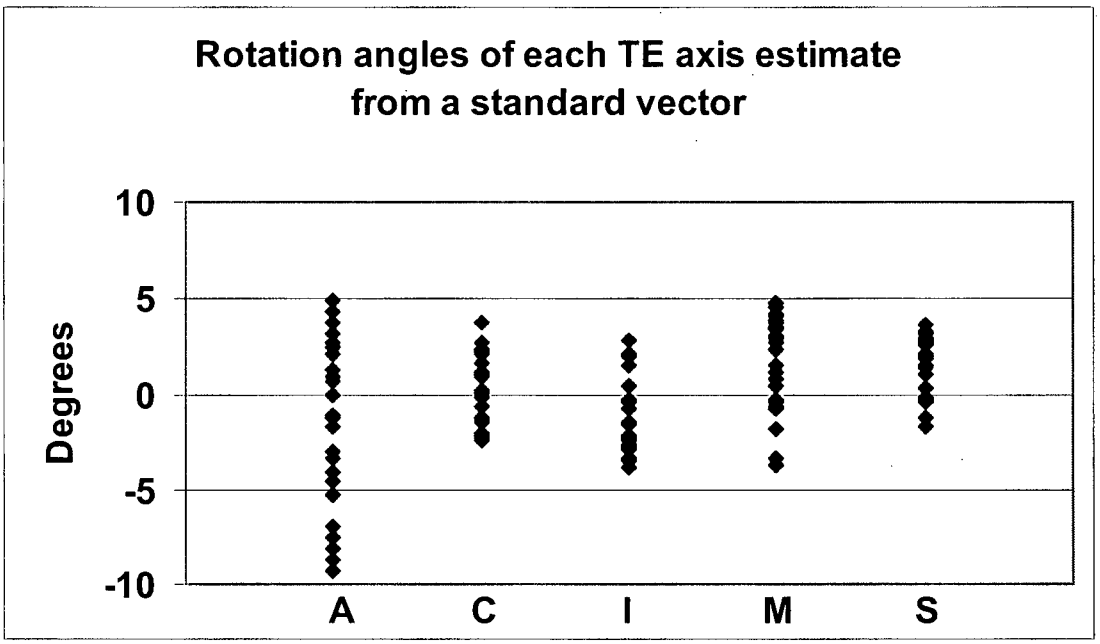

Figure 2.13: Rotation angles for each TE estimate from each operator using the convex hull method. Graph shows the range of 25 values from each operator as well as the bias between operators. [25 values = 5 medial paired with all 5 lateral].

2.3.2 Sphere-fit algorithm

The mean bias locations of the medial and lateral epicondylar estimates, and range for each operator using the sphere-fit method can be seen in Figure 2.14.

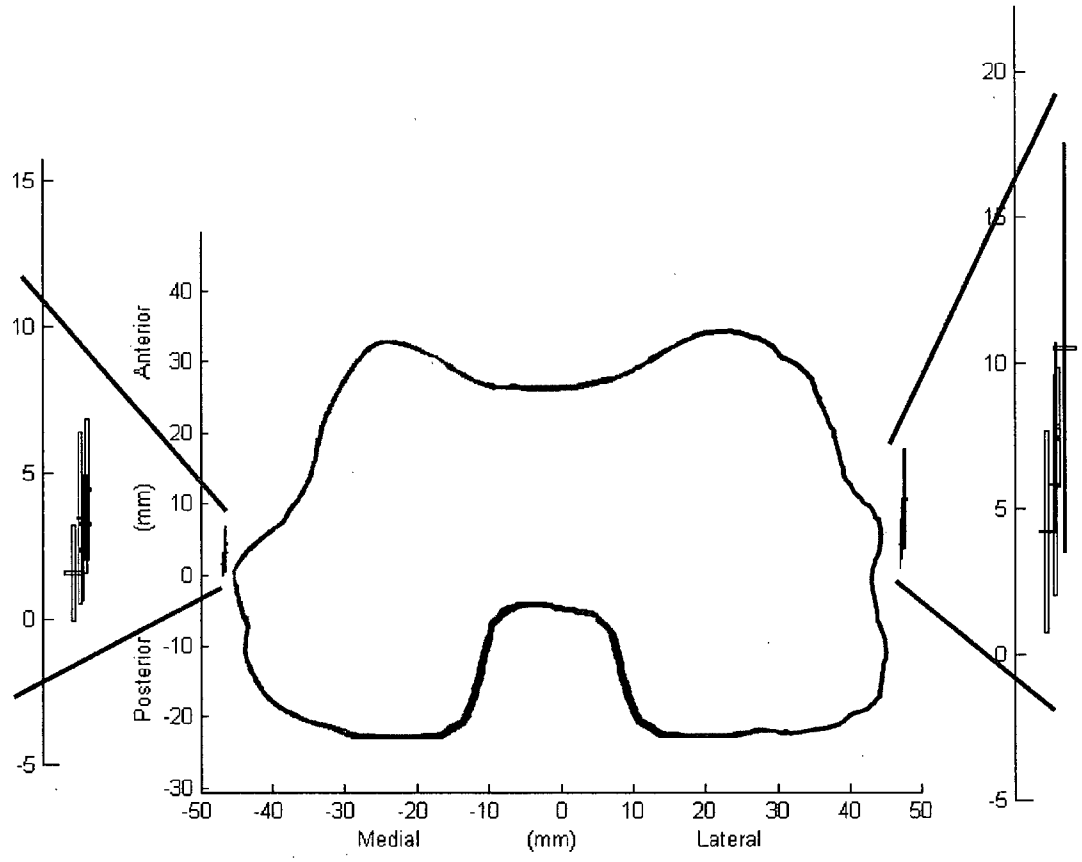

Figure 2.14: Mediolateral and anteroposterior locations of the mean medial and lateral epicondylar estimates for the five operators determined using the sphere-fit method.
Vertical bars show the range in the anteroposterior direction and horizontal bars show the range in the mediolateral direction.

We see that there is also a larger range in the anteroposterior direction over the mediolateral direction for the locations of the medial and lateral epicondylar estimates, similar to results of convex-hull method. The range in the anteroposterior direction is also larger for the lateral epicondylar estimates over the medial epicondylar estimates in this study.

The mean location of all estimates, and the pooled intra-operator variation and associated 95% CI on the SD is shown in Figure 2.15.

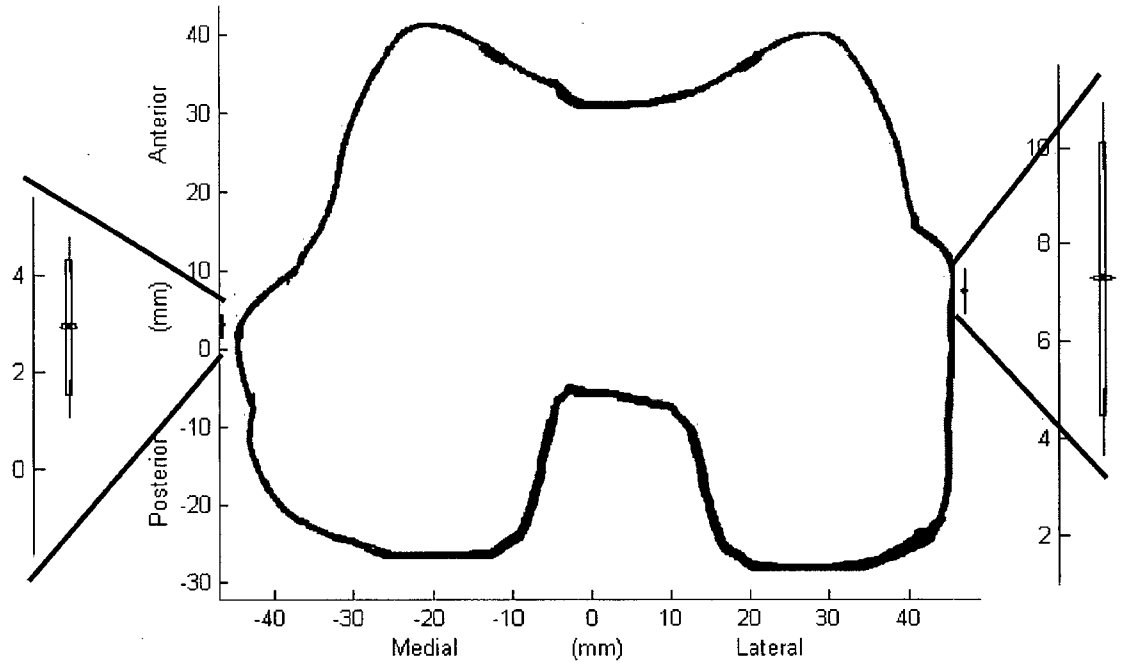

Figure 2.15: Mean epicondylar estimate location for the sphere-fit method.
Horizontal bars represent the pooled standard deviation in the mediolateral direction computed for 40 trials, and vertical bars represent the pooled standard deviation in the anteroposterior direction for the 40 trials. Lines represent 95% CI on the SD. [40 trials = (4 operators*5 trials + 1 operator*20 trials)].

This pooled intra-operator variability and the inter-operator variability using the sphere-fit method for determining the medial and lateral epicondylar estimates are shown in Table 2.2. In terms of locating the femoral knee centre, this translates to a pooled intra-operator variability of 0.1 mm and 1.1 mm in the mediolateral and anteroposterior directions respectively, and an inter-operator variability of 0.05 mm and 0.8 mm in the mediolateral and anteroposterior directions respectively. Total variability for the femoral knee centre was calculated using 5 trials from the four operators and the first 5 trials from the fifth operator (25 trials total), and was 0.1 mm and 1.1 mm in the mediolateral and anteroposterior directions respectively. The variability in locating the femoral knee centre with the sphere-fit method was significantly lower ($p<0.05$) than the convex hull method for all three types of variability reported in all directions except for inter-operator variability of the knee centre in the mediolateral direction only.

Table 2.2: Mediolateral (ML) and anteroposterior (AP) variability for the medial and lateral epicondyles using the sphere-fit method.
All measurements in mm. 95% confidence interval (CI) on each standard deviation is shown in brackets.

Pooled Intra-Operator Variability	ML (95% CI)	AP (95% CI)
Lateral Epicondyle	0.2 (0.1-0.2)	2.8 (2.2-3.6)
Medial Epicondyle	0.1 (0.1-0.2)	1.4 (1.1-1.8)
Knee Centre	0.1 (0.07-0.1)	1.1 (0.9-1.4)
Inter-Operator Variability	**ML (95% CI)**	**AP (95%CI)**
Lateral Epicondyle	0.2 (0.1-0.5)	2.1 (1.2-6.0)
Medial Epicondyle	0.2 (0.1-0.5)	1.0 (0.6-2.9)
Knee Centre	0.05 (0.03-0.2)	0.8 (0.5-2.3)
Total Variability	**ML (95% CI)**	**AP (95% CI)**
Lateral Epicondyle	0.3 (0.2-0.4)	2.9 (2.3-4.0)
Medial Epicondyle	0.2 (0.2-0.3)	1.8 (1.4-2.5)
Knee Centre	0.1 (0.07-0.13)	1.1 (0.8-1.5)

There was no significant difference between the pooled mediolateral intra-operator variability for the lateral and medical epicondylar estimates using the sphere-fit method. However, the anteroposterior intra-operator variability for the lateral epicondylar estimates was significantly higher ($p<0.05$) than the variability for the medial epicondylar estimates.

The pooled intra-operator variability was statistically significantly lower ($p<0.05$) than all estimates computed using the convex hull method in both directions on both sides.

There was no significant difference in inter-operator variability comparing the medial and lateral epicondylar estimates. There was also no statistical significant difference between the inter-operator variability of this method compared to the convex-hull method.

The total variability for the lateral epicondylar estimates using the sphere-fit method was significantly higher ($p<0.05$) than the medial epicondylar estimates in the anteroposterior direction only. This total variability was statistically significantly lower ($p<0.05$) than estimates computed using the convex hull method for both directions of the lateral epicondylar estimates and for the anteroposterior direction of the medial epicondylar estimates only.

Each medial epicondylar estimate was paired with every other lateral epicondylar estimate to determine rotation alignment variability (Figure 2.16). The intra-operator

rotational variability ranged from 1.2° SD (95% CI from 0.9 to 1.7) to 1.8° SD (95% CI from 1.3 to 2.4) for this method, statistically smaller ($p<0.05$) than the convex-hull method for operators A and M. The inter-operator rotational variability was 1.3° SD (95% CI from 0.8 to 3.8) not significantly different from convex hull method ($p>0.05$). The total variability was 1.8°, significantly lower ($p<0.05$) than the convex-hull method. The range of rotation seen for the sphere-fit algorithm was 7°.

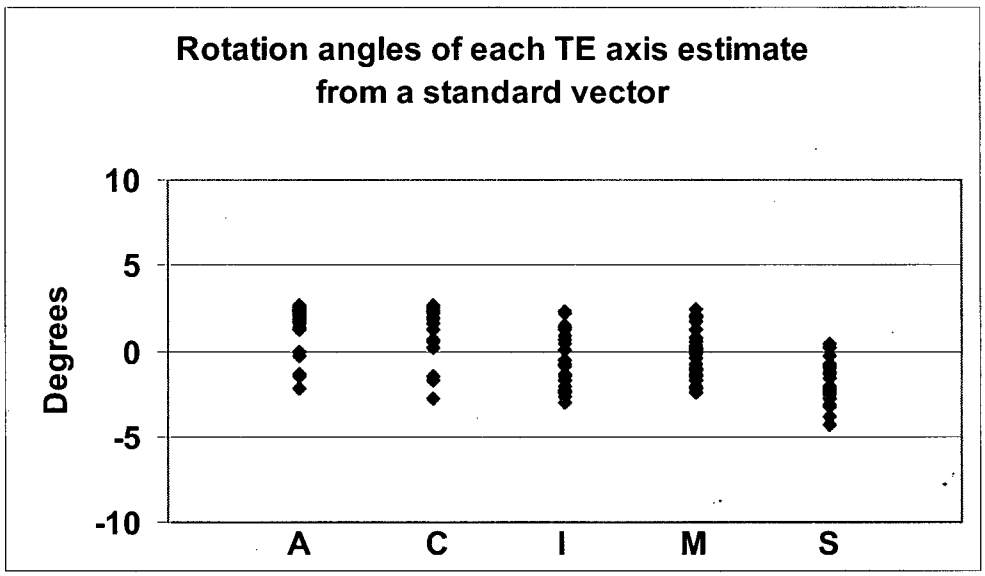

Figure 2.16: Rotation angles for each TE axis estimate from each operator using the sphere-fit method. Diagram shows the range of 25 values from each operator as well as the bias between operators. [25 values = 5 medial paired with all 5 lateral].

2.3.2.1 Bootstrapping results from the sphere-fit algorithm

Most operators' trials were bootstrapped with a high percentage of convergence except for subject M.

2.3.2.1.1 Intra-operator variability

When each trial's planes were bootstrapped 1000 times, and the epicondylar estimates combined, the intra-operator variability (~5000 estimates for operators A, C, I and M and ~20000 estimates for operator S) in the medial-lateral direction ranged from 0.2 mm SD to 0.6 mm SD for the lateral epicondylar estimates, and from 0.1 mm SD to 0.3 mm SD for the medial epicondylar estimates (Figure 2.17). This was significantly smaller than the anterior-posterior direction ($p<0.05$) for all operators, where the intra-operator

variability ranged from 2.5 mm SD to 4.1 mm SD for the lateral epicondylar estimates, and from 1.3 mm SD to 2.9 mm SD for the medial epicondylar estimates.

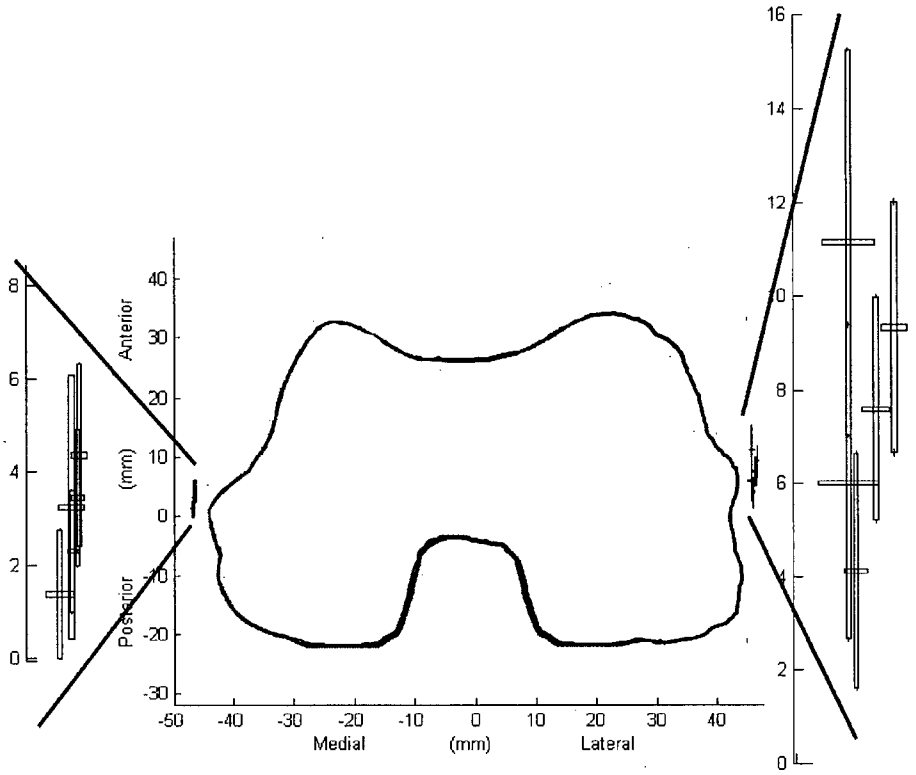

Figure 2.17: Mean mediolateral and anteroposterior locations of the medial and lateral epicondylar estimates from 5000 bootstrapped trials from 4 operators, 20000 bootstrapped trials from 1 operator. Vertical bars show ± 1SD in the anteroposterior direction and horizontal bars show ± 1SD in the mediolateral direction. Lines show the 95% upper and lower confidence limits on the standard deviation.

This can be compared to the variability seen when all the planes collected from each subject were pooled (~500 planes for operators A, C, I, and M and ~2000 planes for operator S) and bootstrapped 1000 times. The mediolateral variability ranged from 0.1 mm SD to 0.4 mm SD for the lateral epicondylar estimates, and was less than 0.2 mm SD for all operator's medial epicondylar estimates (Figure 2.18). The anteroposterior variability ranged from 0.9 mm SD to 3.1 mm SD for the lateral epicondylar estimates, and from 0.8 mm SD to 1.7 mm SD for the medial epicondylar estimates.

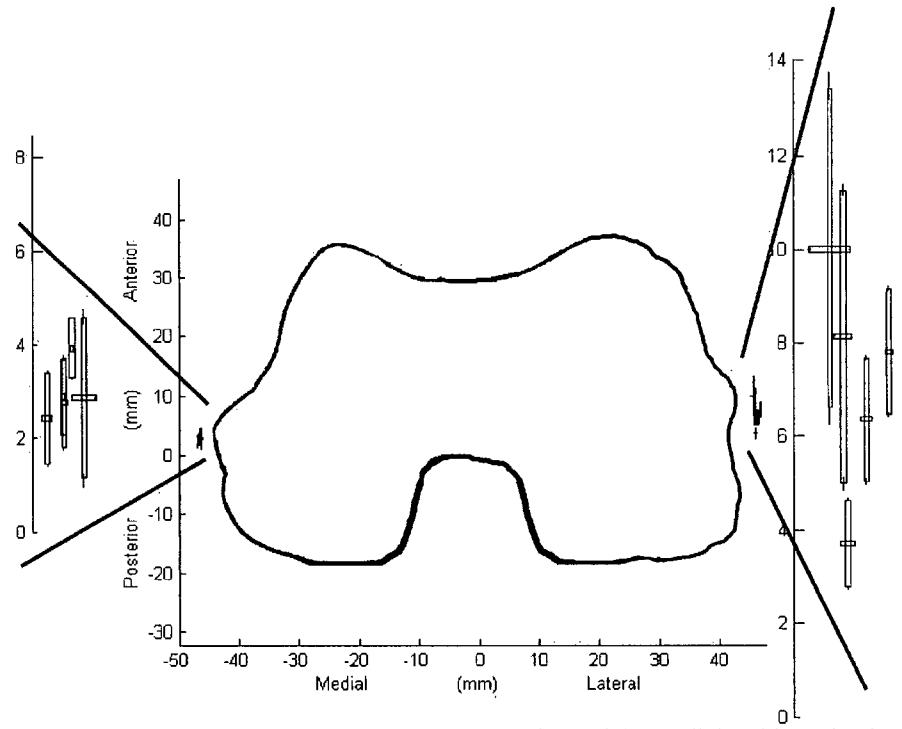

Figure 2.18: Mean mediolateral and anteroposterior locations of the medial and lateral epicondylar estimates from the 1000 bootstrapped trials for the 500 planes from 5 operators. Compared to the 1000 bootstrapped trials from pooling all planes from all operators (*). Vertical bars show ± 1SD in the anteroposterior direction and horizontal bars show ± 1SD in the mediolateral direction. Lines show the 95% upper and lower confidence limits on the standard deviation.

F-test comparisons within each operator comparing the variability from the intra-operator variability for the combined bootstrapped trials (~5000 estimates - Figure 2.15) to the intra-operator variability from the combined bootstrapped planes (~1000 estimates – Figure 2.16) showed that all SD for the combined bootstrapped planes were significantly smaller ($p<0.05$) than that of the combined bootstrapped trials for all operators in all directions except for the anteroposterior location of the lateral epicondylar estimates for Operator C. This shows that there was an overall intra-operator bias between trials for all operators.

2.3.2.1.2 Inter-operator variability

There were a total of 3760 planes collected from the lateral epicondyles and 3398 planes collected from the medial epicondyles. When all these planes were bootstrapped 1000 times (1000 estimates), we see variability of 0.2 mm SD in the mediolateral direction for

the lateral epicondylar estimates, and 0.1 mm SD for the medial epicondylar estimates. In the anteroposterior direction, we see a variability of 1.5 mm SD for the lateral epicondylar estimates, and 0.7 mm SD for the medial epicondylar estimates. Convergence occurred in 872 of the 1000 bootstrapped trials.

F-test comparisons between this variability (1000 estimates) and the variability between the means of the estimates calculated from the individual trials show a significant decrease ($p<0.05$) in SD for all operators in all directions. This means that bias differences exist between operators.

In summary, our results show that:

- variability in the anteroposterior direction (sagittal plane) was significantly higher than variability in the mediolateral direction (frontal plane).
- AP variability (in the sagittal plane) on the lateral epicondyle was generally significantly higher than AP variability on the medial epicondyle.
- the sphere-fit method was more repeatable than the convex-hull method, and
- biases exist between the results from each operator.

2.4 Discussion

2.4.1 Interpretation of results and comparison to other studies in the literature

We conducted an in-vitro study to compare the repeatability in identifying the lateral and medial epicondyles using two algorithms, the convex-hull method and the sphere-fit method, and to determine if using a plane probe is more repeatable than using a point probe. Our results show that in general the sphere-fit algorithm seems to be a more repeatable way over the convex-hull algorithm in identifying both epicondyles for all the important criteria, and is more repeatable than point probe techniques quantified in other studies (7° compared to 11.8° (Fuiko et al., 2003)).

There are three main issues in locating these epicondyles. They are used to determine the mediolateral and anteroposterior location of the femoral knee centre, and rotational alignment for the femoral component. When the variability seen is separated into components corresponding to mediolateral and anteroposterior directions, we see that anteroposterior variability is much greater than mediolateral variability for the resulting

knee centres. However, the magnitude of the total anteroposterior variability seen for the sphere-fit method is 1.1 mm SD (95% CI on the SD from 0.9-1.4). This means that if 95% of the time the knee centre were located anterior or posterior to its true location, there would be 0.2° of flexion in the component, a value that is less than the 3 degree window allowed (Jeffery et al., 1991). The mediolateral variability seen is less than the SD inherent in the measuring equipment (Flashpoint 5000 SD: 0.35 mm) and would only correspond to 0.03° of varus or valgus mal-alignment – an order of magnitude below that tolerated by the component (Jeffery et al., 1991). There are no previous studies to compare the variability of the knee centres determined by the plane probe with that determined by a point probe.

In terms of rotational alignment, the sphere-fit algorithm for this study shows a total angular variability of 1.8° SD (95% CI from 1.7-2.1), and a range of 7°. Previous studies show the inter-operator variability in identifying the lateral and medial epicondyles with a pointed object to have a 11.8 - 23° range (Fuiko et al., 2003; Jerosch et al., 2002; Kessler et al., 2003). This study therefore shows that using the plane probe may be an effective way in removing operator bias in distinguishing extreme points, and prove to be more a more repeatable way in identifying the TEA.

The sphere-fit algorithm is more robust than the convex-hull algorithm as it is less dependent on the actual planes collected. While an outlier plane that lies closer to the bone has the potential to drastically change the results of the convex-hull formed by the convex-hull algorithm, the sphere-fit algorithm is unaffected by this. Instead, as the sphere-fit algorithm is based on fitting all the planes to a sphere, outlier planes are outweighed by the other planes and only have a minimal effect on the radius of the sphere. Outlier planes may be a result of noise in the system, or operator motion that may be faster than the sampling rate of the system.

The disadvantage of the sphere-fit algorithm is that it is based on the assumption that the epicondyles are spherical in shape with an associated radius of curvature. Yet, this is not unlike the convex hull algorithm that assumes that the epicondyles have an associated convex shape. The sphere-fit algorithm therefore relies on the operator collecting planes that would essentially map out a curved surface. Our results show the assumption of a

spherical shape is valid as convergence occurs in all initial trials with an acceptable degree of variation for most operators. The radius of the spheres fit to the condyles was about 15 mm on the medial epicondyle and 30 mm on the lateral epicondyle.

The epicondyles are known not to have similar shapes (Griffin et al., 2000), leading to the different amounts of variation in identifying them with the two techniques. Jerosch et al (2002) found the medial epicondylar points to be projected over 102 mm^2, and the lateral epicondylar points to be projected over 116 mm^2. Kessler et al (2003), found similar trends. His study reports the medial epicondylar points projected over 278 mm^2, and the lateral epicondylar points projected over 298 mm^2.

The medial epicondyle consists of a bony ridge surrounding a central sulcus. The deep MCL attaches in the sulcus, and the superficial MCL attaches on the horse-shoe shaped ridge surrounding the sulcus (Figure 2.19). Surgeons tend to use the high point of the medial condyle as the medial epicondyle. This high point can be anywhere along that ridge and a surgeon could choose points 10 – 15 mm apart, leading to significant variability in the chosen axis for the component. While the sulcus is a more consistent anatomical landmark, its depth can be quite small (0.2 – 2.2 mm), making it difficult to locate (Griffin et al., 2000).

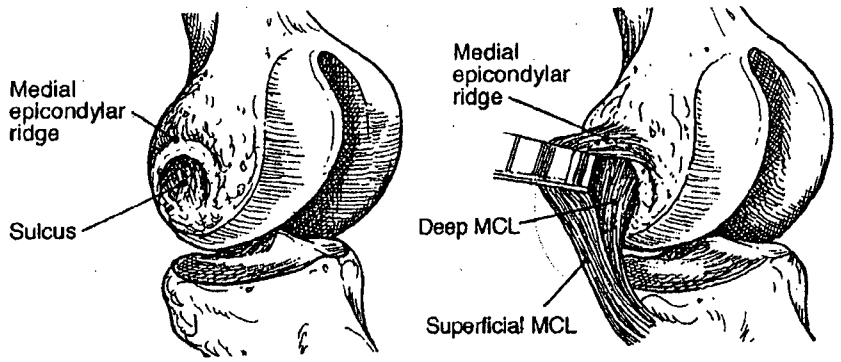

Figure 2.19: Anatomy of the medial epicondyle.
This drawing shows the horseshoe ridge as the attachment of the superficial MCL and the sulcus as the attachment of the deep MCL (Griffin et al., 2000).

The sphere-fit algorithm is beneficial in the identification of the medial epicondyle over the lateral epicondyle. The horse-shoe shaped ridge forms a natural surface to rock the

probe, and once the operator covers the entire ridge, a curved surface should enter the algorithm, with the centre of radius of curvature of the sphere in the sulcus. This contrasts the point probe technique, where the surgeon should essentially palpate and draw out the entire ridge, and choose the centre as the location of the sulcus. Yet, surgeons almost never perform this palpation of the entire ridge (Griffin et al., 2000).

Williams and Warwick (1980) [Gray's Anatomy] describes the lateral epicondyle as flatter and less prominent than the medial epicondyle (seen by the increased radius of this sphere to the medial). This may be an explanation for the increased variation in its identification. Unfortunately, this characteristic is not beneficial to the sphere-fit algorithm, as we see a significant increase in anteroposterior variability over the medial epicondyle.

2.4.1.1 Bootstrapping

Bootstrapping the planes from the trials is a clever way to expand the datasets as well as investigate intra- and inter-operator technique. We see similar intra-operator variability between the bootstrapped trials and the original datasets for the mediolateral and anteroposterior variability in identification of the medial and lateral epicondyles. There was a slight increase seen in operators C and M anteroposterior variability of the MCL. This suggests that these trials may have included a large area of planes collected with differences in technique used between their 5 trials. When the individual trial is bootstrapped, this may lead to an increased variability seen. The inter-operator variability in the bootstrapped trials is slightly higher than the inter-operator variability seen in the original datasets. This suggests that there were bias differences between operators that are exaggerated when the dataset is expanded.

Variability was seen to decrease when trials were bootstrapped from the pooled dataset of all the planes from all the trials. This variability dropped for all operators except operator C. The decrease in variability can be explained by the more complete set of planes that better represent a sphere than the previous individual trials.

When all the planes from all the operators' trials were bootstrapped, we saw an even greater decrease in variation. This suggests that a combination of all the planes from all operators gave rise to a pool of planes that were more repeatable in forming the same

sphere. This implies that training of the operators to perform data collection in a manner that encompasses a greater range of collected planes may lead to less variation of results.

There were 872 trials that converged. This suggests that the random sampling of planes could choose some that were not adequate enough to form a sphere within the tolerance that was allowed.

2.4.2 Strengths and Weaknesses of Study

This study was performed on a fresh cadaveric knee of a 76 year old female. While the ligaments were present as in a typical TKA patient, there was no osteoarthritis present in this subject. This study was performed on a single cadaveric knee. Anatomic variations of the medial and lateral epicondyles are seen (eg. ridge width) (Griffin et al., 2000), and can also depend on then age and gender of the specimen. Further testing on more specimens is necessary to determine whether anatomic variations will have a significant effect on the robustness of the sphere-fit algorithm.

The convex hull algorithm maps out a shape of the epicondyle based on the tangential planes collected. This algorithm is particularly susceptible to sampling rate and movement of the plane probe. As exact planar locations are used to map out the surface of the condyle, an outlier plane manufactured from noisy data (due to system inherent error or effect of moving probe faster than frequency of data acquisition) would have a large effect on the outcome of the algorithm.

The anatomical reference frame defined to compare mediolateral and anteroposterior variation was defined by digitizing specific points on the cadaveric limb. This may not be the same points digitized on cadaveric specimens in other studies. While rotational variation in the transverse plane has been compared between studies, there is a certain amount of uncertainty that should be associated with this comparison.

The inter- and intra-operator variability for the plane probe technique was not explicitly compared to the point probe technique on this particular specimen (using the same subjects). This was not done for two reasons. Graduate students in our lab were the subjects in this experiment. Their perception of the location of the medial and lateral epicondyles may be very different, as they do not possess adequate training in this area. This would therefore be an inaccurate representation of inter-operator variability. In

terms of intra-operator variability when using a point probe, previous studies in our lab (a pilot study on a wooden knee and experiments performed on locating the medial and lateral malleoli (Shute, 2002)) showed that there is typically high intra-operator repeatability when using a point probe as the subject would typically focus on a point and repeatedly digitize the same point. This is uncharacteristic of typical procedures as the operator would not be exposed to the same knee. If a measure of intra-operator repeatability would have to be performed on the same specimen, the subject should only be allowed to digitize a point every 24 hours to ensure that the image is erased from their mind. Limited access to the fresh cadaveric specimen in this study did not allow us to perform this procedure. Further investigation is needed to decide whether the location of the epicondylar estimates found from the plane probe method is the 'correct' location of the epicondyles. The true location of the epicondyles should be the location of the attachments of the medial and lateral collateral ligaments onto the condyles. The plane probe technique is a way of repeatedly locating a point for the medial and lateral epicondyles. Some investigators argue that this is more important than its true location. Further investigation is therefore necessary to determine if a bias should to be applied to our results. This investigation would have to performed on multiple cadaveric knees with further dissection of the soft tissues to determine the exact attachments of the ligaments.

This study was performed using an optoelectronic camera with a specified accuracy of 0.35mm SD RMS in three dimensions. Further investigation could be performed on the robustness of the algorithms using optoelectronic cameras with higher precision (e.g. Optotrak). This would allow clarification between the variability present within the equipment and algorithm, compared to the variability of the algorithm alone.

2.4.4 Conclusions

The use of a plane probe in conjunction with the sphere-fit algorithm may be a more repeatable way of identifying the lateral and medial epicondyles over the traditional point probe method. Using this plane probe method has a range of rotational alignment variation of 7° for the five operators in this study.

2.5 Acknowledgements

We thank Dr. David Kirkpatrick (UBC Department of Computer Science) for his assistance in applying the convex hull algorithm in this situation. We also thank Dr. Bassam Masri for opportunities to observe numerous total knee replacement procedures and discussions on surgical technique.

2.6 References

Andriacchi, T. (1994) Dynamics of malalignment. *Orthop Clin North Am* **25** (3): 395-403.

Anouchi, Y.S., Whiteside, L.A., Kaiser, A.D., and M. Milliano (1993) The effects of axial rotational alignment of the femoral component on knee stability and patellar tracking in total knee arthroplasty demonstrated on autopsy specimens. *Clin Orthop* (287): 170-7.

Arima, J., Whiteside, L. A., McCarthy, D. S., and S.E. White (1995) Femoral rotational alignment, based on the anteroposterior axis, in total knee arthroplasty in a valgus knee. A technical note *J Bone Joint Surg Am* **77** (9): 1331-1334.

Barber, C. B., Dobkin, D.P., and H. Huhdanpaa (1996) The quickhull algorithm for convex hulls. *ACM Trans Math Software* **22**: 469-483

Barrack, R. L., Schrader, T., Bertot, A.J., Wolfe, M. W., and L. Myers (2001) Component rotation and anterior knee pain after total knee arthroplasty. *Clin Orthop* (392): 46-55.

Berger, R.A., Rubash, H.E., Seel, M.J., Thompson, W.H., and L.S. Crossett (1993) Determining the rotational alignment in total knee arthroplasty using the epicondylar axis. *Clin Orthop* (286): 40-7.

Churchill, D. L., Incavo, S. J., Johnson, C. C., and B.D. Beynnon (1998) The transepicondylar axis approximates the optimal flexion axis of the knee. *Clin Orthop* (356): 111-118.

DiCiccio, T.J., and B. Efron (1996) Bootstrap confidence intervals. *Statist Sci* **11** (8): 189-228.

Dorr L.D., and R.A. Boiardo (1986) Technical considerations in total knee arthroplasty. *Clin Orthop* (205): 5-11.

Eckhoff, D. G., Metzger, R. G., and M. V. Vandewalle (1995) Malrotation associated with implant alignment technique in total knee arthroplasty. *Clin Orthop* (321): 28-31.

Elias, S. G., Freeman, M. A., and E.I. Gokcay (1990) A correlative study of the geometry and anatomy of the distal femur. *Clin Orthop* (260): 98-103.

Fehring, T.K. (2000) Rotational malalignment of the femoral component in total knee arthroplasty *Clin Orthop* (380): 72-79.

Feinstein, W.K., Noble, P.C., Kamaric, E., and H.S. Tullos (1996) Anatomic alignment of the patellar groove. *Clin Orthop* (331): 64-73.

Fuiko, R. Kotten, B., Zettl, R. and P. Ritschl (2003) Landmarks for navigated implantation of total knee arthroplasty (TKA). In Langlotz, F, Davies, B.L., and A. Bauer (Eds): *3rd Annual Meeting of CAOS-International Proceedings*:108-109.

Griffin, F.M., Math, K., Scuderi, G.R., Insall, J.N., and P. Poivache (2000) Anatomy of the epicondyles of the distal femur – MRI analysis of normal knees. *J Arthroplasty* **15** (3): 354-359.

Hofmann, A.A., Bachus, K.N., and R.W. Wyatt (1991) Effect of the tibial cut on subsidence following total knee arthroplasty. *Clin Orthop* (269): 63-69.

Hofmann, S., Romero, J., Roth-Schiffl, E., and T. Albrecht (2003) Rotational malalignment of the components may cause chronic pain or early failure in total knee arthroplasty. *Orthopade* **32**: 469-476.

Insall J.N. (1985) Technique of total knee replacement. In Dorr L.D (ed): The Knee. Papers of the first scientific meeting of The Knee Society. *University Park Press,* Baltimore.

Jeffery, R., Morris, R., and R. Denham. (1991) Coronal alignment after total knee replacement. *J Bone Joint Surg Br* **73-B** (5): 709-714.

Jerosch, J., Peuker, E., Phillips, B., and T. Filler (2002) Interindividual reproducibility in perioperative rotational alignment of femoral components in knee prosthetic surgery using the transepicondylar axis. *Knee Surg Sports Traumatol Arthrosc* **10** (3): 194-7.

Katz, M.A., Beck, T.D., Silber, J.S., Seldes, R.M., and P.A. Lotke (2001) Determining rotational alignment in total knee arthroplasty: reliability of techniques. *J Arthroplasty* **16** (3): 301-305.

Kessler, O.C., Moctezuma de la Barrer, J.L., Streicher, R.M., Stockl, B., Krismer, M., and M. Nogler (2003) Variation in the entry point selection for the transepicondylar axis and its quantitative effects. In Langlotz, F, Davies, B.L., and A. Bauer (Eds): *3rd Annual Meeting of CAOS-International Proceedings*: 176-177.

Kunz, M., Strauss, M, Langlotz, F., Deuretzbacher, G.., Ruther, W., and L.P. Nolte (2001) A non-CT based total knee arthroplasty system featuring complete soft-tissue balancing. In: Niessen W, Viergever M (Eds) MICCAI 2001. *LNCS* **2208**, Springer-Verlag: 409-415.

Kurosawa, H., Walker, P.S., Abe, S., Garg, A., and T. Hunter (1997) Geometry and motion of the knee for implant and orthotic design. *J Biomech* **18**: 487-499.

Lotke, P.A., and M.L. Ecker (1977) Influence of position of prosthesis in total knee replacement. *J Bone Joint Surg Am* **59** (1): 77-79.

Martelli, S., and A. Visani (2002) Computer investigation into the anatomic location of the axes of location of the knee. In Dohi, T., and R. Kikinis (Eds) MICCAI 2002. *LNCS* **2489**: 276-283.

Miller, M.C. Berger, R.A., Petrella, A.J., Karmas, K., and H.E. Rubash (2001) Optimizing femoral component rotation in total knee arthroplasty. *Clin Orthop* (392): 38-45.

Moreland, J.R. (1988) Mechanisms of failure in total knee arthroplasty. *Clin Orthop* (226): 49-64.

Muller W. (1983) The knee: form function and ligament reconstruction. Springer Verlag, New York.

Nagamine, R., Miura, H., Inoue, Y., Urabe, K., Matsuda, S., Okamoto, Y., Nishizawa, M., and Y. Iwamoto (1998) Reliability of the anteroposterior axis and the posterior condylar axis for determining rotational alignment of the femoral component in total knee arthroplasty. *J Orthop Sci* **3**(4): 194-198.

Nordin, M., and V.H. Frankel (Eds) (1989) *Biomechanics of the Knee: Basic biomechanics of the musculoskeletal system.* Lea and Febiger, Philadelphia: 116.

Olcott, C.W., and R.D. Scott (2000) A comparison of 4 intraoperative methods to determine femoral component rotation during total knee arthroplasty. *J Arthroplasty* **15** (1): 22-26.

Poivache, P.L., Insall, J.N., Scuderi, G.R., and D.E. Font-Rodriguez (1996) Rotational landmarks and sizing of the distal femur in total knee arthroplasty. *Clin Orthop* (331): 35-46.

Rhoads, D.D., Noble, P.C., Reuben, J.D., and H.S. Tullos (1993) The effect of femoral component position on the kinematics of total knee arthroplasty. *Clin Orthop* (286): 122-129.

Scuderi, G.R., and J.N. Insall (2000) Rotational positioning of the femoral component in total knee arthroplasty. *Am J Knee Surg* **13** (3): 159-161.

Sharkey, P.F., Hozack, W.J., Rothman, R.H., Shastri, S., and S. Jacoby (2002) Why are total knee arthroplasties failing today. *Clin Orthop* (404): 7-13.

Stiehl, J., and B.D. Abbott (1995) Morphology of the transepicondylar axis and its application in primary and revision total knee arthroplasty. *J Arthroplasty* **10** (6): 786-789.

Stulberg, S.D., Loan, P. and V. Sarin. (2002) Computer-assisted navigation in total knee replacement: results of an initial experience in 35 patients. *J. Bone Joint Surg,* **84A** (S2): 90-98.

Tanavalee, A. Yuktanandana, P. and C. Ngarmukos (2001) Surgical epicondylar axis vs anatomical epicondylar axis for rotational alignment of the femoral component in total knee arthroplasty. *J Med Assoc Thai* **84** (S1): S401-408.

Tetsworth, K., and D. Paley. (1994) Malalignment and degenerative arthroplasty. *Orthop Clin North Am* **25** (3): 367-377.

Uehara, K., Kadoya, Y., Kobayashi, A., Ohashi, H., and Y. Yamano (2002) Bone anatomy and rotational alignment in total knee arthroplasty. *Clin Orthop* (402): 196-201.

Whiteside, L.A. and J. Arima. (1995) The anteroposterior axis for femoral rotational alignment in valgus total knee arthroplasty. *Clin Orthop* (321): 168-72.

Chapter 3: Repeatability in identifying the tibial knee centre for application to computer assisted total knee replacement surgery

3.0 Abstract

It is necessary to locate the tibial knee centre for determining the tibial mechanical axis of the lower limb. The tibial component should be perpendicular to this axis in the frontal plane, and is referenced from this axis in the sagittal plane to provide posterior slope. Malalignment in these planes have been correlated to potentially adverse clinical outcomes. Other computer-assisted techniques digitize the centre of the tibial eminences as the tibial knee centre. The centre of the tibial component should be in a position that provides optimal bone coverage of the tibial plateau, similar to the conventional idea. We digitized the perimeter of the tibial plateau on a Sawbones model and on a cadaveric knee, and showed that using an ellipse-fit algorithm provided a repeatable mediolateral and anteroposterior centre (<2 mm SD) for trials performed with a single operator. Though this centre was similar to the centre of the tibial eminences in the frontal plane in our model, it may not be similar in the sagittal plane. This use of the tibial eminences to locate the tibial knee centre may not always represent a centre that reflects optimal coverage of the tibial plateau.

3.1 Introduction

3.1.1 Clinical application for repeatably identifying the tibial knee centre

The tibial knee centre is important in determining the mechanical axis of the tibia. This mechanical axis joins the tibial knee centre to the ankle centre in the frontal and sagittal planes. Errors in locating the tibial knee centre can therefore lead to varus/valgus alignment errors in the frontal plane (Figure 2.2), and can lead to flexion/extension errors in the sagittal plane. Location of this tibial knee centre also should be in a position that provides optimal bone coverage of the tibial plateau when the tibial component is centered on it.

3.1.1.1 Implications in the frontal plane

Frontal/Coronal plane alignment of the tibial component has long been recognized to be crucial in total knee replacement surgery and numerous studies have correlated

valgus/varus malalignment to early failure (Lotke and Ecker, 1977; Moreland, 1988; Jeffery et al., 1991). The tibial component should be placed perpendicular to the mechanical axis of the knee, with the centre of the component on the tibial knee centre (Dorr and Boiardo, 1986). This ensures an equal balance of loads in the lateral and medial compartment. A detailed description on the effects of malalignment in the frontal plane can be found in Section 2.1.1.2.

3.1.1.2 Implications in the sagittal plane

The tibial knee centre in the sagittal plane influences the posterior cut angle of the tibial component with respect to the mechanical axis. If the estimated tibial knee centre is more anterior on the plateau, an anterior cut is made on the plateau. Similarly, a knee centre more posterior on the plateau will make a cut with posterior slope.

There is a relationship between tibial cut angle in the sagittal plane (anterior/posterior slope) and tibial component longevity (Dorr and Boiardo, 1986; Ecker et al., 1987; Hofmann et al., 1991). The natural tibial plateau is generally sloped 5-10° posteriorly to assist femoral rollback on the tibia when the knee is flexed. Though it has been shown that duplicating this anatomic angle in the tibial component reduces anterior subsidence and failure compared to components cut perpendicular to the mechanical axis in the sagittal plane (Hofmann et al., 1991), later biomechanical studies have shown that a 0 – 3° posterior slope actually provides the greatest tibial component stability (Bai et al., 2000). Yet, a recent finite element model of the polyethylene tibial component showed only a 9% increase in cancellous bone stress for an implant modeled in 7° posterior slope over the neutral position (Perillo-Marcone et al., 2000). This modest increase in stress may explain the range of accepted posterior slope angles seen in different instrumentation sets that have a built in posterior slope, allowing the surgeon to make a cut perpendicular to the mechanical axis in the sagittal plane.

Though there appears to be a range of accepted posterior slope values, there are consequences if this posterior slope is excessive. Though an increase in the angle of posterior slope decreases strain in the anterior tibia, it significantly increases anterior displacement of the tibial polyethylene component and posterior strain in the tibia, which has been shown to reduce the lifespan of tibial polyethylene (Hofmann et al., 1991).

Other consequences of excessive slope include posterior tibiofemoral subluxation, lack of femoral rollback in flexion, and impingement of posterior structures restricting flexion (Bai et al., 2000; Laskin, 1991; Walker and Garg, 1991).

3.1.1.3 Bone coverage

Another important factor in tibial component placement is the position that provides the optimal bone coverage of the tibial plateau. Optimal bone coverage is achieved when the component has maximum cortical bearing over the plateau circumference (Lemaire et al., 1997), with posteromedial and anterolateral support. A component with excessive overhang in any direction can be harmful to surrounding soft tissues. It has been concluded that exact-size or smaller components should be positioned equidistant from the cortices of the underlying tibial plateau as the subchondral bone of the tibial plateau is more resistant in the centre of the condyles directly under the weight-bearing zones (Lemaire et al., 1997). This leads us to believe that the centre of the tibial component should lie on a tibial knee centre that is determined using total coverage of the tibial plateau.

3.1.2 Current approaches in CATKR

Though the range of navigation systems for TKR is quite extensive, published literature on these systems is somewhat limited. Most of the algorithms on these commercial systems are proprietary, so their details are unknown.

There are currently two groups of image-free navigation systems on the market. The first group is landmark based, and does not possess geometric and morphologic 3D data. In the landmark based systems category, published literature on the OrthoPilot states that identification of the knee centre occurs kinematically by flexing and extending the knee from 0 to 90°, and rotating the tibia on the femur at 90° knee flexion. This manipulation creates a plane that the tibial component should be aligned with. Other non-commercial systems digitize the sulcus between the tibial spines as the medial-lateral and/or anterior-posterior centre of the knee (Krackow et al., 1999; Kunz et al., 2001)

In the second category that uses bone morphing, Surgetics uses the digitized centre of the tibial eminences as a check against the tibia centre calculated from the reconstruction of the proximal tibia from the cloud of surface points digitized (Stindel et al., 2002). The

VectorVision Knee also morphs a generic 3D model of the leg to the patient's specific anatomy from surface registration. However, the exact equations and algorithms used to calculate these centres, and the repeatability of these centres have never been published.

While there are many studies on the reproducibility of landmarks used to identify proper femoral component position (Berger et al., 1993; Churchill et al., 1998; Mantas et al., 1992; Poivache et al., 1996; Whiteside and Arima, 1995), very few studies have been performed on the tibia. To my knowledge, Dalury, 2001 is the only published study regarding reproducible landmarks that can be used as guidelines for proper tibial component position. Conventionally, he states that a line drawn 1mm medial to the medial border of the tibial tubercle that goes through the midsulcus of the tibial spines is a reproducible landmark for the tibia. In his study, a perpendicular cut made relative to this line produced 46 out of 50 knees cut in alignment within 3° of the mechanical axis in the frontal plane. However, though he planned for a 7° posterior slope in the sagittal plane, his study shows a range of 4-9° posterior slope achieved. Fuiko et al., (2003) also reported an average 3D inter-operator precision (SD) of 2.0mm and an average intra-operative precision (SD) of 2.3mm in identifying the tibial centre in a study performed on 27 tibias. However, he defined the tibial centre as the middle of the tibial eminences, and neither frontal nor sagittal plane variations were distinguished. This tibial centre also does not consider overall coverage of the plateau.

3.1.3 Limitations of these approaches

Our system falls into the category of Image-free systems using Landmarks. Existing Image-free systems using Landmarks only use the centre of the tibial eminences as the tibial knee centre (Kunz et al., 2001) and do not take into consideration whether this centre is equidistant from the cortices of the underlying tibial plateau in the frontal or sagittal plane, or relates to optimal bone coverage. As well, OrthoPilot's use of kinematic manipulation of a pathological knee may not truly represent the desired frontal plane for proper alignment.

3.1.4 Purpose of study

To our knowledge, there has been no reported work on finding the tibial knee centre based on full coverage of the tibial plateau, with the optimum centers lying equidistant from the cortices of the tibia in the mediolateral and anteroposterior direction.

We hypothesized that if the perimeter of the tibial plateau were digitized, an elliptical shape could approximate the area within (Figure 3.1). The centre of this ellipse would represent the centre of the tibial plateau in terms of optimal coverage. Also of interest was the relationship of this centre to the middle of the tibial eminences (used by some CATKR techniques) in the mediolateral and anteroposterior directions.

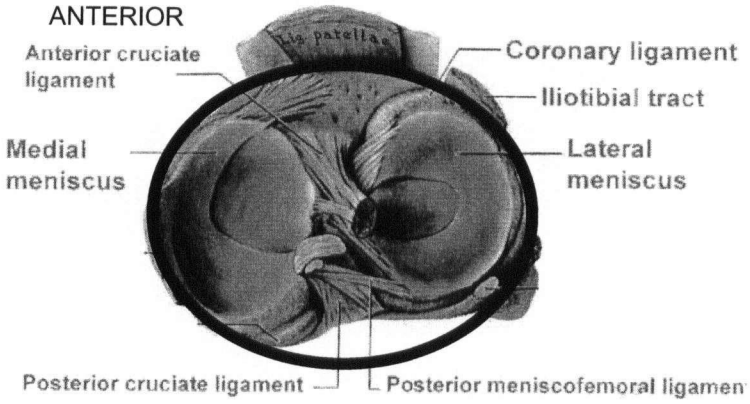

Figure 3.1: Diagram of an ellipse superimposed onto the tibial plateau (Grant's Atlas).

We therefore conducted an experiment using a plastic Sawbones (Pacific Research Laboratories, Vashon, WA) tibia and a cadaveric knee to determine the feasibility and repeatability of fitting an ellipse to the tibial plateau. Specifically, we addressed the research questions: Is the tibial knee centre found by an elliptical fit method a repeatable method in the frontal and sagittal plane, and, how does this centre compare to that used in other CATKR techniques?

3.2 Methods and materials

3.2.1 Measurement equipment and setup

We used a Flashpoint 5000 localizer (SD of noise 0.35mm RMS; Boulder Innovator Group, Boulder, CO, USA) for all measurements. This system tracks infrared emitting diodes within a 1 metre volume with a standard deviation of 0.35mm RMS. We used a

135 mm two-emitter point probe to digitize the points. The manufacturer supplied this point probe (Figure 3.2).

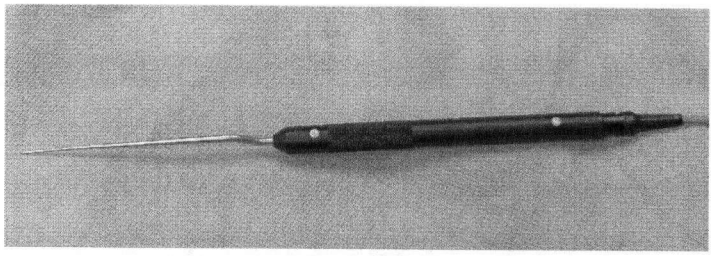

Figure 3.2: Photo of 135mm point probe used in this study.

We attached an array to the tibia so that all measurements could be taken with respect to this local co-ordinate frame irrespective of camera position. This reference frame is defined by a triad of infrared markers 120 mm on a side.

3.2.2 Measurement procedure

In order to relate the results to anatomical reference planes, we defined a nominal body reference frame with respect to the tibial reference frame. The operator digitized three points on the tibial plateau, a centre point defining an origin, a point on the medial side of the tibial tubercle defining the anterior direction, and a point to the right of the tibial tubercle on the tibial plateau defining the x-z plane. A right-handed orthogonal co-ordinate frame was then constructed from these three points (Figure 3.3).

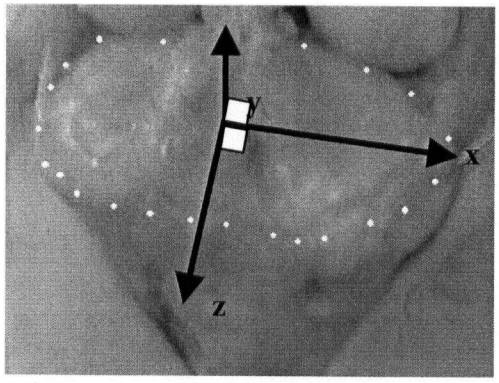

Figure 3.3: Body co-ordinate frame for determining mediolateral and anteroposterior variability.

We then recorded points at least every 5 mm around the perimeter of the tibial plateau starting from the front centre, and proceeding in an anti-clockwise direction. This was done first on a Sawbones model devoid of ligaments and soft tissues (18 trials), and then

on an intact fresh cadaveric knee (76 year old female) (10 trials) (Figure 3.4). There were 28 ± 7 (mean ± 1SD) points collected for the Sawbones trials and 35 ± 4 (mean ± 1SD) points collected for the trials on the cadaveric bone.

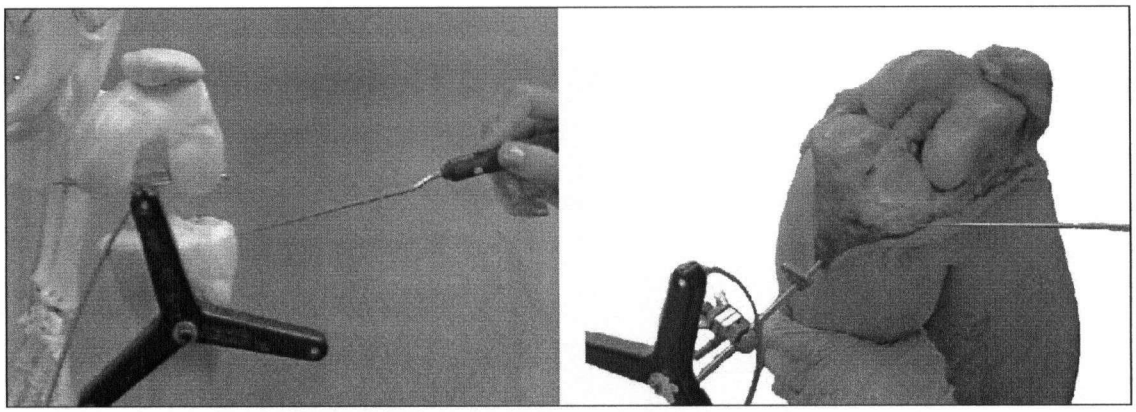

Figure 3.4: Points are digitized on a Sawbones model (left), and on a fresh cadaveric knee (right).

We prepared the cadaveric knee as in a total knee replacement procedure. An experienced surgeon made a midline longtitudinal incision initiating proximally from the midshaft of the femur over the medial third of the patella to the medial margin of the tibial tubercle. As this testing did not involve the patella, the surgeon snipped the patella tendon and moved it out of the way. He then dissected the soft tissues to expose the femur and tibia. He cut the anterior cruciate ligament, and distracted the knee joint to expose the tibial plateau.

It must be noted that the points digitized on the tibial plateau were not as evenly distributed as those digitized on the Sawbones model. The posterior tibial plateau was very difficult to reach with the point probe and at times only three or four points were digitized in this region. We hypothesized that since the posterior condyles of the tibial plateau does not contribute to the elliptical shape, the repeatability of the ellipse-fit algorithm may not be significantly compromised.

3.2.2 Ellipse-fit algorithm

We chose to model the tibial plateau as an ellipse because it returns a clearly defined centre point which can be used as a tibial knee centre. The major and minor axis of the ellipse can also represent the mediolateral and anteroposterior directions respectively.

We first used the digitized points to fit a plane. I used the multidimensional unconstrained nonlinear minimization (Nelder-Mead simplex method – Matlab 6.1 (The Mathworks, Natick, MA) fminsearch) to minimize the distance between the plane and all the points on the plane.

All the points were then projected onto this plane. A right-handed co-ordinate system was formed using three of the points projected into the plane (first point, fifth point, and median point), and all the data were transformed into this co-ordinate system so that the z co-ordinate could be eliminated (Figure 3.5).

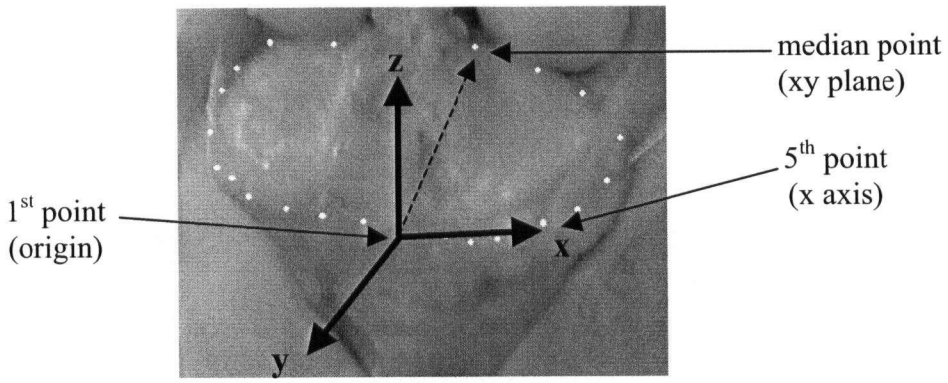

Figure 3.5: Co-ordinate system used to eliminate z co-ordinate in horizontal plane.

The points, now represented in two-dimensional space (all in the plane of the tibial plateau), were entered into an ellipse-fitting algorithm. This algorithm first computes an initial centre from algebraically fitting a circle to the points. With the centre of this circle as an initial input, an ellipse was then geometrically fitted onto the set of points using non-linear least squares.

The parametric equation of an ellipse is as follows:

$$\bar{x} = \bar{z} + Q(\alpha)\bar{x}', \bar{x}' = \begin{pmatrix} a\cos\gamma \\ b\sin\gamma \end{pmatrix}, Q(\alpha) = \begin{pmatrix} \cos\alpha & -\sin\alpha \\ \sin\alpha & \cos\alpha \end{pmatrix}$$

where $\bar{x}$ is each point on the ellipse (dependent variable), $\bar{z}$ is the centre of the ellipse, a and b are the semi-major and semi-minor axis lengths respectively, α is the angle between the major axis and the x axis, and γ as the independent variable (0-360°). We minimized the sum of the squares of the distances of the given points to the "best" ellipse by solving the problem:

$$g_i = \begin{pmatrix} x_{i1} \\ x_{i2} \end{pmatrix} - \begin{pmatrix} z_1 \\ z_2 \end{pmatrix} - Q(\alpha) \begin{pmatrix} a\cos\gamma_i \\ b\sin\gamma_i \end{pmatrix} \approx 0, i = 1,\ldots,m.$$

where (x_{i1},x_{i2}) represents the points collected. This algorithm calculates the best centre (z), major and minor axis lengths (a and b) and the angle from the x axis to the major axis (α). The algorithm also records the number of iterations it takes to fit the ellipse (Gander et al., 1994).

The ellipse fit centre is then adjusted to optimize coverage of the tibial plateau. The ellipse fit created may have overlapped in the mediolateral or anteroposterior direction, with the centre based on this best fit. To ensure that the calculated centre is based on actual digitized points, the digitized points are projected onto the major and minor axes. The centre is then adjusted in the mediolateral and anteroposterior directions by the average of the maximum and minimum projected distances. This concept is presented in Figure 3.6.

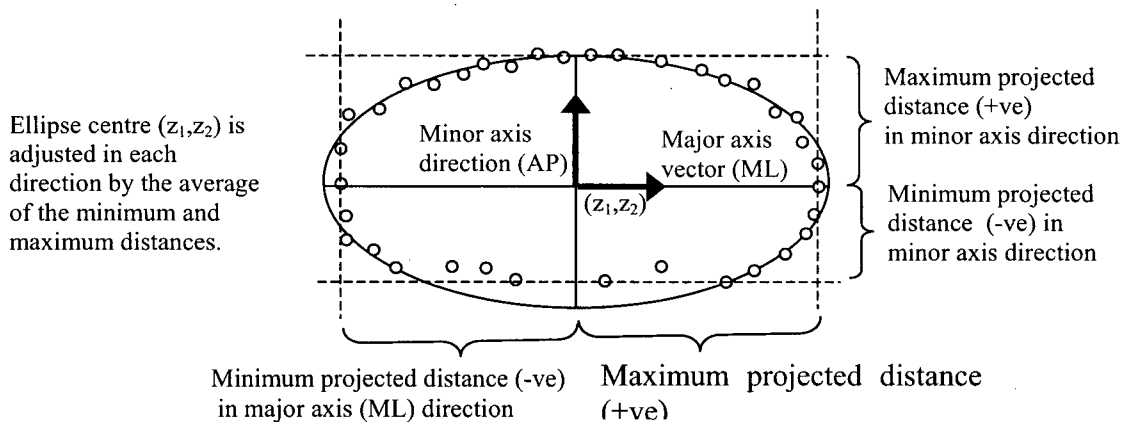

Figure 3.6: Diagram of points digitized on the perimeter of the tibial plateau in the horizontal plane. The initial ellipse centre (z_1,z_2) is adjusted to optimize bone coverage.

3.2.3 Data analysis

For both specimens, the centres were transformed into the body reference frame (b) [created at the beginning of the experiment] from the tibial array reference frame (t) using the anatomical position transform between these two frames.

$$X_b = T_{bt} * X_t$$

where T_{bt} represents the transformation between the body frame and the tibial array reference frame.

To evaluate the variability of the tibial knee centres in the mediolateral direction and anteroposterior directions, we used standard parametric methods, standard deviation (SD), to compare the intra-operator variability between the 18 trials on the Sawbones model and the 10 trials on the cadaveric knee. The 95% confidence interval of the standard deviation was then calculated using the χ^2 distribution.

$$LowerLimit = \sqrt{\frac{(n-1)\sigma^2}{\chi^2_{n-1,1-\alpha/2}}}, UpperLimit = \sqrt{\frac{(n-1)\sigma^2}{\chi^2_{n-1,\alpha/2}}}$$

In order to investigate bias on the location of the digitized middle of the tibial eminences to the centre found by the algorithm, we also digitized the middle of the tibial eminences on the Sawbones specimen.

3.2.3.1 Bootstrapping

We also wanted to investigate what would be an accepted number of points to digitize for a reasonable standard deviation in the mediolateral and anteroposterior directions. We therefore combined all the digitized points from the cadaveric trials into four groups representing quadrants of the perimeter of the plateau. These quadrants would ensure an even resampling of points around the entire ellipse for proper convergence. We resampled groups of 4, 8, 12, 16, 20, 24, 28, 32, 36, and 40 points with replacement from each quadrant representing 16, 32, 48, 64, 80, 96, 112, 128, 144, and 160 points around the entire perimeter. We performed this resampling 140 times for each group of points. We then processed these sets of points and calculated the resulting ellipse centres. We only accepted the trials if the ellipse had converged within the specified number of iterations that had occurred in regular trials. We then computed and compared the mediolateral and anteroposterior SD for the centres calculated from each group of points.

3.3 Results

Using an ellipse to fit the tibial plateau seems to be a reasonable assumption for these trials. Figure 3.7 shows all the points digitized transformed to the body co-ordinate

frame, and the resulting ellipses that were fit to the 10 trials perfomed on the cadaveric knee.

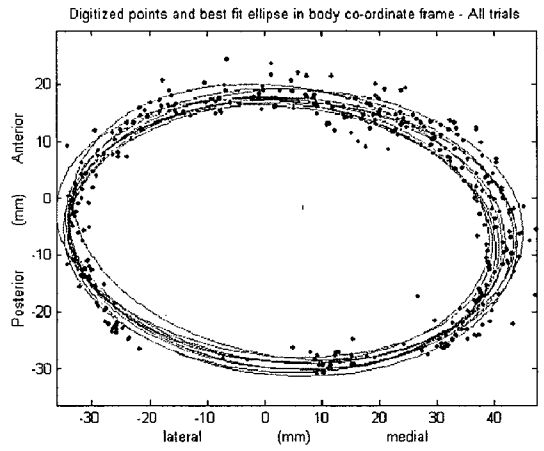

Figure 3.7: All digitized points and best-fit ellipses for the 10 cadaveric trials. All points and ellipse shown in the body co-ordinate frame.

3.3.1 Characterization of intra-operator repeatability on the sawbones model

Figure 3.8 shows a diagram of a sample of the projected planar digitized points (from Trial 8) on the plateau. The centers of the fitted ellipses from each of the eighteen trials are superimposed on the diagram. The mediolateral standard deviation for the 18 trials was 0.8 mm (95% CI from 0.6-1.3). The AP standard deviation was 0.5 mm (95% CI from 0.4-0.7).

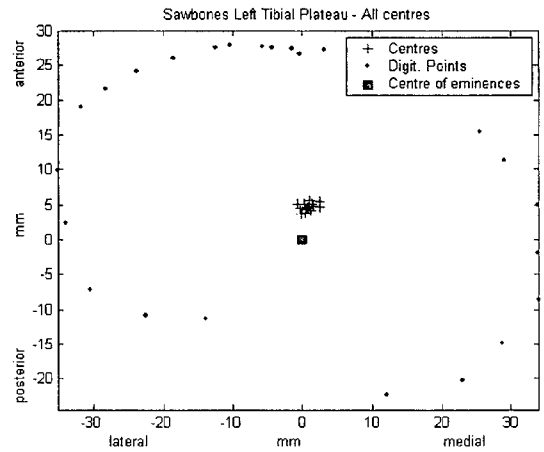

Figure 3.8: Mediolateral and anteroposterior locations of the centres of the ellipses from the 18 trials performed on Sawbones in this study:

3.3.2 Bias from the centre of the tibial eminences

The mean tibial centre was biased from the origin (centre of the tibial eminences) by 0.7 ± 0.4 mm (mean ± 95% confidence interval) medial and 4.6 ± 0.3 mm (mean ± 95% confidence interval) anterior for the Sawbones model in this study.

3.3.3 Characterization of intra-operator repeatability on the cadaver model

Figure 3.9 shows a diagram of a sample of the projected planar digitized points on the plateau (Trial 1), with all the calculated centers from the cadaveric model superimposed on the graph. The mediolateral SD for the 10 trials was 1.7 mm (95% CI from 1.2-3.1). The anteroposterior SD was 1.3 mm (95% CI from 0.9-2.4). This represents an increase in 2-2.5 times SD over the Sawbones model.

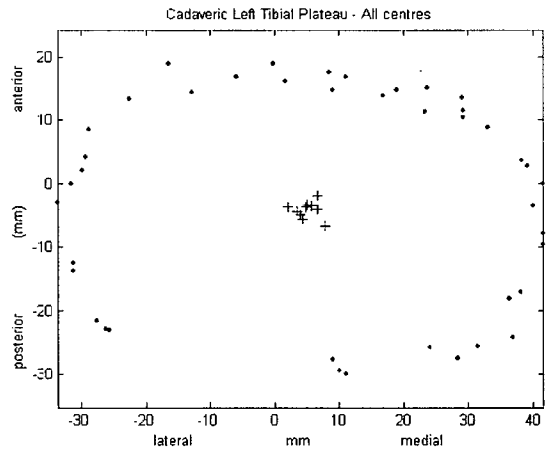

Figure 3.9: Mediolateral and anteroposterior locations of the calculated tibial knee centers on the cadaveric knee

2.3.4 Bootstrapping

Figure 3.10 shows the complete set of points that were collected during all the cadaveric trials. These points were loosely divided into quadrants as shown, and randomly resampled with replacement. There were a total number of 349 points collected around the tibial plateau.

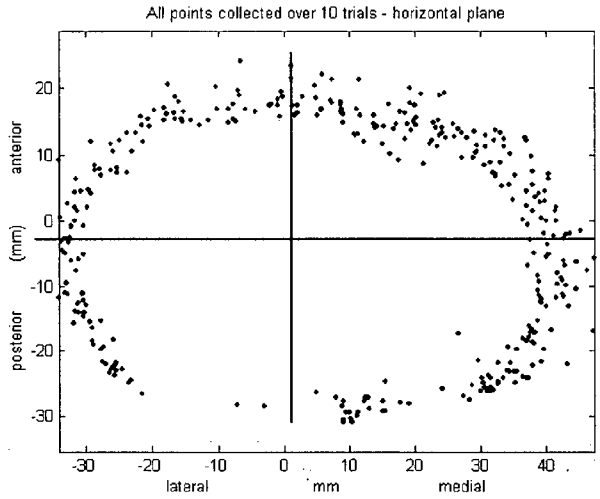

Figure 3.10: Total number of points collected over the 10 trials.
These are the points that were used to bootstrap. An equal number of points were randomly resampled from each quadrant.

Figure 3.11 shows the mediolateral (ML) and anteroposterior (AP) SD computed from each set of 140 resampled trials versus the number of points used to fit the ellipse. We see a definite decrease in standard deviation in both directions dependent on the number of points resampled. The anteroposterior variation is also seen to be greater than the mediolateral. The decrease is the most significant from when 16 points are used to fit the ellipse to when 48 points are used. The SD eventually levels off to about 1 mm AP SD and around 0.8 mm ML SD.

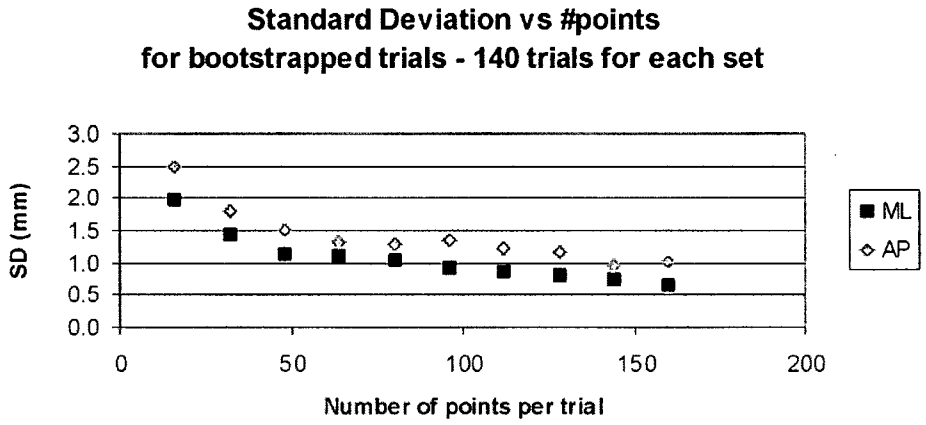

Figure 3.11: SD for each set of 140 bootstrapped trials in the mediolateral and anteroposterior directions. Trials consisted of 16, 32, 48. 64, ,80, 96, 112, 128, 144 and 160 points around the perimeter

3.4 Discussion

3.4.1 Interpretation of results

We conducted this study to determine if the method of digitizing the perimeter of the tibial plateau and using this information to find a tibial centre based on tibial plateau coverage was repeatable with respect to the number of digitized points used and differences in the digitized points on the perimeter of the tibial plateau. The tibial plateau was fitted geometrically as an ellipse, and our results show that this is a reasonable assumption in terms of repeatability in finding a centre (Figure 3.7).

There was a reduction in the number of points collected from the cadaveric specimen compared to the Sawbones model on the posterior tibial plateau due to the reduced access caused by the PCL ligament. Our study shows that this reduction may affect the repeatability of the procedure, as there is an increase between the SD of the centers found on the Sawbones model and on the cadaveric bone (0.8 mm to 1.7 mm ML; 0.5 mm to 1.3 mm AP). This increase may also be due to the uncertainty of the location of the edge (perimeter) on the tibial plateau with the presence of the meniscus and other soft tissues that did not exist on the Sawbones model. However, our bootstrapped results on the cadaveric model show that increasing the number of points sampled around the perimeter of the plateau may decrease the SD to within an acceptable variation.

We also compared the centre calculated from the ellipse-fit algorithm to a digitized centre (centre of the tibial eminences) that is typically used in some CATKR procedures (on the Sawbones model). From this Sawbones experiment, we see that the bias from our calculated centre to the centre of the tibial eminences is less than 1 mm in the ML direction, but around 5 mm anterior in the AP direction. Digitizing the centre of the tibial eminences in the cadaveric model was overlooked during our experiments.

The mediolateral location supports studies that report placement of the tibial component to be in proper alignment when the mediolateral centre lies in line with the centre of the eminences (that lines up with 1 mm medial to the tibial tubercle) (Dalury, 2001). However, our algorithm reports the tibial centre to be anterior to the digitized tibial eminence centre for the Sawbones model. Also, the location of the tibial eminences on the plateau is variable and may not always represent an accurate AP centre of the knee.

A study that measured the reproducibility of tibial landmarks in 27 tibia stated that in 24% of the knees the medial eminence was difficult to obtain. For the tibias in which they could identify a medial eminence, the SD of the distance between the medial eminence to the posterior border of the ACL was variable, it was concluded that the location of the medial eminence should not be used as a landmark for ACL reconstructive surgery (Hutchinson and Bae, 2001).

In conventional TKA, the anterior posterior location of the tibial component is usually decided by coverage of the component on the tibial plateau. However, the posterior tibial cut is based on the mechanical axis that joins the tibial knee centre to the ankle centre. Changes in AP deviations contribute to a change of angle of the posterior tibial cut (5mm = 1°) (Johnson & Johnson Orthopaedics).

A bias between the centre of the tibial eminences and the calculated tibial centre from coverage of the plateau means that what is thought to be a neutral cut in a CATKR that has used the centre of the tibial eminences as the tibial centre can actually contribute to unaccounted-for posterior or anterior slope. While proper tibial component placement with respect to posterior slope is a topic of debate, most implant companies have posterior slope already built into their component. What is known is that the tibial component should not be in excessive posterior slope or anterior slope. The uncertainty that exists in the anteroposterior relationship between the centre of the tibial eminences and the tibial knee centre suggests that the 0 – 3° posterior slope that was proved to be biomechanically the most stable (Bai et al., 2000) may be difficult to achieve with previous methods.

3.4.2 Strengths and weaknesses of study

This study was performed on an intact fresh cadaveric knee of a 76 year old female. While the ligaments were present as in a typical TKA patient, osteoarthritis was not present in this subject. This study was performed on a single cadaveric knee. Anatomic variations of the tibial plateau are inherent in a population (Dalury, 2001; Hutchinson and Bae, 2001). Further testing on more specimens is necessary to determine whether anatomic variations will have a significant effect on the robustness of the ellipse-fit algorithm.

This study was performed using one operator. This was due to limited access to the fresh cadaver, allowing time for one subject to perform the experiment. After performing the experiment on the cadaver, we observed that presence of soft tissues on the perimeter of the plateau of a fresh cadaver may be subject to operator judgment as the rim is not as well defined as the Sawbones model. Further experiments are necessary using more subjects to determine inter-operator repeatability of this method on a cadaveric knee.

The anatomical reference frame defined to compare mediolateral and anteroposterior variation was defined by digitizing specific points on the cadaveric limb. This may not be the same points digitized on cadaveric specimens in other future studies. It is therefore difficult to compare mediolateral and anteroposterior variation between other studies.

This digitization is performed before the tibial cut is made. The tibial knee centre defined by this algorithm assumes that when bone is resected from the plateau, the remaining bone has a similar shape to the original plateau so that the centre remains true. While this assumption may be valid for a small depth of resected bone, this may not be the case if a large depth of bone is resected. In this case, it may be more beneficial to digitize the perimeter of the tibia at the specified resection depth from the tibial plateau. Special instrumentation attached to a digitizing probe may be needed to keep this depth constant, but this may provide a more accurate centre location for the centre on which the tibial implant will eventually be placed.

An ellipse is fit to the tibial plateau in this study. This easily implemented algorithm shows promise for good repeatability. While an ellipse-fit was chosen because it returns a well-defined centre, and mediolateral and anteroposterior directions (major and minor axes), a shape more representative of the tibial plateau could also be used. Possibilities for this shape include the anatomical shape of the tibial plateau or the shape of typical tibial implants. The tibial plateau may fit these shapes more repeatably. The computation of the fitting cost function will be somewhat more complex as it will be somewhat more difficult both to represent the tibial outline and to compute the distance from the digitized points to the outline.

3.4.3 Conclusions

The use of an ellipse-fit algorithm to define a tibial knee centre based on optimum coverage of the tibial plateau shows good repeatability on this knee (1.3 mm SD AP, 1.7 mm SD ML). The ellipse centre is shifted anteriorly by 4.6 mm on the Sawbones model relative to the centre of the tibial eminences. Use of the tibial eminences to locate the anteroposterior tibial centre should therefore not be used as the primary reference for anteroposterior tibial plateau coverage.

3.5 References

Andriacchi, T. (1994) Dynamics of malalignment. *Orthop Clin North Am* **25** (3): 395-403.

Bai, B., Baez, J., Testa, N., and F.J. Kummer. (2000) Effect of posterior cut angle on tibial component loading. *J Arthroplasty* **5**: 916-920.

Berger, R.A., Rubash, H.E., Seel, M.J., Thompson, W.H., and L.S. Crossett (1993) Determining the rotational alignment in total knee arthroplasty using the epicondylar axis. *Clin Orthop* (286): 40-7.

Confalonieri, N. Saragaglia, D., Picard, F., Cerea, P., and K. Motavalli (2000) Computerised OrthoPilot system in arthroprosthesis of the knee. *J Orthopaed Traumatol* **2** (91): 91-98.

Churchill, D. L., Incavo, S. J., Johnson, C. C., and B.D. Beynnon (1998) The transepicondylar axis approximates the optimal flexion axis of the knee *Clin Orthop* (356): 111-118.

Dalury, D. (2001) Observations of the proximal tibia in total knee arthroplasty. *Clin Orthop* (389): 150-155.

Delp, S.L., Stulberg, D.S., Davies, B., Picard, F., and F. Leitner (1998) Computer assisted knee replacement. *Clin Orthop* (354): 49-56.

Dorr L.D., and R.A. Boiardo (1986) Technical considerations in total knee arthroplasty. *Clin Orthop* (205): 5-11.

Ecker, M.L., Lotke, P.A., Windsor, R.E., and J.P Cella (1987) Long-term results after total condylar knee arthroplasty. Significance of radiolucent lines. *Clin Orthop* (216): 151-158.

Fuiko, R., Kotten, B., Zettl, R., and P. Ritschl. (2003) Landmarks for navigated implantation of total knee arthroplasty (TKA). In Langlotz, F, Davies, B.L., and A. Bauer (Eds): *3rd Annual Meeting of CAOS-International Proceedings*: 108-109.

Gander, W., Golub, G.H., and R. Strebel. (1994) *Fitting of circles and ellipses least squares solution.* Technical document ETH Zurich Departement Informatik, Institut fur Wissenschaftliches Rechen.

Hofmann, A.A., Bachus, K.N., and R.W. Wyatt (1991) Effect of the tibial cut on subsidence following total knee arthroplasty. *Clin Orthop* (269): 63-69.

Hutchinson M.R., and T.S. Bae (2001) Reproducibility of anatomic tibial landmarks for anterior cruciate ligament reconstructions. *Am J Sports Med* **29** (6): 777-80.

Jeffery, R., Morris, R., and R. Denham (1991) Coronal alignment after total knee replacement. *J Bone Joint Surg Br* **73-B** (5): 709-714.

Krackow, K.A., Serpe, L., Phillips, M.J., Bayers-Thering, M., and W.M. Mihalko. (1999) A new technique for determining proper mechanical axis alignment during total knee arthroplasty: progress towards computer-assisted TKA *Orthopedics* **22** (7): 698-702.

Kunz, M., Strauss, M, Langlotz, F., Deuretzbacher, G., Ruther, W., and L.P. Nolte (2001) A non-CT based total knee arthroplasty system featuring complete soft-tissue balancing. In: Niessen W, Viergever M (Eds) MICCAI 2001. *LNCS* **2208**, Springer-Verlag: 409-415.

Laskin, R.S. (1991) Bone resection techniques in total knee replacement. In Laskin R.S. (ed): *Total knee replacement.* Springer Verlag, London Limited.

Lemaire, P., Piolette, D., Meyer, F., Meuli, R., Dorfl, J., and P. Leyvraz. (1997) Tibial component positioning in total knee arthroplasty: bone coverage and extensor apparatus alignment. *Knee Surg Sports Traumatol Arthrosc* **5**: 251-257.

Liau, J. Cheng, C., Huang, C., and W. Lo. (2002) The effect of malalignment on stresses in polyethylene component of total knee prostheses – a finite element analysis. *Clin Biomech* **17**: 140-146.

Lotke, P.A., and M.L. Ecker (1977) Influence of positioning of prosthesis in total knee replacement. *J Bone Joint Surg* **59A** (1): 77-79.

Mantas, J.P., Bloebaum, R.D., Skedros, J.G., and A.A. Hofmann (1992) Implications of reference axes used for rotational alignment of the femoral component in primary and revision knee arthroplasty. *J. Arthroplasty* **7** (4): 531-535.

Moreland, J.R. (1988) Mechanisms of failure in total knee arthroplasty. *Clin Orthop* (226): 49-64.

Nizard, R. (2002) Computer assisted surgery for total knee arthroplasty. *Acta Ortopaedica Belgica* **68** (3): 215-230.

Perillo-Marcone, A., Barrette, D.S., and M. Taylor (2000) The importance of tibial alignment – Finite element analysis of tibial malalignment. *J Arthroplasty* **15** (8): 1020-1027.

Poivache, P.L., Insall, J.N., Scuderi, G.R., and D.E. Font-Rodriguez (1996) Rotational landmarks and sizing of the distal femur in total knee arthroplasty. *Clin Orthop* (331): 35-46.

Sharkey, P.F., Hozack, W.J., Rothman, R.H., Shastri, S., and S. Jacoby (2002) Why are total knee arthroplasties failing today. *Clin. Orthop* (404): 7-13.

Stindel, E., Briard, J., Merloz, P., Plaweski, S., Dubrana, F., Lefevre, C., and J. Troccaz. (2002) Bone morphing: 3d morphological data for total knee arthroplasty. *Comp Aid Surg* **7**: 156-168.

Stulberg, S.D., Loan, P. and V. Sarin. (2002) Computer-assisted navigation in total knee replacement: results of an initial experience in 35 patients. *J Bone Joint Surg* **84A** (S2): 90-98.

Tetsworth, K., and D. Paley. (1994) Malalignment and degenerative arthroplasty. *Orthop Clin North Am* **25** (3): 367-377.

Walker, P.S., and A. Garg (1991) Range of motion in total knee arthroplasty - A computer analysis. *Clin Orthop* (262): 227-235.

Chapter 4: Kinematic model and evaluation of an adjustable cutting guide for use in computer assisted total knee replacement surgery

4.0 Overview

The next stage in implementing the CAKTR was to integrate and evaluate a prototype adjustable cutting guide designed previously. This chapter will describe the need for such a guide, the guide that was developed as a student project, the kinematic model developed by the author to relate the desired cutting plane to the actual cutting plane, and an evaluation of the resulting implementation.

4.1 Use of an adjustable cutting guide in CATKR surgery

Once the surgeon performs the necessary manipulations and digitization to determine the desired cutting guide plane either for the proximal tibial cut or the distal femoral cut, it is necessary to accurately locate these planes with a cutting guide so that the appropriate bone cut can be made. The plane of the cutting guide must be tracked so the surgeon can line it up with the desired cutting plane. There are two ways in which this can be done. In some CATKR systems, (e.g. Surgetics, VectorVision), the surgeon holds the tracked cutting guide in his or her hand and lines up the coloured lines representing the desired cutting plane and the guide cutting plane while watching the computer screen in real time (Figure 4.1).

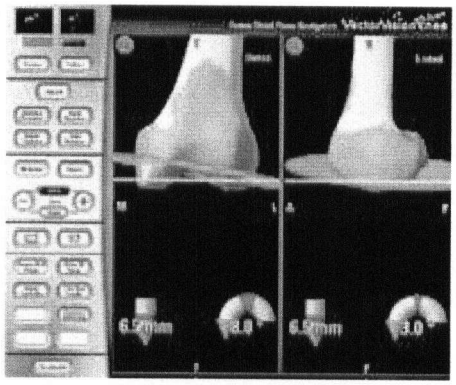

Figure 4.1: Interface for VectorVision Knee (Image courtesy BrainLAB).
The cutting block plane is lined up with the desired cut plane using hand-eye co-ordination.

These planes must line up in both the frontal and sagittal views. This can prove to be difficult as the update time may be insufficient for the fine movements of the hand, and

there may be need for constant readjustment. Also, trying to follow the desired movement in both the sagittal and frontal views simultaneously can be difficult and time consuming, and the process of securing the guide in place once positioned freehand is likely to shift the guide.

We decided that a faster and more accurate approach would be to design a device that could first be placed on the bone in approximately the correct position, and then sequentially adjusted under computer guidance. A prototype was already being manufactured at UBC when commercial systems (Orthopilot, Stryker) released similar devices (Figure 4.2) in their latest versions. Our system differs from these commercial systems in that it is intended to be mounted first, then adjusted, whereas the commercial versions appear to be designed for adjusting the position of a conventional cutting guide prior to securing it in position.

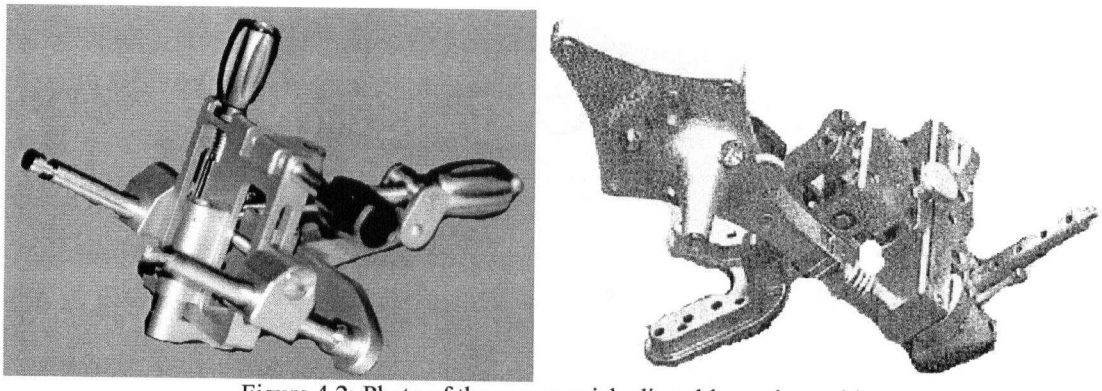

Figure 4.2: Photo of the commercial adjustable cutting guides
from Orthopilot Version 4.0 (left) and Stryker Knee (right).
Orthopilot photo taken by Dr. A. Hodgson at the Orthopilot display table at the CAOS 2003 conference.
Stryker photo from Krackow et al., 2003.

This type of device should eliminate the variability in the manual securing process. However, to our knowledge there is currently no literature on the difference between the desired cut plane and guide cut plane resulting from this hand-held procedure.

The balance of this chapter presents the conceptual and theoretical design of our cutting guide, a description of the physical prototype, a kinematic model used to predict required adjustments, and its incorporation into the computer-assisted technique.

4.2 Design of the cutting guide

The drawings for the first prototype of the adjustable cutting guide for the NCL CATKR system was done by a group of two undergraduate students for their MECH 455 course project. The students reported jointly to the author, Dr. A. Hodgson (lab director), and Christopher Plaskos, a doctoral student in our lab whose work focused on bone cutting techniques.

This design was subsequently manufactured by the BCIT Health Technology Group.

4.2.1 Prototype design (from Eaton and Bouchard, 2003)

The main objectives for the design of the guide were as follows:

- 3 degrees of freedom of adjustable motion (rotation about the coronal and sagittal planes and linear translation in the axial plane) easily controlled by the operating surgeon; this enables the cutting plane to be adjusted to the joint line and be easily placed into varus/valgus or posterior slope/flexion.
- a modular base mounted with bone screws/pins onto bone; a base is necessary to interface the adjustable part of the guide to the bone. It must be easily secured to the bone, and account for shape differences in the tibia and femur.
- the cutting guide must be mounted on bone exposure of less than 4 cm in the proximal-distal (PD) direction; this is similar to the bone exposure currently present in conventional surgery.
- overall PD length of less than 15 cm; this criteria was chosen so that the design was not excessively bulky for ease of use.

The final design consisted of an alignment adjustment system, a resection tool–guide interface, and a base to attach the guide onto the bone (Figure 4.3).

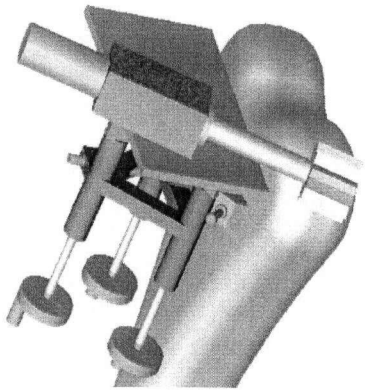

Figure 4.3: CAD drawing of the cutting guide design
(Image courtesy of Dan Eaton and Devan Bouchard).

The final design incorporates an alignment adjustment system that used a minimum constraint approach - three adjustable degrees of freedom of the guide plate are controlled by three screws fixed to the base (Figure 4.4a). Spherical balls are fixed onto the ends of the screws, and fit inside three cylindrical channels that are mounted onto the guide plate. These channels converge to a common centre and are spaced 120 degrees apart in an inverted Y- formation. As the screws rotate, the spheres spin and translate inside these cylindrical channels, causing the attached plate to tip in each direction (Figure 4.4b).

The resection tool-guide interface is a flat guide plate against which the surgeon can press a flat surface of a milling tool (Figure 4.3). The reference array would be attached to this flat guide plate (Figure 4.4b)

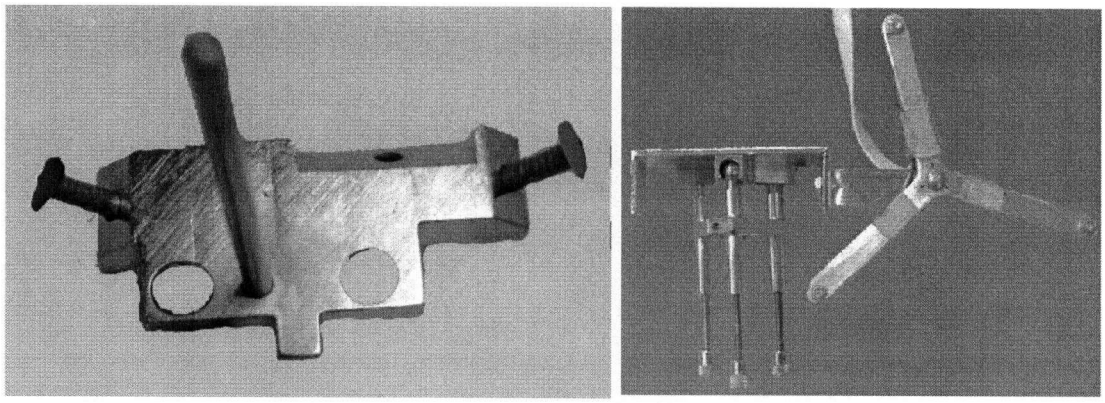

Figure 4.4: (a) Cutting guide base (left), (b) alignment adjustment system attached to guide resection plate. An array is rigidly attached to the guide plate so its location can be calibrated (right).

The base chosen was similar to that of a tibial cutting block. It consists of a small block constrained with three pins that enter the bone in different directions (Figure 4.4a). Bone pins were chosen to minimize installation time and keep the procedure similar to the current technique. Three pins positioned off centre would constrain all six degrees of freedom. Two pins in different directions constrains all three degrees of freedom axially, and two degrees of freedom rotationally. The third pin constrains the last degree of rotational freedom.

Though the base is an important component of the design, it was not the primary focus of the undergraduate project. At this stage in the development, we were more concerned with the workings of the alignment control system.

The author performed the remainder of the work described in this chapter.

4.2.2 Integration of the design

Once the cutting guide is attached to the bone and is in a nominally correct position, the system must advise the surgeon how much to turn each screw to bring the guide into proper alignment. To do this we required a kinematic model. This model would allow us to calculate differences between the actual and desired guide cutting planes, and inform the user how much to turn each screw to bring these planes into alignment.

4.2.2.1 Kinematic model

The cutting guide is adjusted by lengthening or shortening three legs: the medial, lateral and anterior (Figure 4.4b). The values calculated for adjusting each of these legs assumes that the normal to the cutting guide plane is perpendicular to the adjustment legs (Figure 4.5), as distances that are calculated along the direction of the normal to the cutting guide plane are then divided by the pitch of the screw of the adjustment legs to provide a value. Though this angle may never be perpendicular, the iterative process evaluating whether the cutting guide plane has reached the desired cut plane allows for the number of turns value to be approximate.

The contact points must therefore digitized on the guide plane surface so that the distance (d) between these points to the desired cutting plane along the normal of the guide plane can be calculated. This distance is then converted to the number of turns by dividing by

the pitch of the screw (Figure 4.5). Both planes must have unit normals pointing in the same direction, and be in the same reference frame.

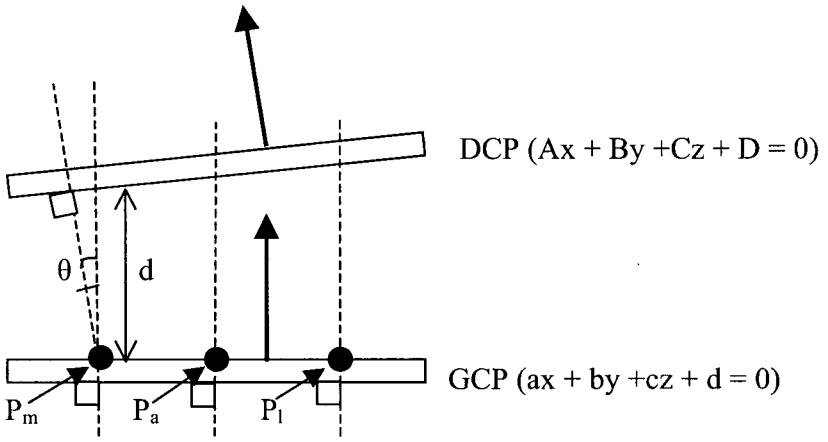

Figure 4.5: Diagram of the Guide Cut Plane (GCP) and the Desired Cut Plane (DCP).
The distances (e.g. d) from each point contact P_m, P_a, and P_l in the direction of the normal to the guide cut plane is calculated.

The details of the calculations and the procedure are as follows:

The guide cutting plane must be evaluated in the same bone array reference frame as the desired cut plane. The guide plane has a dynamic reference plane attached to it, and is a rigid body with the reference frame.

The guide plane (GCP_g) is first digitized with a point probe in the guide array reference frame (g). At least three points are necessary to define this plane. Typically, about 6 points should be digitized. A plane is then fit to these points (ax+by+cz+d=0). This equation of the plane in the guide array reference plane does not change. The location of the contact points P_{mg}, P_{lg} and P_{ag} must also be known in the guide reference array. These points are also digitized with the point probe.

When the user evaluates the location of the guide cutting plane in the bone reference frame (GCP_b), the system actually determines the location of the guide reference array in the bone reference array. We first determine transformations between these two reference arrays, and then transform the guide plane (GCP_g) into the bone array reference

frame (b) by first transforming the normal (a,b,c), and then adjusting the distance (d) term.

The normal to the guide cutting plane (N_{GCP}) must be in the same direction as the normal to the desired cutting plane (N_{DCP}) [both in the bone reference frame]. The normal to the desired cutting plane is known, as it uses a known joint centre (hip and ankle for desired cut planes of the femur and tibia respectively) to ensure proper orientation. The angle between the normals are then checked using the equation:

$$\vartheta = a\cos(N_{GCP} \bullet N_{DCP})$$

If the normals are greater than 90 degrees from each other, the guide cutting plane equation is converted so that the normal lies in the opposite direction:

$$GCP_b = -1 * GCP_b$$

The contact points P_a, P_m, and P_l are also transformed into the bone array reference array.

$$P_{(x)b} = T_{bg} * P_{(x)g}$$

where x = m, l, or a. The distance between these points and the DCP_b is calculated in the direction of the normal to the GCP_b. For example, the distance between the guide cutting plane and the desired cutting plane along the guide cutting plane normal for the medial leg of the guide is (from Figure 4.5):

$$d = \frac{(A,B,C) \bullet (x_{Pm}, y_{Pm}, z_{Pm}) + D}{(A,B,C) \bullet (a,b,c)}$$

Distances are calculated for each contact point (P_m, P_l, and P_a). Using the pitch of the screw (0.71 mm), the number of turns is calculated for each adjustable leg:

$$No.turns = {}^{d(mm)}\!/_{0.71mm}$$

4.2.2.2 User Interface

The distance and number of turns that allow each contact point (P_{mb}, P_{lb}, and P_{ab}) on the GCP_b to achieve the DCP_b should be displayed to the user. In our current user interface, a bar graph is displayed each time the user evaluates the status of the planes (Figure 4.6). This graph shows the positive or negative distance that the contact points should travel

(+ve distance and #turns represent upward travel and turning of the knobs to the right). Above each distance bar is the number of turns required to achieve this distance.

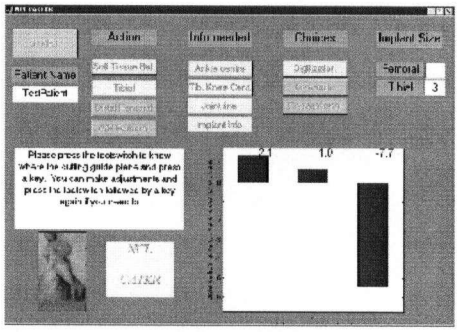

Figure 4.6: Graphic User Interface (GUI) of the bar graph prompting the user to adjust the screws by the number of turns displayed on the screen.

Once the distances between the contact points (P_{mb}, P_{lb}, and P_{ab}) on the GCP_b, and the DCP_b are within 0.1 mm of each other, the system exits and the user can proceed to make the cut.

4.3 Evaluation of the cutting guide prototype

After building the prototype, we evaluated it for overall capabilities and unwanted movement. This allowed the surgeon to have specifications about the range of proximal/distal movement, varus/valgus angle and posterior slope angle that can be achieved and the amount of time that it takes to achieve this motion. Unwanted movement of the cutting guide during use could also occur due to excessive clearances between sliding parts introduced during manufacturing and also due to inadequate fixation at the bone-guide interface. Such movements while cutting could affect the implant in both the frontal and sagittal planes (varus/valgus and flexion/extension errors). If there is movement in the proximal or distal direction, the joint line may be elevated or lowered.

4.3.2 Methods for quantifying range and unwanted movement

In order to test the design of the cutting guide we mounted the base of the cutting guide and a dynamic reference frame onto a rigid body (block of wood). We used wood, as it was easier to mount the base onto wood as opposed to the Sawbones model for this

benchtop evaluation. Also, the wood provided the use of a flat surface that could be independently digitized for initial testing of the kinematic model (Figure 4.7).

We then inserted the adjustable portion of the cutting guide (with an attached dynamic reference frame) to its base and adjusted the cutting guide plane to its lowest height (Figure 4.7).

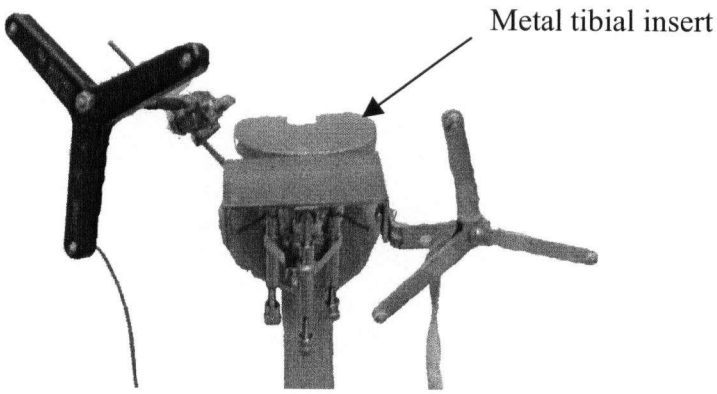

Figure 4.7: Equipment setup used to evaluate the range and uncertainty of the cutting guide (benchtop evaluation). The metal tibial tray provided a desired cut plane for testing the kinematic model.

We used a Flashpoint 5000 optoelectronic localizer (SD 0.35 mm; Boulder Innovators, Boulder, CO) to measure the locations of the cutting guide plane in the wood reference frame. We pressed the foot button to capture the location of the guide reference frame in the wood reference frame for each plane location that we wanted to measure.

4.3.2.1 Quantifying range

In order to determine the precision of the measuring system (an estimate of the noise in the system), we first measured the location of the plane at its lowest height 20 times.

We then determined the proximal/distal range of the guide by measuring the location of the cutting plane after adjusting all legs to their highest height. We also measured the time taken to perform this manipulation.

We then adjusted the medial leg to its lowest height to measure the maximum angle that could be achieved in this direction, and measured the time for this adjustment. We returned this leg to its highest height so that the plane was once again horizontal, and

repeated this for the lateral then anterior leg. We calculated maximum angles for the plane sloping to the medial, lateral, and posterior directions.

These manipulations were performed without applying any pressure to the guide plane.

We computed the angle between the normals to compare all measured planes. For the proximal/distal range, the planes were levelled so that the normals were the same, and we compared the d-value of the plane equation.

4.3.2.2 Quantifying unwanted movement

Unwanted movement of the guide could occur at three interfaces, bone (wood) to base, base to the adjustable portion of the guide, and between the adjustable portion of the guide to the guide plane. We removed the adjustable portion of the guide and applied pressure to the base to investigate movement between the wood and the base.

We then placed the adjustable part of the guide on the base, and investigated movement at this interface by applying pressure to the legs.

In order to investigate movement between the guide plane and the adjuster, we then adjusted the plane to its maximum height and captured this plane location. We applied a force using the hand to the cutting plane surface on the medial and lateral sides of the plate and if a change was noticed, we measured the new location of the plane, and tried to identify the cause of the movement. Quantifying this movement would tell us valgus or varus error that could be encountered while using a cutting instrument on the plane.

This was repeated in the anterior/posterior part of the guide plane (for posterior slope or flexion error).

4.3.3 Evaluation on a Sawbones model

The cutting guide was then attached to a plastic tibia model (Sawbones, Pacific Research Laboratories, Vernon, WA) and further comments were made about the feasibility of the design (Figure 4.8) in the discussion section.

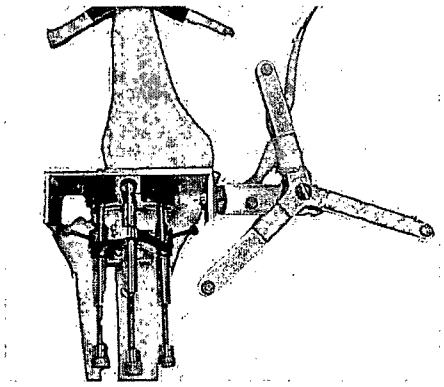

Figure 4.8: Equipment setup to evaluate the use of the cutting guide on a 'Sawbones' tibia model.

4.3.4 Results

Table 4.1 summarises the range, precision, and error of the various adjustments outlined.

Table 4.1: Range and error for the cutting guide evaluated on the block of wood.

Specification	Value	Time taken to achieve (s)
Precision of measuring cutting plane in one location	0.0003° SD (20 samples)	n/a
Proximal/distal range	32.8 mm	60
Right leg range	19.4°	20
Left leg range	18.8°	20
Anterior leg range	17.8°	20
Valgus/varus error with pressure applied	0.7°±0.03 (20 samples)	n/a
Posterior slope/flexion error with pressure applied	0.8°	n/a

4.4 Discussion and Recommendations

This prototype of the cutting guide revealed that the cutting guide range was larger than needed for its application. We had chosen a large range of motion (ROM) for this prototype so that it could be adjusted into alignment regardless of the placement by the surgeon.

A second version of the cutting guide could have shorter adjustable legs if a specific adjustment range could be quantified for this particular technique. A resident/surgeon could use this prototype to assess on average the necessary adjustment range needed after attaching a base onto bone and making adjustments to known desired cutting planes. In

this way it may be possible to reduce the proximal-distal range to only 10 mm, and posterior slope/flexion adjustments to the 10° range.

We found that we could induce a deviation of roughly 1° when applying pressure to the cutting guide plane. We identified the cause of this valgus/varus error to be due to manufacturing of the adjustable legs. Though we specified slide fit between the barrel and the screw, one of the legs had a slight play, giving rise to toggle in the cutting guide plane. The actual tolerance between the barrel and the screw was specified to be 0.002". Calculations for this value were based on a cutting plane accuracy of 0.1° (Eaton and Bouchard, 2003).

Varus or valgus malalignment alters the loading distribution and kinematics at the knee. The mechanical axis (load line) no longer passes through the centre of the knee, but instead may shift medially in varus, or laterally in valgus. The corresponding compartment may become overloaded leading to an accelerated breakdown of the bone-cement/prosthesis interface. These unstable loading conditions can result in component loosening, excessive wear, subsidence, and ultimately revision TKA (Insall, 1985; Jeffery et al, 1991; Moreland, 1988). There are many factors influencing varus/valgus malalignment and a 1° contribution from the deviations in the cutting plane is unacceptable. Overall, for the entire surgery, valgus or varus malalignment should be no more than a 2-3° window in order to ensure high success rates.

We identified the cause of the posterior slope/flexion error to be due to the attachment bar between the cutting guide base and the adjustable portion. Applying pressure to the front of the cutting guide plane caused this bar to flex allowing the cutting plane to change location by 0.8°. This bar is currently 1/8" in diameter. Modeled as a simple cantilever beam, we calculate that for an estimate of 10 N applied to the plate, the displacement angle is 0.6° [0.44 mm movement]. Therefore, for less than 0.1 mm movement, the diameter of this attachment bar should be 1/5" so that this does not occur.

Flexion/extension errors contribute to abnormal kinematics, soft tissue imbalances, and component subsidence (Hofmann et al, 1991). These errors are caused when the mechanical axis (load line) passes anterior or posterior to the centre of the knee in the sagittal plane. On the femur, this can result in incorrectly referenced anterior and

posterior resections causing notching of the anterior cortex (leads to high risk of femoral fracture) or a fixed flexion contracture (Hungerford et al, 1985). Though the attitude for posterior slope angles in tibia sagittal alignment varies, unwanted movement that may cause an anteriorly sloped cut can decrease the flexion range of motion and diminish the size of the flexion space posteriorly. This leads to posterior wedging, increased polyethylene wear or even anterior lift-off of the tibial component (Bai et al, 2000; Dorr and Boiardo, 1986; Walker and Garg, 1991). It is necessary to reduce this 1° error so that these complications do not occur.

There was also a slight rotation of the plate in the transverse plane. Though this does not affect the angle of the plane, we isolated the cause to be the attachments between the base and the adjustable portion. There were three fixtures designed to stop motion between these two pieces. These are a circular pin and an oval pin fitting into appropriate slots, and a plate that made contact with another plate. These fixtures were supposed to be manufactured with a tolerance of 0.005". It is necessary for these specifications to be met to ensure proper performance.

After the cutting guide was attached to the plastic tibia model, a few shortcomings in the design were revealed. The minimum distance between the base of the guide (attached to the bone), and the cutting guide plane was 14 mm. This is due to the guide channels being in the way of the base. For the guide-cutting plane to be manipulated, the cutting guide base must be placed at least this distance away from the desired cutting guide plane before manipulation can occur. Taking into account the resected bone, for this version of the cutting guide to work, the base of the guide would have to be mounted below the patella tendon attachment. This is clinically unrealistic. The cause of this oversight may be that the emphasis of the MECH 455 project was on the adjustment mechanism of the device. The design of the base, and its interaction with the bone and the adjustment component was not subjected to the same rigorous design discussion prior to it being manufactured.

A revised version of the cutting guide should allow the base to fit in between the guide channels so that they are not in the way. The angles between the guide channels (instead of 120°) could be changed for two of the legs to accommodate this.

The cutting guide was also presented and evaluated during a review process of the current stage of our integrated computer assisted knee technique by an expert surgeon (Dr. B. Masri). The following further recommendations were made for ease of use, and to accommodate the move towards minimally invasive surgery.

The surgeon stated that there was need for the attachment between the adjustable control system and the base to include accommodations for muscles overlying bone in this area. The surgeon also suggested making a sleeve to cover exposed screw threads that may get dirty during the procedure.

The current interface has a graph that showed the distance between the desired plane and the guide plane combined with the # of turns necessary for each leg for them to be aligned. The surgeon thought that the # of turns necessary should simply be superimposed on a diagram of the cutting guide so that it is clear which leg must be adjusted. He suggested that future real-time capabilities of the system would also be beneficial to the adjustment procedure, and hence reduce the amount of time and iterations necessary for the guide plane to align with the desired cutting plane.

In minimally invasive procedures, only a small medial portion of the proximal tibia is exposed compared to conventional surgery. The base should therefore be redesigned so that it only sits in this small section of exposed bone (Figure 4.9).

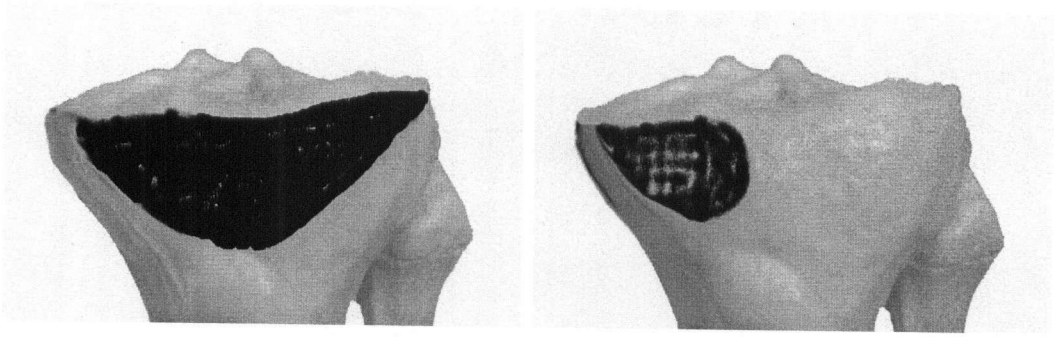

Figure 4.9:(a) The portion of exposed bone in a conventional surgery (photo taken in our laboratory – information on exposed bone from J&J Orthopaedics Primary TKR manual), (b) The portion of exposed bone that would be available in a minimally invasive surgery.

It is hoped that with these recommendations, the future design of the cutting guide would prove to be more conducive to this application.

This evaluation was performed only on our guide and we have not compared its performance to others currently on the market. Performance could be compared in terms of ease of use, and attachment and adjustment times to accurately locate the plane. As the base of this prototype is similar to a conventional tibial cutting guide, it can be assumed that attachment times would be similar as the accuracy of this position is not critical. During the evaluation by the expert surgeon it was found that about four iterations were necessary before the guide cut plane aligned with the desired cut plane. This may take about two minutes dependent on the care taken in turning the legs by the specified amount. Real time capabilities would greatly reduce this time. There is currently no literature on the performance of other similar adjustable cutting guides. The OrthoPilot and Stryker Knee recently incorporated adjustable cutting guides into their systems (Figure 4.2), but they were only on display at the Computer Assisted Orthopaedic Surgery 2003 conference and its adjustment times and performance cannot be discussed.

4.5 Conclusions

The main contribution of the current version of the adjustable cutting guide is its adjustable mechanism, and the kinematic model that allowed us to integrate the cutting procedure into our overall system. However, for our adjustable cutting guide to be clinically acceptable, modifications to the guide channels and the leg length are necessary. Real-time position display capabilities would also be highly beneficial to our system. With these changes, our adjustable cutting guide should eliminate the uncertainty associated with the current technique of securing the cutting guide currently used in other commercially available computer assisted systems.

4.6 References

Bai, B., Baez, J., Testa, N., and F.J. Kummer. (2000) Effect of posterior cut angle on tibial component loading. *J Arthroplasty* **5**: 916-920.

Dorr L.D., and R.A. Boiardo (1986) Technical considerations in total knee arthroplasty. *Clin Orthop* (205): 5-11.

Eaton, D., and D. Bouchard (2003) *Adjustable cutting guide for knee replacement surgery.* Report submitted for requirement of MECH 455, UBC, Vancouver, BC.

Hofmann, A.A., Bachus, K.N., and R.W. Wyatt (1991) Effect of the tibial cut on subsidence following total knee arthroplasty. *Clin Orthop* (269): 63-69.

Hungerford, D.S., Kenna, R.V., and K.A. Krakow (1985) Alignment in total knee arthroplasty. In Dorr LD (ed): *The Knee. Papers of the first scientific meeting of the Knee Society.* University Park Press, Baltimore: 9.

Insall J.N. (1985) Technique of total knee replacement. In Dorr L.D (ed): *The Knee. Papers of the first scientific meeting of The Knee Society.* University Park Press, Baltimore.

Jeffery, R., Morris, R., and R. Denham (1991) Coronal alignment after total knee replacement. *J Bone Joint Surg Br* **73-B** (5): 709-714.

Krackow,K.A., Phillips, M.J., Bayers-Thering, M., Serpe, L., and W.M. Mihalko (2003) Computer-assisted total knee arthroplasty: navigation in TKA. *Orthopedics* **26** (10): 1017-1023.

Moreland, J.R. (1988) Mechanisms of failure in total knee arthroplasty. *Clin Orthop* (226): 49-64.

Chapter 5: Design and integration of the NCL CATKR (Computer Assisted Total Knee Replacement) System

5.0 Abstract

In this chapter I describe the current status of the integrated system that we have developed in our lab. The system was developed as a Graphical User Interface (GUI) supported by Mathlab 6.1 (The MathWorks, Natick, MA). I outline all the required steps and choices of the procedure and describe details of the co-ordinate frames, algorithms and benefits of each choice. The integrated system was demonstrated to an expert surgeon on a mock-up lower limb model, with the surgeon performing the required digitization of the bone. The recommendations were either incorporated into the software or discussed as future work.

5.1 Introduction

A computer-assisted procedure is meant to complement and assist the surgeon. The techniques developed are essentially more accurate than conventional procedures. However, there are negative aspects to introducing new technologies into clinical practice. These are the system costs, increased operating time, and surgeon acceptance (DiGioia, 2003). In the end, however, adoption of computer-assisted technologies should improve patient outcomes due to the accessibility of more accurate, more reliable and less invasive techniques.

Despite these advantages, surgeons will encounter some difficulties when learning a computer-assisted surgical (CAS) system. Though descriptive and procedural knowledge is preserved, there is an increase in the complexity of operational and interactive knowledge (De Siebenthal and Langlotz, 2003). Mathematical algorithms are replacing the mechanical instrumentation of conventional total knee replacement procedures, and the registration for these algorithms require different components such as a computer, specific tools, and arrays. These tools are very different from those currently used in conventional surgeries.

Though many commercial systems exist on the computer-assisted total knee replacement market, these first generation systems are still in need of refinement to smoothly integrate

into current care models. They have to be refined and streamlined, particularly in the ways that they interface with the surgeon (Di Gioia, 2003).

The Neuromotor Control Lab (NCL) has been developing an image-free landmark based computer-assisted total knee replacement procedure since 1997. Since that time, many commercial systems have been released on the market. However, validation and repeatability of the algorithms used in these systems are either unknown or not verified. The goal of our lab is to provide a system that has been fully verified. It will provide a platform for research and development in this field. From 1997 to now, various researchers in our lab have worked on determining and verifying proper algorithms to accomplish all the goals of a CATKR procedure.

Integration of the entire system is the final step in software development. Each algorithm has been individually tested for repeatability, and an overall assessment of the system would be the next step after integration has occurred.

We have integrated our system creating an open architecture for research. Our system allows an easier transition between a CATKR and conventional TKR procedure. Other image-free landmark based systems (e.g. OrthoPilot) walk the surgeon through the procedure, allowing the surgeons no decisions or choices. The surgeon must perform all the registration and cuts in an exact order (Stulberg et al, 2002). While some may argue that this decreases the complexity of the system, surgeons tend to have different preferences in performing the order of cuts in surgery. This is seen in current conventional total knee replacement surgery where some surgeons have certain preferences in the order they perform the femoral, tibial or patella cuts. Also, differences in patient pathology may make it necessary to undertake actions in a non-standard sequence.

Our objective is to provide a system with modularity built into its design. We have designed our system so that any performed manipulation can be rejected or accepted, in the case of a known error. The user also always knows exactly the current stage in the procedure, and what still has to be done. The buttons on the interface are one of three colours representing 'ready', 'in progress', and 'complete'. An overview of the technical details of the program for our system can be found in Appendix C.

5.2. Design of integrated system

There are five required activities in an image-free landmark based computer-assisted total knee replacement procedure (CATKR). These are registration (gathering the necessary data for determining cutting planes and implant size), goal planning and bone cutting, implantation, and measuring success. Figure 5.1 represents the stages for an image-free landmark based CATKR procedure.

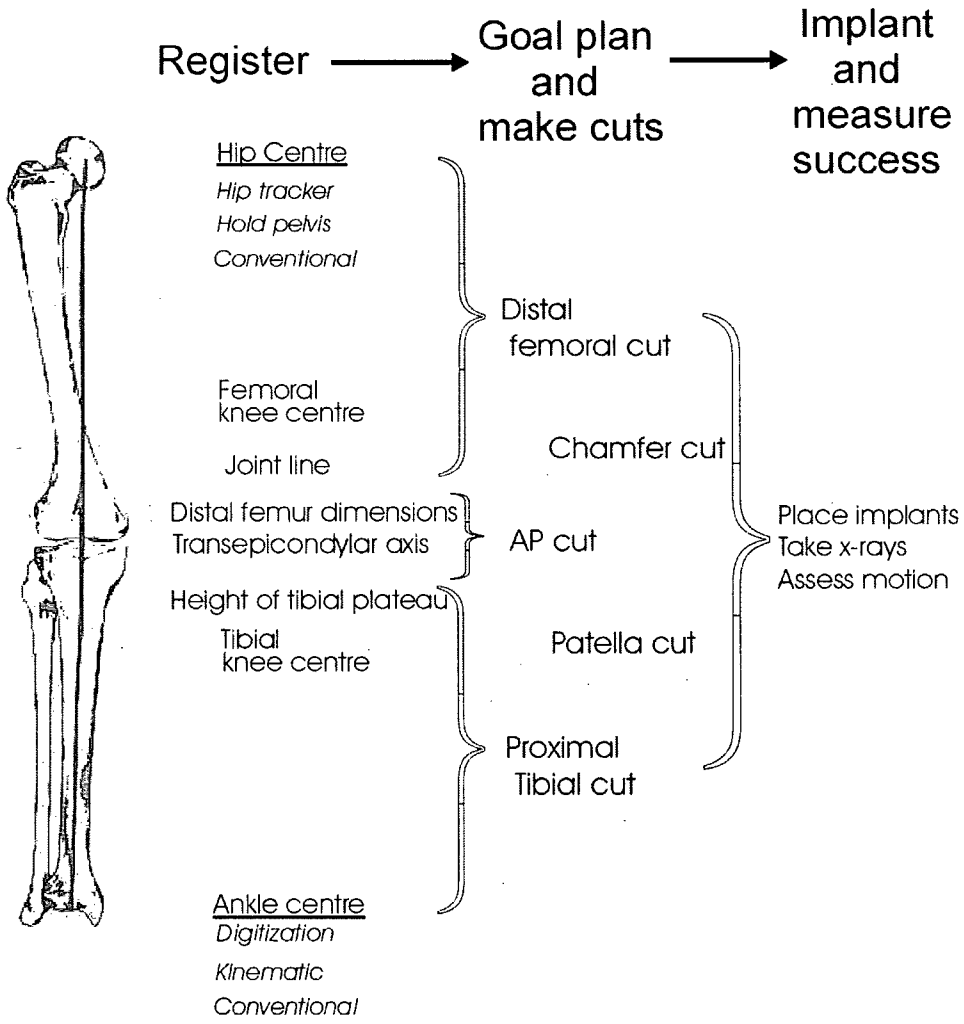

Figure 5.1: The stages of a computer-assisted total knee replacement procedure.
The surgeon must first gather necessary information specific to patient anatomy. This will define the mechanical axis of the leg, the rotational axis, dimensions for implant sizes, and joint lines. This information is used to determine the placement of the cuts so that the components can be implanted. Soft tissue balancing/assessment is also considered as part of the goal planning step.

There are many paths that one can take to get to the end. Our system allows users the flexibility to choose the path that they are most comfortable with, as in a conventional

surgery. The sequences that may occur are combinations of: assess alignment from soft tissues, register and cut the femur, and register and cut the tibia. While all specific algorithms have been tested on cadavers, the integration software has only been tested on a Sawbones (Pacific Research Laboratories, Vashon, WA) model thus far.

5.2.1 Equipment necessary for our CAS procedure

The necessary equipment in our system includes:

- an optoelectronic localizer (Flashpoint 5000, Boulder Innovators, Boulder, CO)
- rigid bodies containing light-emitting diodes
- adjustable cutting guide with rigid body attached
- point probe and plane probe
- computer, monitor and foot switch

Optional equipment includes:

- hip and ankle trackers designed to hold the rigid bodies to the pelvis and calcaneous

5.3 Steps in our CAS procedure

Figure 5.2 shows the initial interface at the start of the program.

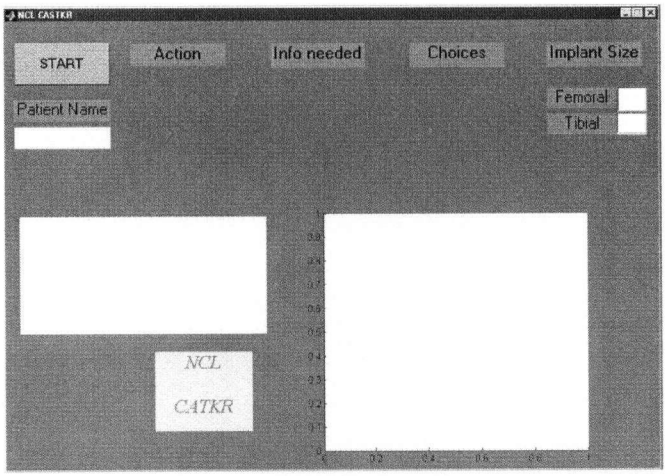

Figure 5.2 Graphical User Interface (GUI) at the start of the procedure.

Once the START button is pressed, a window pops up that requests the patients name and the leg on which the surgery is performed (Figure 5.3). This enables various pieces of information to be specifically saved throughout the procedure. This can be useful as a research tool allowing future cross-patient comparisons of various landmarks and centre locations.

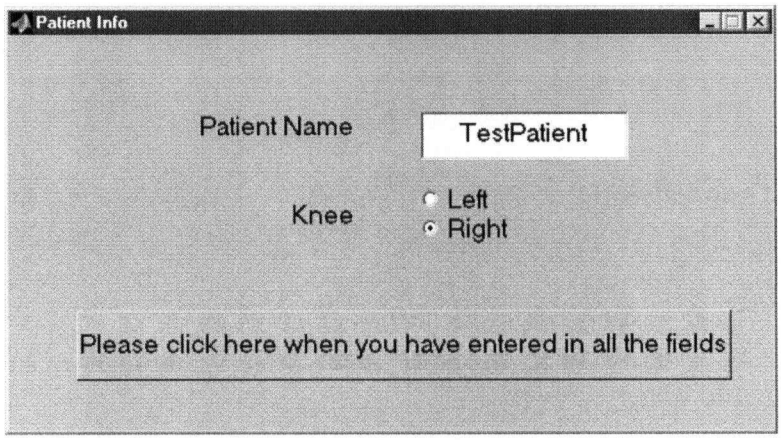

Figure 5.3: Patient Info pop-up screen.
On this screen, the surgeon informs the system which leg is being operated on.

5.3.1 Registration

Registration as it applies to image-free computer-assisted orthopaedic surgery is the process of collecting data to determine the critical features necessary for a landmark based image-free CATKR surgery. The critical features needed are:

- the hip and femoral knee centre for the femoral mechanical axis
- the tibial knee and ankle centre for the tibial mechanical axis
- the transepicondylar axis for proper rotational alignment.
- various other landmarks for appropriately sizing the femoral and tibial components and for preserving the joint line (Figure 5.1).

Before registration can occur for each bone, the active marker arrays must be rigidly attached to the femur and tibia. In order to keep the midline knee incision as small as possible, a small incision is typically made about 10 cm away from the exposed knee to allow the percutaneous fixation of these arrays via bone pins or screws. The base of the

array is designed for quick release so that it can be removed and replaced in the exact location (prototype only).

Registration for image-free landmark based systems occur entirely in the operating room. Once the patient name is entered, the program allows the surgeon to choose the first action. The recommended procedure is from top to bottom. The choices are: alignment from assessing the state of the soft tissues, performing registration for the femoral cut, and performing registration for the tibial cut (Figure 5.4). When each button is pressed, it turns from pink to yellow to show that the user is performing the particular action, while other buttons are grayed out (disallowed) so that they cannot be chosen until complete registration for the cut has occurred.

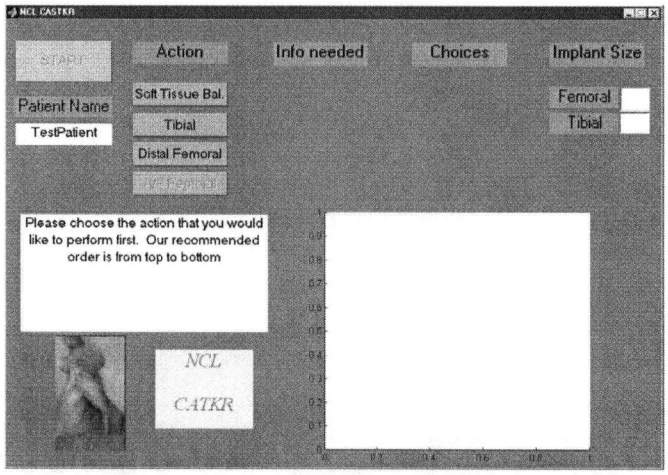

Figure 5.4: The GUI that allows the surgeon to make choices in the cut sequence. The name of the patient is also displayed on the screen.

After each stage of the procedure, the surgeon must give the go ahead to accept and move on. Therefore after each manipulation, a window pops up to this effect (Figure 5.5).

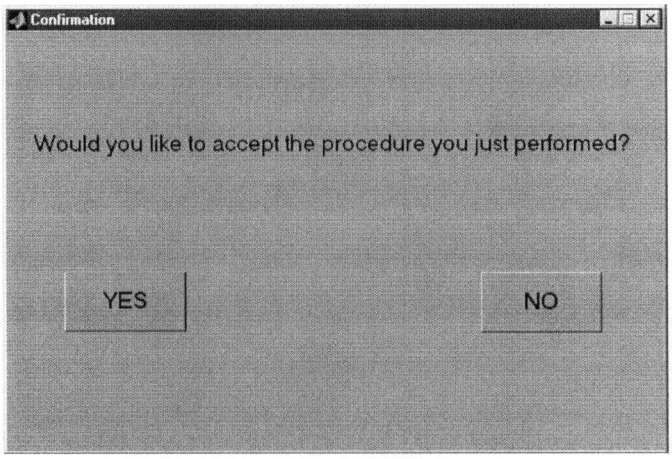

Figure 5.5: GUI for the confirmation step that allows the surgeon to repeat a procedure if he/she thinks that there was uncertainty in the way the manipulations or digitization was performed.

5.3.1.1 Soft tissue assessment

When the soft tissue button is pressed, the system should potentially allow the surgeon to perform manipulations to determine the state of the soft tissues. The system would then predict an alignment of the components so that these soft tissues are balanced.

This feature is in the initial development stage. Though previous research has been performed in this area, testing has never been performed on cadavers. Pig knees were used to test the feasibility of kinetic manipulations to determine the optimal placement of the components from the balanced soft tissues. Illsley (2002) found that this placement may be different from the mechanical or rotational axis alignment. He proposed a choice between placement determined from alignment with the mechanical axis, and from balancing soft tissues using kinematic manipulations. The system has not been tested with this button as all tests have been performed on a Sawbones model without soft tissues. Further development of the system will include integration of the soft tissue manipulation into this procedure.

5.3.1.2 Tibial cut (registration)

When the tibial cut button is pressed, all other actions are inaccessible. The required inputs for this cut are the ankle centre, tibial knee centre, joint line height, and the implant size (Figure 5.6). The user is able to perform the manipulations and measurements in any desired order.

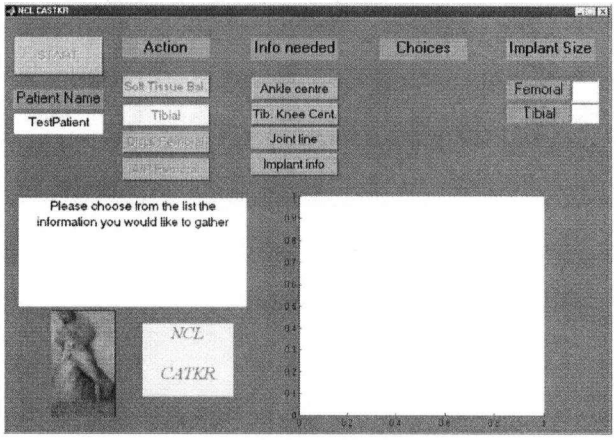

Figure 5.6: GUI that allows the surgeon choices in the sequence for collecting the requirements of the proximal distal cut.

5.3.1.2.1 Ankle centre

The surgeon may choose to find the ankle centre conventionally, by digitizing the malleoli, or by using a kinematic manipulation technique (Figure 5.7). The end result of this button (excluding the conventional choice) is the (x,y,z) location of the ankle centre in the tibial array frame. This location is also saved in a file for future use.

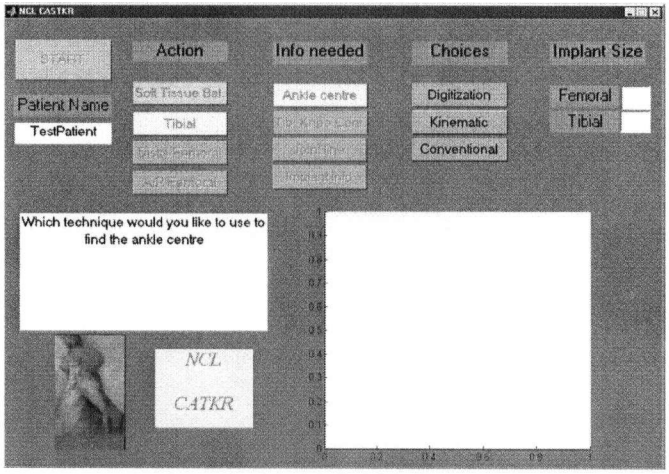

Figure 5.7: GUI that allows the surgeon to determine the ankle centre by three different choices - by digitizing the malleoli (centre determined using a built in off-set), by kinematic manipulation of the foot, or by using conventional instrumentation.

5.3.1.2.1.1 Digitization

Digitization of the lateral and medial malleoli is one method that the surgeon may choose to locate the ankle centre. This is currently the procedure in other CATKR systems. The system prompts the surgeon to pick up the point probe and digitize the most prominent

point of the medial, then lateral malleoli (Figure 5.8). An offset is then applied by the system to address the fibula bone resting on the talus. Research in our lab showed that though this technique may offer good mediolateral repeatability, bias effects in the anterior-posterior direction are somewhat larger than with the kinematic technique (another choice).

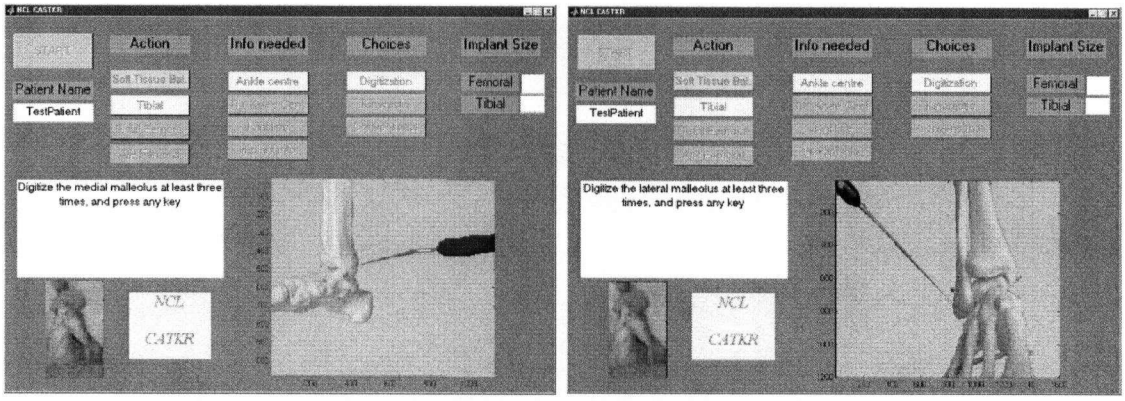

Figure 5.8: GUI showing that the medial (left) and lateral malleoli (right) must be digitized.

5.3.1.2.1.2 Kinematic

The kinematic technique uses measurements of the calcaneous relative to the tibia in conjunction with a spherical joint model to estimate the location of the ankle centre. Choosing the kinematic option prompts the user to place the calcaneal tracker on the patient. The foot is manipulated in dorsi/plantarflexion with the ankle in the neutral, inverted and everted positions, in/eversion with the ankle in the neutral, dorsiflexed and plantarflexed positions, and lastly a cycle of circumduction (Shute, 2002). The points collected by the calcaneal tracker in the tibial frame are fitted to a sphere whose centre represents a repeatable non-weight bearing centre. As the proper load bearing axis (mechanical axis) should actually link the weight-bearing ankle centre to the tibial knee centre, an offset is built into the system to accommodate this. The algorithm used to perform the spherefitting is the homogeneous transform (HT) method based on the fact that if two rigid bodies are connected with a spherical joint, the vector to the joint centre in the moving frame maps to a constant point in the fixed frame for all positions.

This algorithm was derived and validated in a previous study (Shute, 2002), and has been tested for repeatable ankle centre locations in 12 subjects with a resulting SD of 0.7 mm in the ML direction and 0.4 mm in the AP direction. The average bias applied to the non-

weight bearing centre determined in a population of young adults was a lateral and posterior shift of 2.7 mm and 6.9 mm respectively.

5.3.1.2.1.3 Conventional

If the conventional option is chosen, the system terminates registration for this cut. The cut is made with conventional instrumentation, and the user proceeds to the next cut. This conventional procedure is based on x-ray images to determine the joint line, a visual estimation of the tibial mechanical axis with an extra-medullary rod (Figure 1.4), and clamps to determine the ankle centre.

5.3.1.2.2 Tibial knee centre

For this step, the system prompts the surgeon to pick up the point probe and digitize the perimeter of the tibial plateau starting from an anterior point moving to the right (this ensures a right-hand co-ordinate frame for system calculations). Each digitized point should be no more than 5 mm from its nearest neighbour (Figure 5.9a). An exception for this is inaccessible areas of the posterior tibial condyles. The system fits the points to an ellipse using a geometric-fit algorithm that uses least squares (Gander et al, 1994)). This fits the ellipse based on maximum coverage of the tibial plateau. The centre of the ellipse is then slightly modified as the tibial knee centre (Chapter 3). The repeatability of this algorithm has been performed on a Sawbones models and on a fresh cadaveric knee. The mediolateral intra-operator repeatability for the cadaveric knee was 1.7 mm SD, and the anteroposterior intra-operator repeatability was 1.3 mm SD.

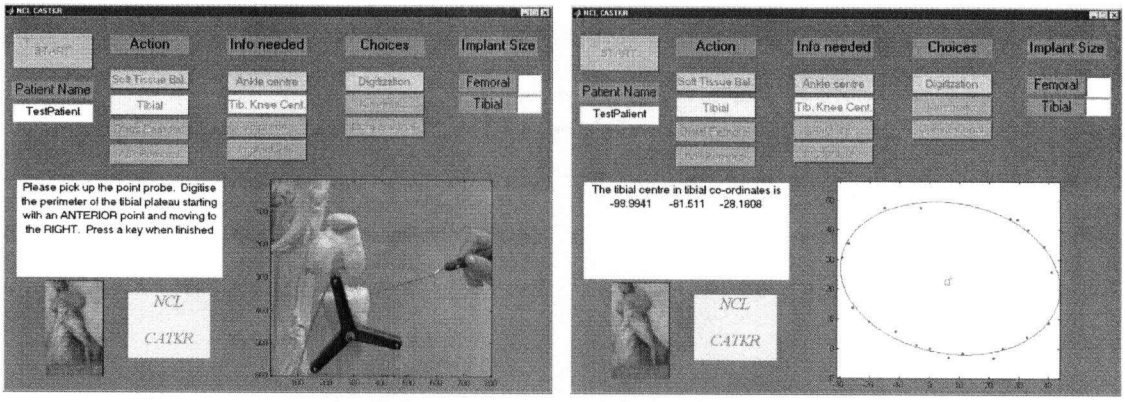

Figure 5.9: (a) GUI showing the digitizing procedure necessary to determine a tibial knee centre estimate. (b) GUI showing the best fit ellipse to the points digitized on the perimeter of the tibial plateau. The tibial co-ordinates displayed are for development purposes only.

The end result of this procedure is an (x,y,z) estimate of the tibial knee centre in the tibial array frame. A figure shows the digitized points and the best fit ellipse (Figure 5.9b) so that the surgeon can verify that the best fit ellipse was a reasonable estimate of the tibial plateau. This centre is also saved in a file in the case of future research.

5.3.1.2.3 Joint Line

The system prompts the user to use the point probe to digitise the highest point on the least damaged tibial condyle (Figure 5.10). This ensures the least amount of bone resection, and ensures that the joint line is not changed, which could otherwise lead to a loss of extension or flexion. This information is collected in the tibial array frame.

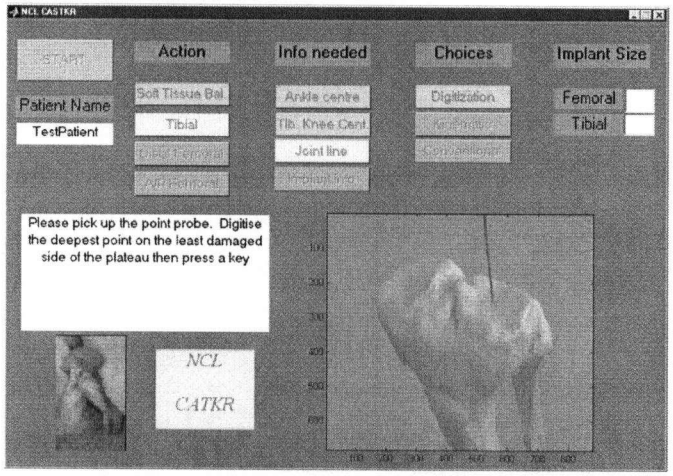

Figure 5.10: GUI showing the procedure for digitizing the joint line.

5.3.1.2.4 Implant Info

The surgeon inputs the type of implant that he or she would like to use in the procedure (e.g. Posterior Cruciate Retaining (PCR) curved, Posterior Stabilizing (PS)) (Figure 5.11). The system assumes a 10 mm default resection depth for the tibial plateau. The user is prompted whether this value should be increased/decreased depending on the state of the tibial plateau (theoretical only).

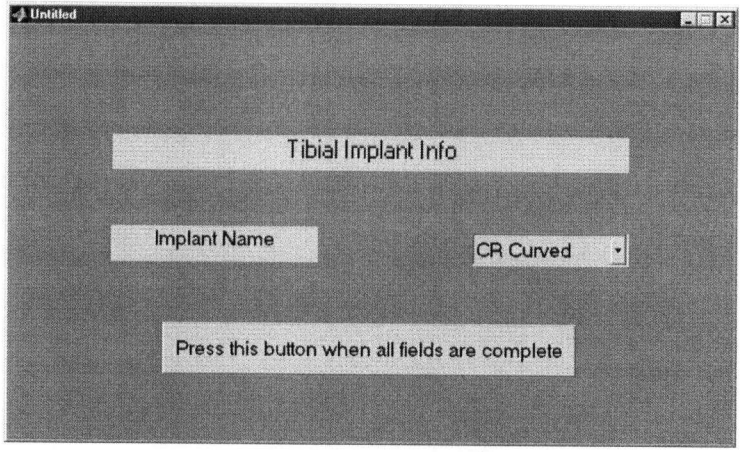

Figure 5.11: GUI that allows the surgeon to choose the tibial implant that he would like to use.

After all the required registration steps are complete for the tibial cut, the button changes colour to signify that the cut can now be performed. The user must press the tibial button again when they are ready to perform the cut. This will be addressed in a Section 5.3.2 'Bone Cutting'.

5.3.1.3 Femoral cut (registration)

If the femoral cut button is pressed, other action buttons become inaccessible. The four necessary requirements for proper femoral distal cut alignment are then displayed. These are hip centre, femoral knee centre, joint line, and implant size (Figure 5.12). The surgeon is then allowed to perform these procedures in any order that he chooses.

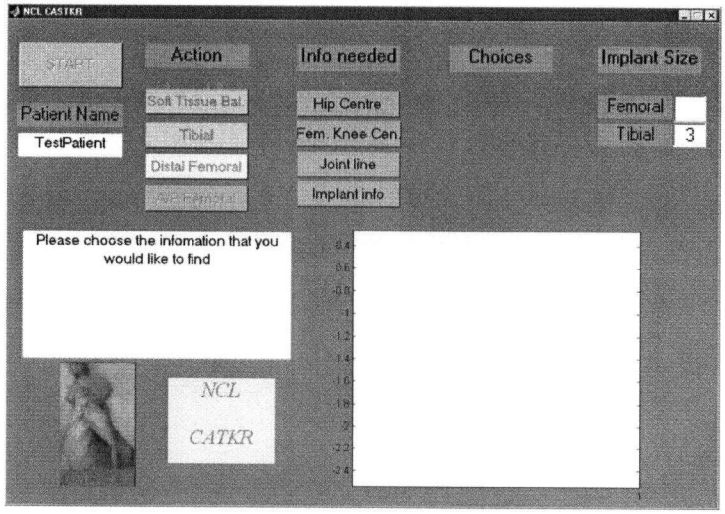

Figure 5.12: GUI showing the necessary information for completing the distal femoral cut.

5.3.1.3.1 Hip centre

The surgeon may choose to find the hip centre conventionally, by using a hip tracker, or by holding down the pelvis (Figure 5.13). The end result of this button (excluding the conventional choice) is the (x,y,z) location of the hip centre in the femoral array frame. This centre is also saved in a file in the case of future research.

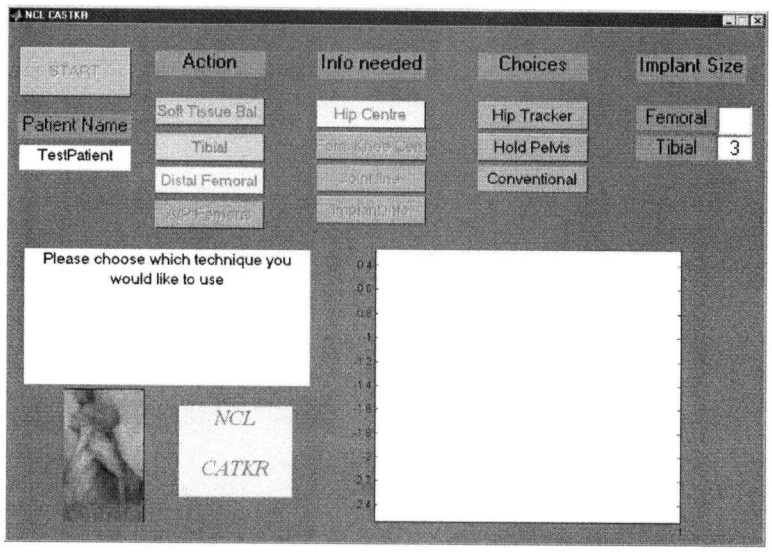

Figure 5.13: GUI showing the choices for determining the hip centre.

5.3.1.3.1.1 Hip tracker

An advantage of the hip tracker is that it accounts for pelvic motion in calculation of the hip centre. When this button is chosen, the user follows the procedure as outlined on the screen. Information is needed about the dimensions of the patient so that calculations could be made regarding the use of the tracker (Figure 5.14a). The surgeon is then prompted to place the tracker on the body. A stance position of the limb is captured to get a transform between the femoral reference array and the hip tracker array (Figure 5.14b). A force plunger is then used to apply a seating force to the tracker while kinematic manipulations are performed.

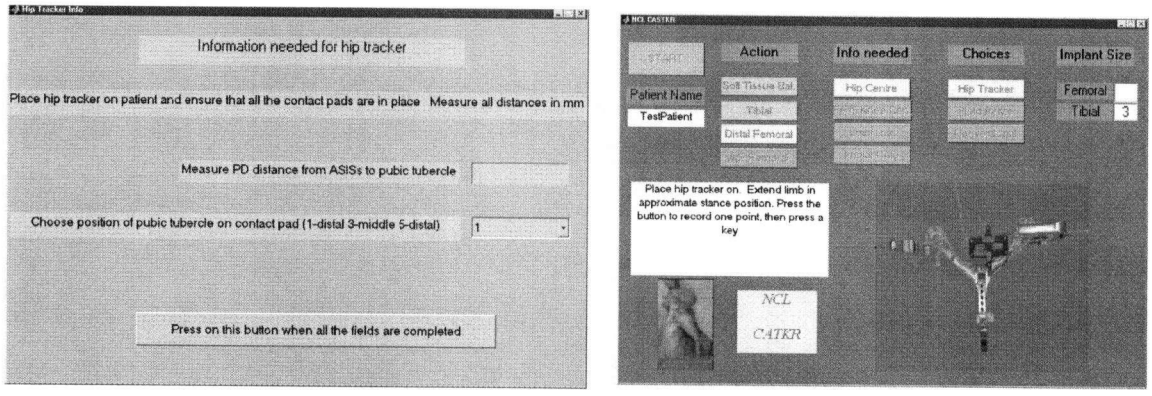

Figure 5.14: (a) GUI showing the information needed for the use of the hip tracker (left).
(b) GUI outlining the initial steps necessary to determine the hip centre using the hip tracker (right).

For this kinematic manipulation, the limb is moved though a range of motion. The femur should be flexed, extended, abducted, adducted and rotated. Points are collected for every 10mm of femoral marker motion in the hip reference frame. At least 50 points should be collected. As the hip joint is approximated by a ball and socket joint, the points are fitted to a sphere with the centre of the sphere as the centre of the hip. The algorithm included in the hip-tracker registration is the non-linear least squares homogenous transform method for fitting a sphere (Inkpen, 1999; Shute, 2002). Use of this algorithm on 10 cadavers showed an angular error of 0.22° SD in the mediolateral direction (Hodgson et al., 2003).

Once registration is complete, the system asks the user whether to accept the procedure. Once the user clicks yes, the hip centre button changes colour to indicate that the hip centre has been found.

5.3.1.3.1.2 Hold pelvis

Holding the pelvis down eliminates the use of the hip tracker. Though pelvic motion is unaccounted for, the increase in the variation may be an insignificant amount. For this manipulation, the hip reference frame is rigidly attached to the table and a stance position is captured similar to the procedure outlined for the pelvic tracker. Manipulations are also performed in the same manner, with the same algorithm to find the hip centre. Holding down the pelvis was implemented in our system, as it is similar to other image-free landmark based systems (Krackow et al, 1999). Validation studies performed on the

same cadavers as the hip tracker showed an angular error 0.25° SD in the mediolateral direction.

5.3.1.3.1.3 Conventional

Once conventional instrumentation has been chosen, the system automatically skips the rest of the registration required for this distal femoral bone cut. The cut is made with conventional instrumentation and the surgeon proceeds to the next cut or step in the procedure. This conventional way of determining the hip centre is based on x-ray images to determine the angle between the anatomical and mechanical axis of the femur. An intra-medullary rod is then used to locate the anatomical axis of the femur (Figure 1.4). Use of this rod may cause fat embolism (entry of bone marrow fat into the venous system). Elimination of this intra-medullary rod by computer-assisted techniques is seen as a major benefit to patients.

5.3.1.3.2 Femoral knee centre

The system first prompts the surgeon to digitize medial and lateral epicondylar estimates with the point probe (Figure 5.15). The system then prompts the surgeon to use the plane probe to collect tangential planes from the surface of each epicondyle (Figure 5.16). A sphere-fit algorithm uses the initial estimates and the captured planes to determine the estimates of the lateral and medial epicondyles. The centre of the transepicondylar axis linking these epicondyles is the femoral knee centre. Repeatability of this algorithm has been performed on a cadaver (Chapter 2).

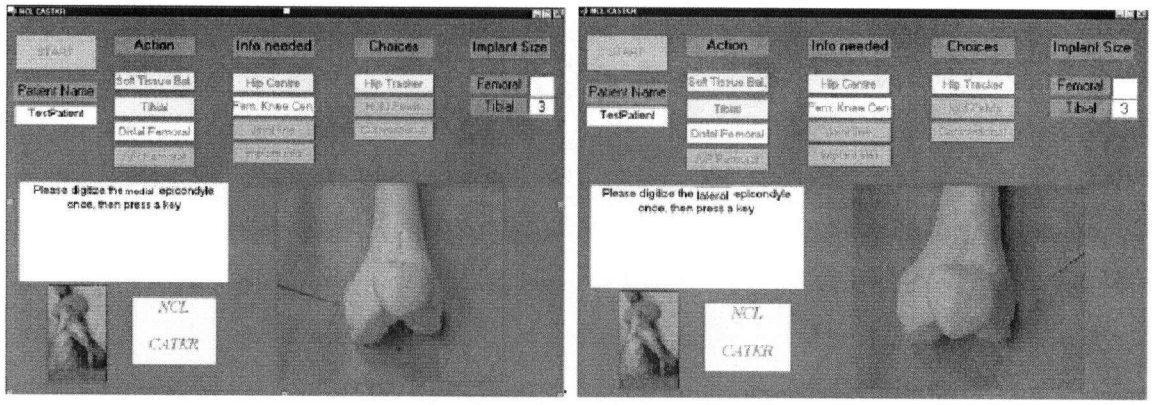

Figure 5.15: GUI prompting the user to digitize the epicondyles as initial inputs into the algorithm.

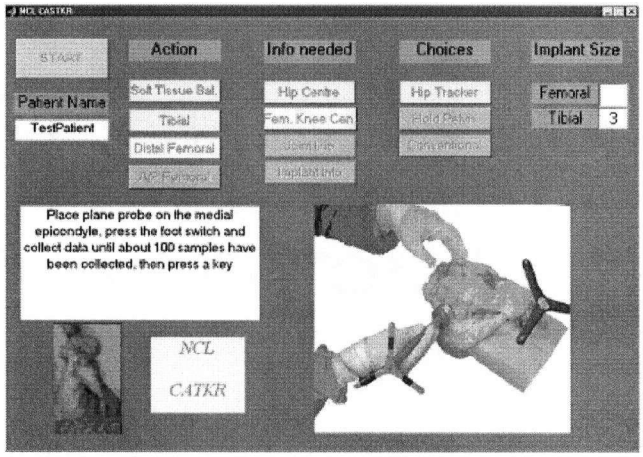

Figure 5.16: GUI prompting the use to digitize the epicondyles with the plane probe.

The total mediolateral variability was 0.1 mm SD, and the total anteroposterior variability was 1.1 mm SD. The surgeon must confirm each stage of data collection. The end result of this button is the (x,y,z) location of the femoral knee centre in the femoral array frame, and the vector for the TE axis.

5.3.1.3.3 Joint line

The system prompts the surgeon to use the point probe to digitize the most distal point of both posterior condyles (Figure 5.17). This is performed in the femoral array reference frame. The thickness of the implant is then subtracted in future calculations so that the joint line remains the same. Moving the joint line in a proximal/distal direction results in a loss of flexion/extension of the knee (Victor and Sint-Lucas, 1998).

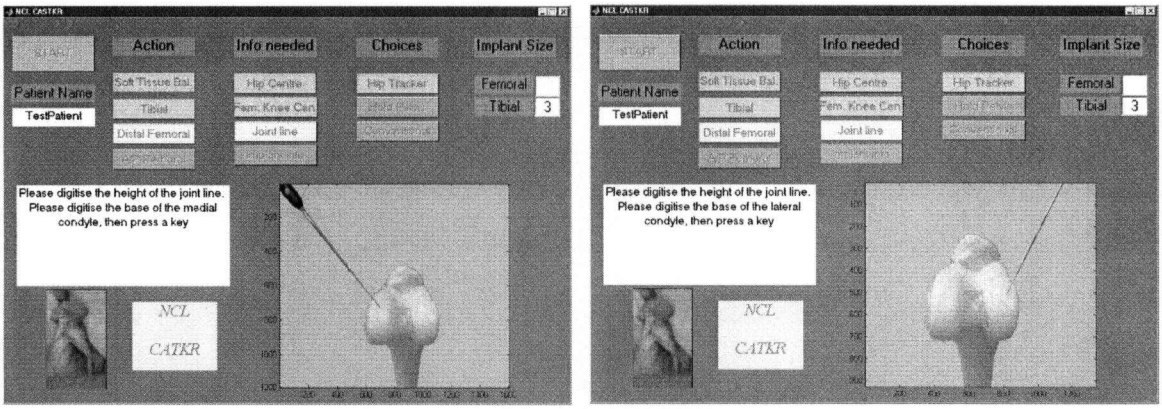

Figure 5.17: GUI prompting the user to digitize the base of the posterior condyles for the femoral joint line.

5.3.1.3.4 Implant size

The femoral implant size is based on the AP dimension of the knee. The system prompts the surgeon to digitize (1) the anterior cortex (Figure 5.18), and (2) the posterior surfaces of the condyles the furthest away from the anterior cortex. The system calculates the size of the femoral component based on a database of component sizes. The current database is Johnson & Johnson components.

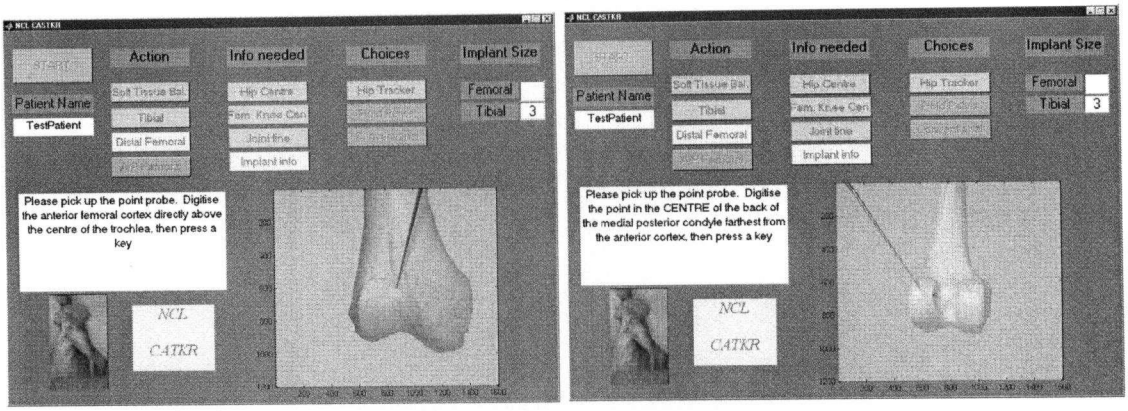

Figure 5.18: GUI that prompts the user to digitize the landmarks necessary to compute the AP dimension of the femoral implant.
(a) the anterior cortex and (b) the posterior condyles furthest away from the anterior cortex.

Care is taken in performing this step as a smaller size creates looseness in flexion and possible notching of the femoral cortex and a larger size creates tightness in flexion and increased excursion of the quadriceps mechanism (Johnson & Johnson Orthopaedics).

The user must then choose the type of implant that to use so that the system can calculate the implant size (Figure 5.19).

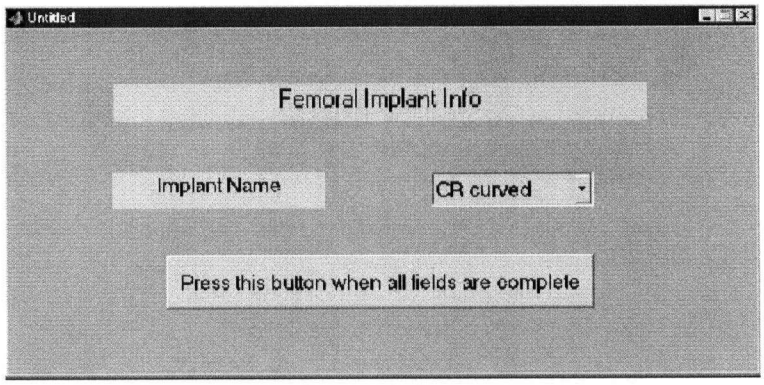

Figure 5.19: GUI that prompts the user to identify the type of femoral component to use.

After all the required registration steps are complete for the femoral cut, the button turns blue. This tells the user that all requirements to make the cut are complete. The user must press the button to enter into the steps required to actually make the femoral cut. The steps necessary in making the cut will be addressed in Section 5.3.2 'Bone Cutting'.

5.3.1.4 AP cut (registration)

Once the all the necessary information has been gathered to make the femoral cut, and the cut has been performed, it is possible to make the anterior-posterior cut of the femur affecting rotational alignment. Registration for this cut ensures that the component is parallel to the transepicondylar axis. The soft tissues should be balanced before this occurs. It is therefore necessary to define the TE axis in this procedure. Once this button is pressed, the surgeon can choose to position the implant using conventional instrumentation, or align the component with the digitized TE axis (Figure 5.20).

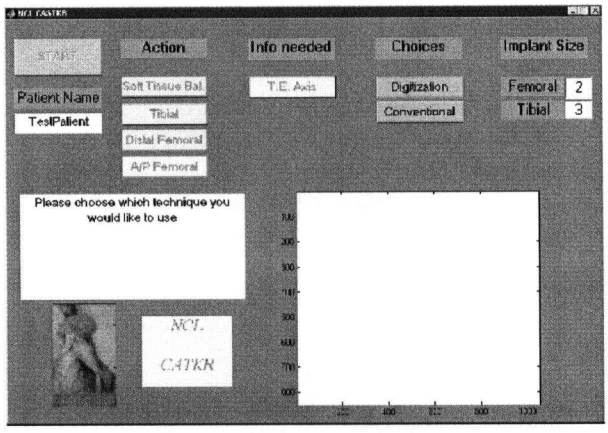

Figure 5.20: GUI that prompts the user to choose which method he would like to use to make the AP cut on the femur.

5.3.1.4.1 Digitization

Registration of the TE axis should have been performed in order to find the femoral knee centre. However if the conventional procedure were used to perform the distal femoral cut, the user is prompted to use the plane probe to collect data for determination of the lateral and medial epicondyles (Figure 5.16). This method located the transepicondylar axis with a rotational variability of 1.8° SD. The locations of the medial and lateral epicondyles are returned in the femoral array frame, and a unit TE axis vector is created.

5.3.1.4.2 Conventional

Once the surgeon chooses the conventional method for determining the AP cut, there is no further registration performed. Conventional AP guides use combinations of the TE axis, Whiteside's line, and the posterior condylar line to determine its proper orientation (Figure 5.21). However, the cut should be aligned with the TE axis (Martelli and Visani, 2002) and other references to this TE axis is variable depending on patient's anatomy (Olcott and Scott, 2000). Locating the TE axis by visual inspection is also highly variable (Jerosch et al., 2002).

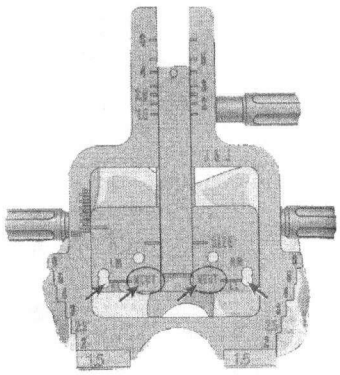

Figure 5.21: Diagram of the AP reference-sizing guide.

5.3.2 Bone Cutting

After all the required registration steps are complete for either cut, the system allows the user to choose to make the cut at this time, or perform further registration for other cuts.

When the surgeon proceeds to make an actual cut, he or she is prompted to alter the overall alignment of the knee. The surgeon can also assess the limb to decide if alterations are necessary from those decided by the system. Options available to change are varus/valgus and posterior slope for the tibial cut, and flexion for the femoral cut. Though most studies state that neutral alignment to the mechanical axis is the best, the surgeon may make changes (Figure 5.22a and 5.22b).

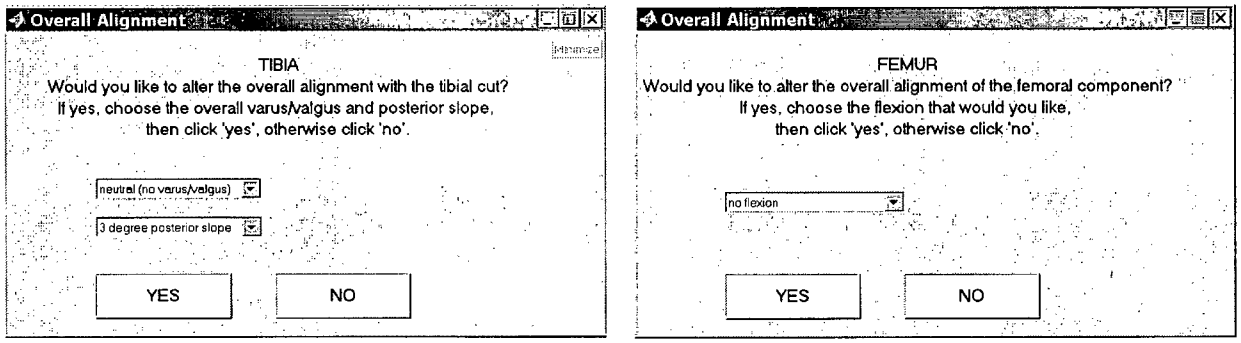

Figure 5.22: GUI that allows the surgeon to alter the overall alignment of the leg.
(a) changes in the varus/valgus alignment and posterior slope are made to the tibial cut,
and (b) changes in flexion affect the femoral cut

5.3.2.1 Tibial cut (goal planning and bone cutting)

The system has calculated the cutting plane of the proximal tibial cut in the tibial array reference frame. This is represented by a normal to the plane, and a distance from the plane to the origin on the array. To ensure proper overall alignment, the co-ordinates of the centres are used to create a body frame. The body frame for the tibial component is defined as the +x axis from the tibial knee centre to the right along the major axis of the ellipse, the –y axis from the tibial knee centre to the ankle centre, and the +z axis anterior (Figure 5.23)

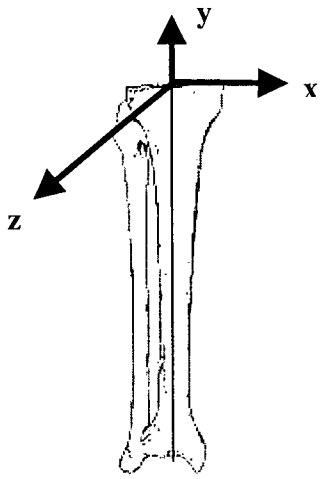

Figure 5.23: Diagram of the tibial body frame used in this study.
The +x axis is defined as the tibial knee centre to the right along the major axis of the ellipse, the -y axis from the tibial knee centre to the ankle centre, and the z axis anterior (right hand co-ordinate frame).

The desired cutting plane (before alterations) is transformed into this body reference frame. Any variation in overall alignment for varus/valgus and posterior slope is then

addressed. The system calculates the change in cutting plane by altering the normal by the varus/valgus angle (VV) and posterior slope (PS) dependent on right or left leg:

$$\text{Desired Cut Normal}_{body} = [\sin(VV) \quad 1-(\sin(VV)*\sin(VV))-(\sin(PS)*\sin(PS)) \quad \sin(PS)]$$

This is in the body (tibia) reference frame. The desired cutting plane in this body reference frame is then transformed back to the tibial array reference frame for instrumentation purposes.

The bone cut can then be performed. The system prompts the user to fix the base of the cutting guide on the bone about 4 mm below the cut line (Figure 5.24).

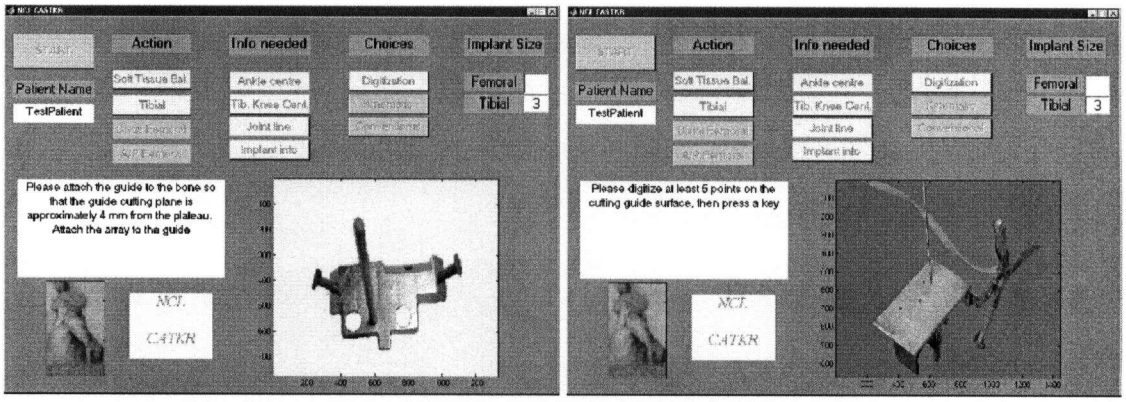

Figure 5.24: (a) GUI that prompts the user to attach the base of the guide to the bone.
(b) GUI that prompts the user to calibrate the cutting plane in its reference frame.

The adjustable cutting guide (seen in Figure 5.24b) must be calibrated to form a relationship between the cutting plane and its rigid guide array. The system prompts the user to digitise at least five points on the cutting guide plane. The system fits a plane to these points using a non-linear least squares minimization (Chapter 4). Included in these points are ones needed for the calculation of adjustments. These are P_m, P_l, and P_a, representing the points above the medial, lateral and anterior adjustable legs of the cutting guide, and are in the guide array frame (Chapter 4).

This step is included because the guide array is removable, and should be only attached to the cutting plane when a cut is necessary as not to obstruct the operation.

The adjustable cutting guide with guide array is then attached to the base (Figure 5.25a).

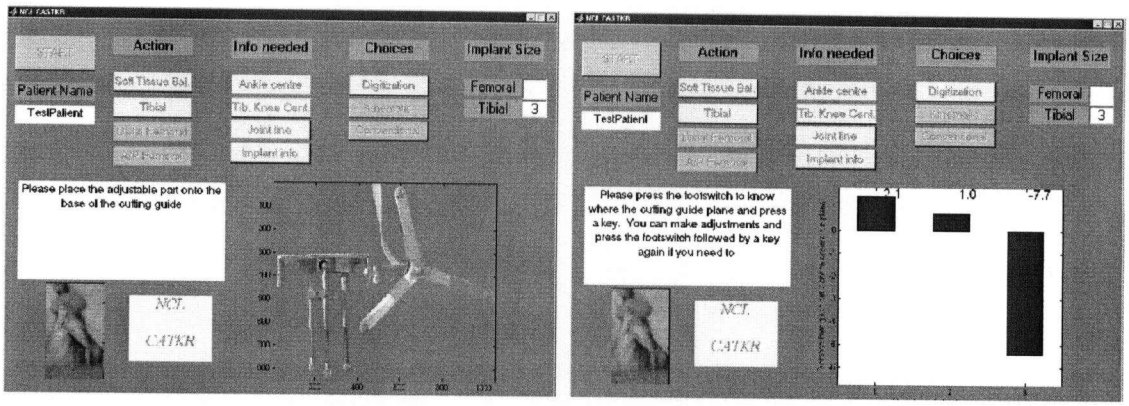

Figure 5.25: (a) GUI prompting the user to place the adjustable portion of the guide onto the base. (b) GUI that shows the surgeon the necessary turns to make on each leg of the adjustable guide.

The normal for the desired cutting plane must be in a known direction. The system checks the location of the ankle centre with the normal of the desired cutting plane. The system alters the form of the plane so that its normal is in the opposite direction of the ankle centre.

This plane is in the guide array frame (GCP_g). The normal of this guide cutting plane must be in the same direction as the desired cutting plane. The angle between the two normals is calculated, and the sign flipped if the angle is between 90° and 180°.

The user then presses the foot-button to check the location of the guide array with respect to the tibial array. Transformations are made between these two reference frames (T_{gt},T_{tg}). The guide cutting plane (GCP_g) and the points (P_m,P_l,P_a) are then converted to the tibial array frame.

$$X_t = T_{tg} * X_g$$

Both the desired cutting plane (DCP_t) and the guide cutting plane (GCP_t) are now both in the tibial array reference frame. The system calculates the number of turns that should be carried out for the guide cutting plane to achieve the desired cutting plane position (Figure 5.25b) (Chapter 4). The user can press the footswitch to make further comparisons. This process occurs until the guide cutting plane is within 0.2 degree of the desired cutting plane in the mediolateral and anteroposterior directions.

The surgeon should then use a milling tool (Midas Rex, TX) to make the cut. A milling tool has been verified to be significantly better than conventional oscillating bone saws

(Plaskos, 2002) as it eliminates deflections. Research is currently underway on the exact size and speed of the milling tool that should be used.

After the cut is made, the surgeon must digitize the most medial and most lateral points on the tibial plateau (Figure 5.26). This allows the system to use built-in dimensions to calculate the correct implant size. Each tibial component is congruent with certain sizes of femoral component. If the displayed sizes determined from measurements do not match up, the surgeon can adjust the component size in the implant size window.

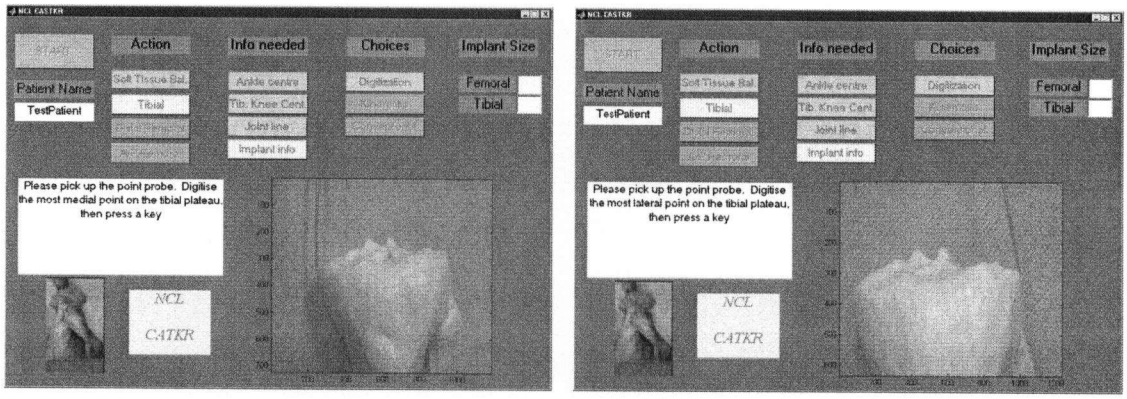

Figure 5.26: GUI showing the required digitization to determine the ML dimension of the implant. This determines the implant size.

5.3.2.2 Femoral cut (goal planning and bone cutting)

The process is similar for the femoral cut. The system has calculated the cutting plane of the distal femoral cut in the femoral reference frame. This is represented by a normal to the plane, and a distance from the origin of the femoral array. The body frame for the femoral component is defined as the +x axis from the knee centre along the transepicondylar axis to the right, the +y axis from knee centre to hip centre, and the +z axis from the knee centre anterior (defines a right handed co-ordinate frame) (Figure 5.27).

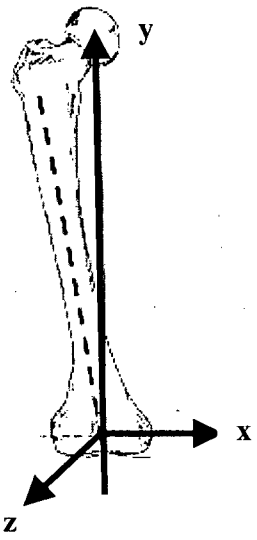

Figure 5.27: Diagram of the femoral body frame used in this study.
Transformations are performed between this frame, and the femoral array frame in order to make calculate the desired cutting planes

After the desired cut plane is transformed into the body frame, flexion (FA) of the femoral component can be addressed by altering the normal by the following equation.

$$\text{Desired Cut Normal}_{body} = [0 \quad 1-(\sin(FA)*\sin(FA)) \quad \sin(FA)]$$

This plane is then transformed back to the femoral reference frame, and the normal checked with the hip centre to confirm its direction.

The cutting guide base is then attached to the distal femur in a similar way as explained for the tibial cut, and with similar procedure, calculations, and adjustments.

5.3.2.3 AP Cut (goal planning and bone cutting)

The AP guide has an array attached to it [theoretical only]. The surgeon must follow the guidelines on the screen, and using two knobs, adjust the AP guide axis to be congruent with the TE axis. When in place, the surgeon would then tap pins into holes present on the guide confirming this position. The position of these holes is the same as those used on current instrumentation for the AP chamfer block. In this way, current AP chamfer instrumentation could still be used. This feature is currently not installed as the hardware is yet to be developed (Figure 5.28).

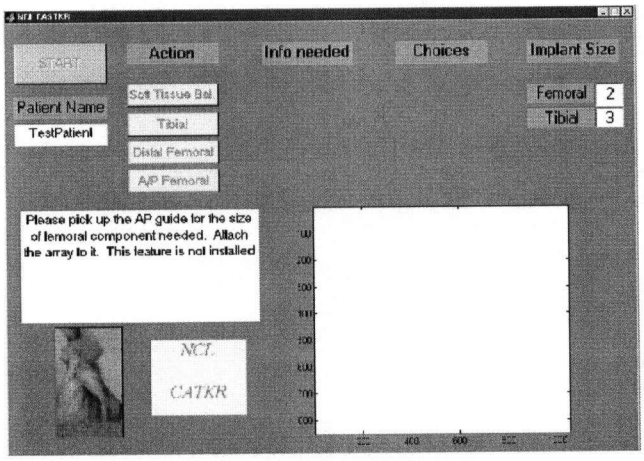

Figure 5.28: GUI that would include the prompts to make the AP cut using an AP guide block.

5.3.3 Implantation

After the three cuts guided by the system (distal and AP femoral, and proximal tibial), the conventional instrumentation can be used to make the chamfer cuts. Final checks can be made concerning the balancing of soft tissues and kinematics. The surgeon can now implant the components and measure success as performed in conventional surgery. The procedure is then complete (Figure 5.29).

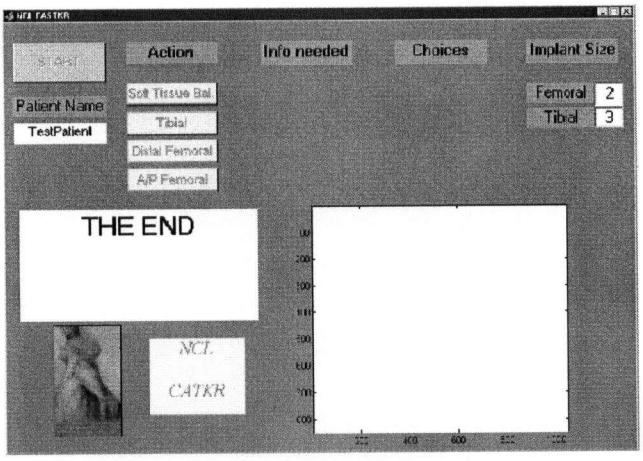

Figure 5.29: GUI that signifies that all cuts have been made, and the procedure is complete.

If the bone cuts have been performed with a milling tool, then it is more beneficial to use press-fit components instead of cemented components, as the introduction of cement could introduce variability in this step of the procedure. A milling tool should be used instead of a bone saw as use of a bone saw was proven to introduce cutting errors (Plaskos, 2002).

5.3.4 Measuring Success

There are many ways to measure success. Immediate (short term) success may be assessed from post-operative x-rays as in conventional surgery. Care should be taken in the placement of the lower limb for these x-rays, as internal/external rotation of the leg could provide an inaccurate frontal or sagittal plane assessment. These x-rays should be long standing weight-bearing radiographs (Krackow et al., 2003). These x-rays should not be the only measurement, as they only show axial alignment in extension, and do not accurately assess overall performance. Varus/valgus deformations should therefore also be assessed in flexion as this shows internal or external rotation (Krackow et al., 2003).

Future assessments of the total knee replacement procedure can then be performed using the Knee Society Score (Insall, 1989). This assessment uses the presence of pain, knee stability, range of motion, and ability to walk to provide knee and function scores out of 100.

5.4 Discussion of GUI and future recommendations for software development

The integrated system was demonstrated to, and evaluated by an expert surgeon (Dr. Bassam Masri) using a mock-up left lower limb with attached pelvis. This Sawbones model was used for kinematic manipulations and digitizing procedures. The surgeon provided feedback on the current system. While some recommendations were incorporated into the current design, others are addressed in this section.

The software component of the NCL system (excluding soft tissues) has been fully integrated using previously verified algorithms designed for each specific area of CATKR. The difference between this system and commercial systems is that each of the algorithms used in our system has been previously tested in our lab. This is not the case for many commercial systems where some of the algorithms used or points digitized are merely a copycat of other systems with no real justification for their use. Because these systems only report clinical outcomes, and it is difficult to isolate which component of their technique is the limiting factor to their system if their algorithms have not been previously verified.

Another main difference between our system and commercial systems is the choice in the sequence of steps for the procedure. This is a beneficial component to our system as

some surgeons have a preference in the sequence of the cuts that they make. As some surgeons move towards minimally invasive procedures, this choice does not limit the surgeon from trying other ways or sequences to reduce exposure of the knee or length of the skin incision.

Our system allows choices in the algorithms for determining the ankle and hip centre. This is also based on surgeon preference. While we can recommend the choice with the highest repeatability, this may not be the best choice in terms of operating room efficiency. The surgeon has the capacity to weigh the options between accuracy and time on a case by case basis.

When the soft tissue capabilities of the system is fully developed and integrated, this would be beneficial to our system. Some surgeons argue that the state of the soft tissues is sometimes more important than mechanics. If soft tissues cannot be balanced with perpendicular bone cuts, it may be necessary to make alternatively angled cuts to ensure proper soft tissue kinematics. Though this may only be the case for a small number of patients, this represents the true benefits of computer-assisted systems over conventional systems in that specific patient anatomy can be accounted for.

After registration has been performed for each cut, the surgeon uses the adjustable cutting guide to make the cut. While this adjustable cutting guide is a first prototype, a version incorporating the feedback from the surgeon will represent an easier method for cutting guide placement versus the commercial systems that use a manually-guided procedure based on two lines on the screen. Future versions of the cutting guide were addressed in Chapter 4.

The total integration of the system has been tested on a Sawbones model, but certain hardware and software requirements are still necessary for the system to be fully verified in the operating room. Evaluation by the expert surgeon was beneficial as it provided insight into the operating room practices, and on feasibility of components of the overall procedure. It also allowed us to evaluate our system considering improvements to make it more conducive for the move towards more minimally invasive surgery.

In general, the most beneficial change to our system would be the incorporation of real time feedback. Real time feedback is currently present in other commercially available

systems, and would be the next step for our system. Our system is currently based on the Matlab 6.1 programming platform (The MathWorks, Natick, MA). We chose this platform for research and development as it is easier to implement and verify algorithms with built-in math functions than it would have been to use a programming language such as C++. Matlab offers realtime capabilities, but the serial device interface used to communicate with the localizer is not particularly robust, and the graphic display subsystem operates comparatively slowly so the visual updates tend to appear somewhat choppy. Once the system is fully verified, then it can be ported to a C++ implementation to incorporate realtime feedback and improve the smoothness of the display relative to what we could achieve with Matlab.

In particular, this real time feedback would be beneficial for adjusting the cutting guide. This would eliminate the iterative process currently implemented in our system. Instead, as the surgeon is adjusting each knob, the displayed differences from the desired positions would decrease to zero as the desired and cutting guide planes become coincident.

Another beneficial addition to our system would be the use of a touch screen to provide responses and feedback to the system. This would be beneficial in a number of areas.

These are:

- allowing the surgeon to interface easily with the computer without the need for a technical assistant,
- 'continue' and 'go back' capabilities; and
- deciding the resection amount for the tibial implant.

A touch screen allows the surgeon to perform the procedure without the need for an additional person operating the computer. This interface would allow for all choices and changes to be made quickly and easily.

After each kinematic manipulation or digitization step is performed, the system confirms with the user if it was acceptable. This is currently performed using a pop-up window. Touching a forward or backward arrow on the screen would reduce the time associated with this confirmation step.

The typical tibial resection amount is about 10 mm to accommodate the tibial tray and polyethylene insert. This is a minimum amount. This amount could change if the plateau were more diseased, and is subject to surgeon judgement. Touch screen capabilities would allow the surgeon to quickly increase or decrease the resection amount that the system calculates between the deepest point on the least diseased plateau to the deepest point on the diseased plateau (resection amount).

The surgeon recommended the use of additional probes that would accelerate the digitization process for certain parts of the procedure. A flat condylar probe was previously built in our lab, but not implemented.

The probe (Figure 5.30) would be used to determine the plane for:

- the joint line (base of the posterior condyles); and
- the posterior part of the posterior condyles for AP sizing of the femoral component.

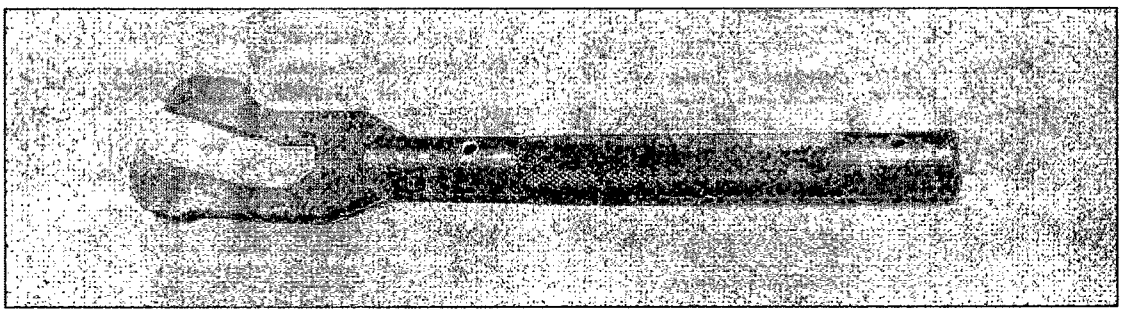

Figure 5.30: Photo of a condylar probe built in our lab.

The plane probe currently in use (Figure 2.5) was built previously, and demonstrates the plane probe technique for finding the lateral and medial epicondyles with the knee exposed. This plane probe could be redesigned for use in minimally invasive, or unicompartmental procedures. A new design would allow the instrument to slide through the skin incision and be placed tangential to the epicondyles without having them in view.

Additional recommendations reflect on specific hardware from the optoelectronic localizer (Flashpoint 5000, Boulder Innovators, Boulder, CO) that is currently used for this integrated system. There are currently other optoelectronic localizers that exist (e.g.

Polaris or Optotrak; Northern Digital, Ontario, Canada) as well as one that is currently in development in our lab. Changes in hardware in Flashpoint 5000 that would be beneficial to CATKR would be:

- active/passive markers and tools that are wireless; and
- incorporating hand-held buttons or building the tools with interfacing buttons on them.

The current hardware (Flashpoint 5000) is an optoelectronic localizer with a wire source of electricity attaching the active emitters to the computer. Infrared light is emitted from these active emitters and detected by the camera. These wires can clutter the operating room, and add an element of confusion to the workspace. It is therefore beneficial to incorporate an active system where the emitter triads are battery operated (e.g. technology used by Stryker), or a passive system (e.g. Polaris), where markers reflect infrared light from another light source. Currently, most commercial systems (e.g. Stryker, VectorVision) are wireless (active or passive) except for the OrthoPilot, which still incorporates the use of wires.

The most common method for digitizing a point with the point probe using Flashpoint 5000 is with a foot button. This is also common to other systems such as the OrthoPilot. A foot button may not always be the best method. A surgeon who stands on a footstool to perform the operation would not be able to use this device. A foot button could also be easily misplaced on the floor of the operating room. A hand held button, or a button attached to the digitizing tool would be the beneficial for the digitizing tools.

All optoelectronic localizers introduce problems with line of sight. There are two solutions that help this problem. These are:

- placing the camera on a boom that could be easily moved around during the operation
- the addition of more LEDs on the tools so that a choice of triads could be recognised by the camera.

In this way, there would be no difference if the surgeon were left or right handed, or were digitizing the medial or lateral side of the patient's lower limb.

The patella cut, and chamfer cuts are not addressed in this system. Research is still needed in this area to decide if it should be incorporated into computer-assisted knee suregery.

5.5 Conclusions

The current integrated system combines all the work performed previously on each aspect of the computer assisted system. This integrated system was designed as a GUI using Matlab 6.1, and incorporates choices in sequence and in technique throughout the entire procedure. It is hoped this system, with the addition of future recommendations in hardware and software, would provide an open architecture for research, and could be tested first on cadavers, and then clinically. In this way, benefits over current commercial systems may be seen.

5.6 References:

De Sienberthal, J. and F. Langlotz (2003) A complete system for training CAS procedures based on a knowledge oriented architecture. In Langlotz, F, Davies, B.L., and A. Bauer (Eds): *3rd Annual Meeting of CAOS-International Proceedings*: 84-85.

DiGioia, A. (2003) Computer assisted orthopedic surgery, robotics and navigation: What have we learned. Round table discussions September 2003 *Orthopaedics Today.* http://www.slackinc.com/bone/ortoday/ottoc.asp Last accessed November 26, 2003.

Gander, W., Golub, G.H., and R. Strebel. (1994) *Fitting of circles and ellipses least squares solution.* Technical document. ETH Zurich Departement Informatik, Institut fur Wissenschaftliches Rechen.

Hodgson, A.J., Inkpen, K.B., Plaskos, C., Bullock, S., and V Stanescu (2003) A comparison of two non-invasive techniques for locating the hip centre in computer-assisted surgical procedures. Final report submitted to DePuy.

Illsley, S.G. (2002) Intraoperatively measuring ligamentous constraint and determining optimal component placement during computer-assisted total knee replacement. MASc Thesis. University of British Columbia, Vancouver, B.C.

Inkpen, K.B. (1999) *Precision and accuracy in computer-assisted total knee replacement.* MASc Thesis. University of British Columbia, Vancouver, B.C.

Insall, J.N.,Dorr, L.D., Scott, R.D., and W.N. Scott (1989) Rationale of the Knee Society clinical rating system. *Clin Orthop* (248): 13-14.

Jerosch, J., Peuker, E., Phillips, B., and T. Filler (2002) Interindividual reproducibility in perioperative rotational alignment of femoral components in knee prosthetic surgery using the transepicondylar axis. *Knee Surg Sports Traumatol Arthrosc* **10** (3): 194-7.

Martelli, S., and A. Visani (2002) Computer investigation into the anatomic location of the axes of location of the knee. In Dohi, T., and R. Kikinis (Eds) MICCAI 2002. *LNCS* **2489**: 276-283.

Olcott, C.W., and R.D. Scott (2000) A comparison of 4 intraoperative methods to determine femoral component rotation during total knee arthroplasty. *J Arthroplasty* **15** (1): 22-26.

Plaskos, C. (2002) *Bone sawing and milling in computer-assisted total knee arthroplasty.* MASc Thesis. University of British Columbia, Vancouver, B.C.

Shute, C. (2002) *Ankle joint biomechanics applied to computer assisted total knee replacement.* MASc Thesis. University of British Columbia, Vancouver, B.C.

Stulberg, S.D., Loan, P. and V. Sarin. (2002) Computer-assisted navigation in total knee replacement: results of an initial experience in 35 patients. *J Bone Joint Surg,* **84A**(S2): 90-98.

Victor, J. and A.Z. Sint-Lucas (1998) Alignment and component positioning in total knee arthroplasty Belgian Orthoweb www.orthoweb.be. Last accessed on October 30, 2000

Chapter 6: Thesis summary and direction of future work

6.0 Thesis summary

The goal of a total knee replacement (TKR) is to restore limb alignment, improve limb function, and relieve patient pain by resurfacing the deformed articular surfaces of the knee joint with femoral, tibial, and patellar components. The femoral component should be perpendicular to the mechanical axis of the femur (line joining the hip and femoral knee centre) in the frontal and sagittal planes, and aligned with the transepicondylar axis in the tranverse plane; the tibial component should be perpendicular to the mechanical axis of the tibia (line joining the tibial knee and ankle centre) in the frontal and sagittal planes, and be congruent with the femoral component in the transverse plane; and the patellar component should align with the femoral component and should not overstuff the patellofemoral joint (i.e. should be the same thickness as the original patella).

Though TKR is considered a successful procedure (>88% of procedures within 3° of the mechanical axis in the frontal plane (Konig and Kirschner, 2003)), component positioning errors, postoperative instability, and component loosening still exist. Computer-assisted techniques aim to remove the inadequacy of mechanical instrumentation and the necessary visual perception present in conventional procedures. This technology should provide optimal alignment, component position, gap and ligament balancing, and hence improve stability and increase range of motion (Krackow et al., 2003). Commercial systems exist, and though there is promise in their application, there is still a lot of work before these systems would be accepted in terms of costs and benefits to the patient and hospital (DiGioia, 2003).

There are two types of computer-assisted systems available - Image-based and Image-free (Krackow et al., 2003). Image-based systems incorporate the use of CT or Fluoroscopic images, whereas Image-free systems are either landmark-based or use a bone morphing algorithm that morphs patient-specific anatomy onto a generic model. Image-free systems tend to be more popular as they are cheaper and do not expose the patient to radiation (DiGioia, 2003).

The Neuromotor Control Lab at the University of British Columbia has been developing an image-free system since 1997. The aim of our lab is to have a complete, accurate, and

cost-effective system based on verified algorithms for each step of the surgery. It can then serve as a research testbed to validate, evaluate, and compare new algorithms before they are implemented clinically. The algorithms in our system have been investigated either by previous graduate students in our lab or by the author. Inkpen (1999) investigated a repeatable method for locating the hip centre; Shute (2002) determined a repeatable method for locating the ankle centre; Plaskos (2002) showed that the use of a milling tool would provide a more accurate cut than the conventional bone saw; and Illsley (2002) investigated an alternative alignment of the components from soft-tissue balancing.

This thesis focused on determining repeatable methods for the requirements of a total knee replacement system that have not been previously addressed, and integrating the system to take steps towards providing an open architecture for research. With this, the true benefits of computer-assistance over conventional surgery may eventually be shown.

In the first study, I investigated two methods for determining the transepicondylar axis, with applications to proper rotational alignment and the femoral knee centre. Current commerical systems digitize the medial and lateral epicondyles with a point probe – a method that has been shown to be highly variable (Fuiko et al., 2003; Jerosch et al., 2002; Kessler et al., 2003). Instead, we developed and tested a plane probe that is used to capture planes tangential to each epicondyle of the femur. We compared the use of a convex-hull based method and a sphere-fit based method to determine the medial and lateral epicondylar estimates. Four students performed 5 trials each, and one student performed 20 trials on a fresh cadaveric knee. We found that using the sphere-fit algorithm was a more repeatable way than the convex-hull algorithm in locating the epicondyles. Variation in the mediolateral (ML) direction was much less than in the anteroposterior (AP), with generally more variation in locating the lateral epicondyle than the medial. Bootstrapping the collected planes showed that the estimated locations could be biased depending on the operator. Applying this to locating a femoral knee centre, this method provided a pooled intra-operator variability of 0.1 mm and 1.1 mm SD in the ML and AP directions respectively, an inter-operator variability of 0.05 mm and 0.8 mm SD in the ML and AP directions respectively, and a total variability of 0.1 mm and 1.1 mm SD in the ML and AP directions respectively. In terms of rotational alignment, this

method showed a standard deviation of 1.8°, and a total range of 7°. This range was less than that presented by other studies using a point probe to locate the epicondyles.

The next component that needed to be verified was the location of the tibial knee centre. Current CATKR procedures digitize the centre of the tibial eminences for the ML and/or AP position of the tibial knee centre on the tibial plateau (Krackow et al., 1999; Kunz et al., 2001). This may not represent a centre that provides optimal coverage of the tibial plateau (Lemaire et al., 1997), and a plane perpendicular to an axis joining this point and the ankle centre may provide a cut that may be varus/valgus or in posterior/anterior slope. A geometric ellipse fit algorithm was used as a novel method to determine the centre based on optimal coverage of the tibial plateau. A single operator digitized the perimeter of the tibial plateau of a Sawbones model (Pacific Research Laboratories, Vashon, WA), and a fresh cadaveric knee. The ellipse-fit algorithm showed a ML variability of 1.7 mm SD, and AP variability of 1.3 mm SD in locating the tibial knee centre on the cadaveric knee. This pilot study showed feasibility in using this method for a tibial knee centre and provided the final method in our lab for the requirements of the mechanical axis of the leg. The desired cutting planes for the tibial and femoral components could now be calculated as perpendicular to these mechanical axes.

Once this desired cut plane has been defined from registration, the cutting guide plane must be tracked to coincide with the desired cut plane, so that the bone cuts can be performed. I was part of a supervisory group for a student project in which a prototype cutting guide was designed and subsequently manufactured. This cutting guide is placed approximately in place, and subsequently adjusted to its final position. This is different from other commercially available systems where the cutting guides are manually guided into place using real time feedback. I determined a kinematic model for this cutting guide, and evaluated it based on range, accuracy, ease of use and feasibility of use. This cutting guide proved to have an extensive range of use for its application and could be redesigned to a smaller size. Changes are also needed so that the base could be properly attached to the amount of bone that would be exposed in a computer-assisted/minimally invasive surgery, and account for muscles and fat overlying the bone.

Finally, once all the requirements for registration and bone cutting had been addressed, integration of the entire procedure could occur. In this way, research can be performed on the overall procedure, using all the algorithms at one time. This integration provides an open architecture, allowing choices and comparisons in the different stages of the knee replacement system. The system was integrated so that it could be evaluated as an entire system. A graphical user interface (GUI) was designed that incorporates modularity and choices in the sequence of steps of the surgery. It also incorporates many different algorithms for each step, allowing the surgeon choices in the method for each step as well as the sequence of steps. I outlined the steps in our procedure from when the START button is pressed until the procedure is complete, and provide the algorithms and transformations that occur in the system. Each step of the procedure was shown from registration to the bone cuts. The system was evaluated by an expert surgeon, and recommendations in hardware and software are addressed. The surgeon made positive comments towards the sequence of steps and choices for each step in our integrated procedure. The most beneficial changes that would enhance our system would be a touch screen to interface with the computer, and the incorporation of real-time feedback to assist in alignment of the cutting guide.

In summary:

- a plane probe may be more repeatable than a point probe in locating the epicondyles.
- the sphere-fit based algorithm was more repeatable than the convex-hull based algorithm for the cadaveric specimen used in this study.
- mediolateral variability was lower than anteroposterior variability in locating these epicondyles.
- the medial epicondyle was more repeatable than the lateral epicondyle.
- biases existed between operators in using the plane probe.
- an ellipse-fit algorithm showed promise in locating the tibial knee centre based on optimal coverage of the tibial plateau.

- though kinematics of the cutting guide will stay the same, evaluation of the cutting guide showed a need for redesign.
- an integrated system allowed our overall system to be assessed, and recommendations were made for future development of the GUI and our entire computer-assisted total knee replacement system.

6.2 Direction of future work

The future work needed for this system can be grouped into three categories: validation, hardware design, and software design.

6.2.1 Validation

The determination of femoral and tibial knee centres in this study can be treated as a pilot study that provided us with methods to implement in the integrated system. More specimens and operators are required to verify the robustness of these methods. To our knowledge, this is the first time that a plane probe has been used to determine epicondylar estimates. While the sphere-fit algorithm is a repeatable method, other algorithms using this concept may prove to be more repeatable. Also, in order to compare the inter-operator repeatability of the plane probe method to the point probe method on the same specimens using the same subjects, the study could be further designed using expert surgeons over a longer period.

In terms of finding a tibial knee centre, to our knowledge this is the first time that an ellipse-fit algorithm has been used to assess overall coverage. Further testing using multiple operators and more specimens would be needed to verify this technique.

There are also other stages of the integrated system that have only been previously verified on test subjects or specimens that are not truly representative of the total knee replacement population. In particular, validation is needed on the soft-tissue component of the integrated system before it can be fully incorporated into the system. The ligament measurement model designed by Illsley (2002) was only verified on porcine specimens using a basic model involving only the primary ligaments of the knee. This simplified model must be verified on cadavers, and clinical feasibility of the method must be shown before it can be incorporated into the system.

Validation of the hip centre identification techniques were performed on fresh cadavers that were smaller than the typical total knee replacement population. Further verification of these methods may be necessary to determine the robustness of these algorithms on larger patients (Hodgson et al., 2003).

The bias that should be applied to the ankle centre identification technique (for an estimate of a weight-bearing centre) was determined from a group of 12 subjects with a mean age of 25 years (Shute, 2002). A larger group of subjects should be tested in order to determine bias values with tighter confidence bounds.

6.2.2 Hardware design

The integrated system would benefit from the development of, and changes to hardware in the current system. Hardware that should be built or redesigned include:

- a distal cutting guide that meets the recommendations outlined in chapter 4.
- an AP cutting guide to complete the integration of the entire system. This cutting guide would allow the AP cuts to be performed parallel to the TE axis of the knee.
- a plane probe that is more conducive to minimally invasive surgery. The surgeon could use the tool to gather planes tangential to the epicondyle without having them in view.
- a flat probe that can be easily used to measure the locations of the base and posterior part of the posterior femoral condyles. The system would then know the exact plane without having the surgeon digitize points as in current commercial systems.
- a point probe with a spherical end to easily glide along the edge of the tibial plateau. This would decrease the amount of time that is currently needed in this procedure, and may increase the repeatability as more points could be gathered in a very short time.
- an ankle tracker that is clinically acceptable. This tracker must be designed so that it is relatively comfortable to wear, and easily adjustable for different patient sizes.

- an optoelectonic localizer that uses wireless technology so that the operating environment is not cluttered with wires.
- handbuttons and a touchscreen to interface with the system, and tools with extra LEDs to increase the ease of use by the surgeon.

6.2.3 Software design

Changes in software are necessary to complete the integration of the procedure, and may be beneficial to the interface between the system and the surgeon. Development and changes in software are needed in the following areas:

- development and incorporation of an algorithm that determines the joint line using the flat probe.
- real-time feedback of the position of the cutting guide, and the number of points collected during kinematic manipulation and digitization.
- determining the patellar cut using computer-assisted techniques. Computerized registration for this cut is not present in other commercial computer-assisted TKA systems and can be specific to the instrumentation and surgeon. Research is needed in this area to determine whether there would be any benefits to making this cut computer-assisted.

The usability of the software and hardware can then be tested as a complete system.

6.3 Conclusions

Combining the contributions of this thesis with that of previous students and the recommended hardware and software changes, our system provides an open architecture for research in the computer-assisted total knee replacement area. This future system should increase the accuracy of TKR thereby increasing implant success and longevity, hence improving the patients quality of life.

6.4 References

DiGioia, A. (2003) Computer assisted orthopedic surgery, robotics and navigation: What have we learned. Special to September 2003 *Orthopaedics Today.*

Fuiko, R. Kotten, B., Zettl, R. and P. Ritschl (2003) Landmarks for navigated implantation of total knee arthroplasty (TKA). In Langlotz, F, Davies, B.L., and A. Bauer (Eds): *3rd Annual Meeting of CAOS-International Proceedings*:108-109.

Hodgson, A.J., Inkpen, K.B., Plaskos, C., Bullock, S., and V. Stanescu (2003) *A comparison of two non-invasive techniques for locating the hip centre in computer-assisted surgical procedures.* University of British Columbia, Vancouver. Final report submitted to DePuy.

Illsley, S.G. (2002) *Intraoperatively measuring ligamentous constraint and determining optimal component placement during computer-assisted total knee replacement.* MASc Thesis. University of British Columbia, Vancouver, B.C.

Inkpen, K.B. (1999) *Precision and accuracy in computer-assisted total knee replacement.* MASc Thesis. University of British Columbia, Vancouver, B.C.

Jerosch, J., Peuker, E., Phillips, B., and T. Filler (2002) Interindividual reproducibility in perioperative rotational alignment of femoral components in knee prosthetic surgery using the transepicondylar axis. *Knee Surg Sports Traumatol Arthrosc* **10** (3): 194-7.

Kessler, O.C., Moctezuma de la Barrer, J.L., Streicher, R.M., Stockl, B., Krismer, M., and M. Nogler (2003) Variation in the entry point selection for the transepicondylar axis and its quantitative effects. In Langlotz, F, Davies, B.L., and A. Bauer (Eds): *3rd Annual Meeting of CAOS-International Proceedings*: 176-177.

Konig, A., and S. Kirschner (2003) [Long term results in total knee arthroplasty] (*In German) Orthopade* **32** (6): 516-526.

Krackow, K.A., Serpe, L., Phillips, M.J., Bayers-Thering, M., and W.M. Mihalko. (1999) A new technique for determining proper mechanical axis alignment during total knee arthroplasty: progress towards computer-assisted TKA *Orthopedics* **22** (7): 698-702.

Krackow,K.A., Phillips, M.J., Bayers-Thering, M., Serpe, L., and W.M. Mihalko (2003) Computer-assisted total knee arthroplasty: navigation in TKA. *Orthopedics* **26** (10): 1017-1023.

Kunz, M., Strauss, M., langlotz, F., Deuretzbacher, G., and W. Ruther (2001) A non-CT based total knee arthroplasty system featuring complete soft-tissue balancing. In Niessen, W., and M, Viergever (Eds): *MICCAI 2001, LNCS* **2208**: 409-415.

Lemaire, P., Piolette, D., Meyer, F., Meuli, R., Dorfl, J., and P. Leyvraz. (1997) Tibial component positioning in total knee arthroplasty: bone coverage and extensor apparatus alignment. *Knee Surg Sports Traumatol Arthrosc* **5**: 251-257.

Plaskos, C. (2002) *Bone sawing and milling in computer-assisted total knee arthroplasty.* MASc Thesis. University of British Columbia, Vancouver, B.C.

Appendix A: Simple explanation of the quickhull convex hull algorithm for 2-d.

This is a 2-d walkthrough of a convex-hull algorithm. There are many ways that a convex hull of a set of points can be computed. This is the 2d version of the quickhull method used in our matlab computations (Barber et al, 1996).

The convex hull of a set of points is the smallest convex set that contains all the points. The algorithm first forms a simplex. In 2-d this simplex is a triangle that contains the origin of all the points (In 3-d this simplex is a tetrahedron).

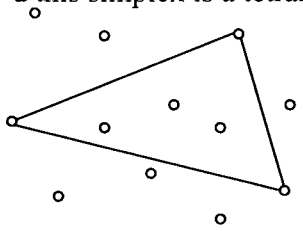

For each face of the triangle, it determines from its outside set of points, which point is the furthest (identified by shaded point).

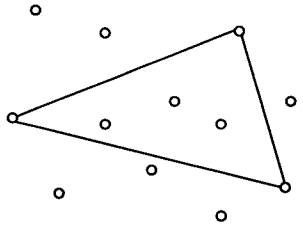

The algorithm creates faces to include that point

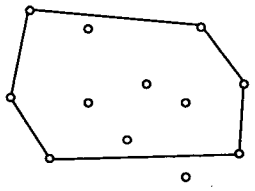

It then performs further iterations until there are no points belonging to the outside set of any face.

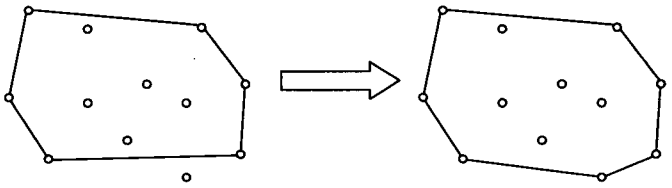

Appendix B: CAOS 2003 Conference Poster

A PLANE PROBE REPEATABLY IDENTIFIES ANATOMICAL FEATURES IN COMPUTER ASSISTED TOTAL KNEE REPLACEMENT SURGERY

Stacy J. Bullock[1], Antony J. Hodgson[1]
[1]Department of Mechanical Engineering
University of British Columbia, Vancouver, BC, Canada
Email: ahodgson@mech.ubc.ca

Motivation

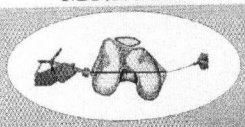

In total knee replacement surgery, accurate rotational alignment of the femoral component is important for normal patellar tracking and proper soft tissue balance. This can be achieved with alignment parallel to the transepicondylar axis, which approximates the flexion-extension axis of the knee.

Conventionally, surgeons must explicitly point to the extrema of the epicondyles, but this shows high variability[1]. We propose that rotating a flat surface over the epicondyles and identifying the extrema of the resulting convex hulls will reduce the effect of operator variability.

Study Design

Overall Goal

To characterize intra- and inter-operator repeatability of the convex hull algorithm in locating the lateral and medial epicondyles on a wooden model

Equipment

Planar probe

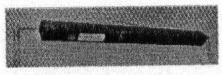

Flashpoint optoelectronic tracker

Measurement Technique

- Operator rocks probe on model – collects planes tangent to 'epicondyle'
- <10s of rotation; ~100 sample planes
- 5 operators 27±3 years
- ~20 trials per operator

Data Analysis

- Transform data to reference frame nominally aligned with transepicondylar axis
- Use convex hull algorithm to compute facets of hull from plane measurements
- Candidate 'epicondylar' tips lie at vertices of hull
- Define transepicondylar axis as most widely separated pair of points on medial & lateral hulls
- Evaluate mediolateral and anteroposterior variation within and between operators

Results

Intra-operator Variation of Features (~20 trials each)

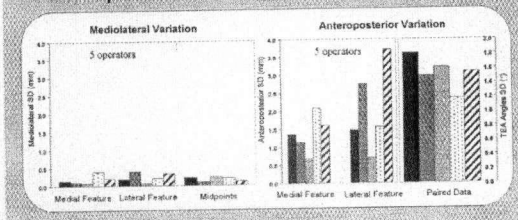

Inter-operator Variation (99 trials)

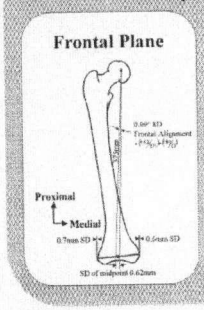

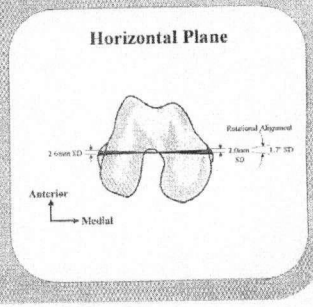

Conclusions

- 1.7° SD for rotational alignment variability
  - 95% CI (~6.8° = ±4 SD) much lower than 23° range reported using point probe technique[1]
- 0.09° SD for mediolateral knee centre variability
  - insignificant contribution to varus/valgus variability

Continuing & Future Work

- Currently validating planar approach on cadaveric knees
- Redesigning planar probe for use in minimally invasive knee arthroplasty

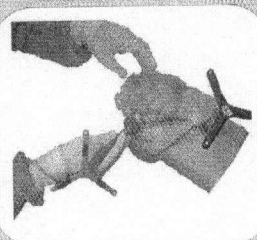

Appendix C

Software

The name of the main GUI for the NCL Computer assisted Total Knee Replacement Procedure is called **TKR_Procedure3.m.** This program is linked to the GUI interface program **TKR_Procedure3.fig.** This file is the main structure for the entire computer-assisted program.

This program calls on 4 embedded GUI's, and many files that either collect data, process data, or display to the screen. These files must all be in the path. These folders that must therefore be in this path for the entire GUI to work are:

- **General**
- **Femur**
- **Tibia**
- **Images**
- **fputilities**

These five folders contain all the files necessary for running the entire GUI. These files are all called from **TKR_Procedure3.m**

Hardware

The hardware for this GUI consists of:

- Flashpoint 3000 optoelectronic tracker. This must be plugged into the COM1 serial port of the host computer.
- A footbutton that is plugged into Port D.
- a DRF on the tibia (MEDDRF) and a DRF on the femur (DRF4). For the current breakout box, MEDDRF is plugged into Port A when in use, and DRF4 is plugged into Port A3 when in use.

- Optional DRFs on the hip tracker and ankle tracker. The DRF from the hip tracker is plugged into Port B2 when in use, and the DRF from the ankle tracker is plugged into Port B3 when in use
- Various tools such as the plane probe and the point probe. The plane probe is plugged into Port B3 when in use; and the point probe is plugged into Port C.
- A cutting guide that is placed in Port B3 when used on the femur (with DRF4 in Port A3 as the DRF), and in Port B3 when used on the tibia (with MEDDRF as the DRF in Port A as the DRF).

Please ensure that all the LEDs are in sight during manipulation and digitization.

NOTE

High pitched beeps are 'good' data (good line of sight), and low pitched beeps are when there is 'bad' data being collected. Explanations for 'bad' beeps include line of sight issues, or tools or DRFs that are not receiving current. They would be either not plugged into the right Ports, or not plugged in at all. The Infrared LED sensor card can be used to detect if the tool in use is receiving current.